

NOVEL ANIMAL MODEL AND *IN VIVO* IMAGING SYSTEM TO STUDY INFLAMMATORY
RESPONSES-MEDIATED CANCER METASTASIS

by

CHENG-YU KO

Presented to the Faculty of the Graduate School of
The University of Texas at Arlington in Partial Fulfillment
of the Requirements
for the Degree of

DOCTOR OF PHILOSOPHY

THE UNIVERSITY OF TEXAS AT ARLINGTON

May 2010

Copyright © by Cheng-Yu Ko 2010

All Rights Reserved

ACKNOWLEDGEMENTS

I would like to sincerely thank people who provide support and guidance during my Ph.D. study in UTA. I deeply thank my parents Mr. Chih-Hua Ko and Mrs. Shu-Ching Kuo for their endless encouragement and support. I greatly appreciate my advisor, Professor Liping Tang for giving me the opportunities to continue my study and for his sincere guidance which made it possible to accomplish this work. I gratefully appreciate all of the committee members (Dr. Kytai T. Nguyen, Dr. Jian Yang, Dr. Wei Chen and Dr. Jer-Tsong Hsieh) who have spend their time to read my thesis and to offer precious advices on my research work. Last but not least, I would also like to acknowledge the contribution of my lab members to the completion of this dissertation.

April 15, 2010

ABSTRACT

NOVEL ANIMAL MODEL AND *IN VIVO* IMAGING SYSTEM TO STUDY INFLAMMATORY RESPONSES-MEDIATED CANCER METASTASIS

Cheng-Yu Ko, PhD

The University of Texas at Arlington, 2010

Supervising Professor: Liping Tang

Cancer metastasis is the leading cause of death in cancer patients. A vast majority of cancer-related mortality is attributed to this rather than the primary tumor itself, making the understanding of cancer metastasis critically important. Inflammatory responses have been implicated to play an important role in cancer metastasis. However, the investigation of the relationship between inflammation and cancer cell migration is limited by the lack of a reproducible cancer metastasis animal model. To fill the gap, we have recently developed an animal model. This model is composed of a two-step procedure. First, poly-L lactic acid (PLA) microspheres were implanted subcutaneously on the back of mice to induce localized inflammatory responses. Second, after PLA microsphere implantation for 24 hours, melanoma B16F10 cancer cells were transplanted in the peritoneal cavity. After cell implantation for different periods of time, animals were sacrificed and all tissues/organs were isolated for assessing the distribution of metastatic cancer cells. In addition, an imaging model was established to visualize and also quantify the cancer cell migration *in vivo*. For that, cancer cells were labeled with X-Sight fluorescence agent. Following transplantation, the distributions of the X-Sight labeled cells could be monitored using Kodak In-Vivo Imaging System. A relationship

between fluorescence intensity and cell numbers was established to quantify the numbers of recruited cancer cells.

Our studies have shown that inflammatory responses are one of the critical determinants of cancer cell metastasis. First, by implanting materials with varying pro-inflammatory properties, we found that there was a good relationship between the degree of biomaterial-mediated inflammatory responses and the numbers of immigrated cancer cells *in vivo*. Inflammatory responses exert similar migration responses of various cancer cells, including B16F10 melanoma cells, Lewis lung carcinoma cell line (LLC), rat prostate cancer cell line (JHU-31), human prostate adenocarcinoma (PC-3), and human breast cancer cell line (MDA-MB231).

Studies were carried out to decipher the mechanisms governing inflammatory responses-mediated cancer metastasis. Our results have uncovered that cancer cells migrated out of the primary transplantation site – peritoneal cavity – *via* lymphatic system and CCR7/CCL21 pathways. Upon entering the circulation, cancer cells navigated to the inflammatory tissue *via* CXCR4/CXCL12 pathway. Rather surprisingly, we found that lymphocytes play an important role in cancer cell migration to inflamed tissue. Such lymphocyte-associated cancer cell migration is mediated, at least partially, by RANTES.

Based on the results obtained from previous work, we have been working on the development of two novel strategies to reduce cancer metastasis. First, using scaffolds to release different chemokines, we tested the influence of chemokine release on cancer cell recruitment. Interestingly, we found that erythropoietin (EPO) -releasing scaffold not only attracts more cancer cells immigrating to the implant area but also prolongs the animal survival duration. On the other hand, the stromal cell-derived factor-1 alpha (SDF-1 α) releasing scaffolds had no significant influence on cancer cell migration. The second approach was aimed to study the potential effect of vascular permeability on cancer cell migration. The feasibility of this approach is supported by the fact that localized release of histamine significantly increases

the numbers of recruited cancer cell to the implantation sites. Since mast cells are the main source of histamine, we further tested the influence of mast cell inactivator/stabilizer (cromolyn) on cancer cell recruitment. Indeed, cromolyn substantially reduced the cancer cell recruitment to the subcutaneous implants. It is our belief that this novel inflammation-induced cancer metastasis model along with *in vivo* imaging systems using either exogenous or endogenous labeling methods should be able to perform high throughput screening of different categories anti-inflammatory drugs for cancer therapy.

TABLE OF CONTENTS

ACKNOWLEDGEMENTS	iii
ABSTRACT	iv
LIST OF ILLUSTRATIONS.....	xi
LIST OF TABLES	xv
Chapter	Page
1. INTRODUCTION.....	1
1.1 Cancer metastasis	1
1.1.1 Mechanisms of cancer metastasis.....	1
1.1.2 Roles of inflammatory responses on cancer metastasis	3
1.1.3 Animal models of human cancer metastasis	4
1.2 Biomaterials-triggered inflammatory responses.....	5
1.2.1 Mechanisms	6
1.2.2 Property of biomaterials affects inflammatory responses	7
1.3 <i>In vivo</i> tracking of cancer cell migration	8
1.3.1 Overview of <i>in vivo</i> imaging	8
1.3.2 Limitation of monitoring cancer cell migration.....	10
1.4 Overview of research project	10
1.4.1 Innovative aspects	11
1.4.2 Successful outcome of the project.....	11
2. INFLUENCE OF LOCALIZED INFLAMMATORY RESPONSES ON CANCER CELL MIGRATION.....	12
2.1 Rationale	12
2.2 Materials and preparation	12

2.2.1 Materials.....	12
2.2.2 PLA microspheres preparation	13
2.2.3 Cancer cell types and culture condition	14
2.2.4 Animal implantation.....	14
2.2.5 Histological evaluation	16
2.2.6 Cancer cell labeling for cell tracking	17
2.2.7 Cancer cell migration imaging.....	17
2.2.8 Statistical analyses.....	18
2.3 Results	18
2.3.1 Reduced inflammation decreases tumor cell immigration	18
2.3.2 Material tissue reactivity dictates the degree of cancer cell recruitment	21
2.3.3 Tumor cells preferentially accumulated n the inflamed tissue	24
2.3.4 <i>In vivo</i> biodistribution of different types of cancer cells.....	31
2.4 Discussion.....	36
2.5 Conclusion.....	37
3. ROLE OF CYTOKINES/CHEMOKINES ON CANCER METASTASIS.....	38
3.1 Rationale	38
3.2 Materials and preparation	38
3.2.1 Materials.....	38
3.2.2 Fabrication of PLA microspheres.....	39
3.2.3 Cancer cell type and culture.....	39
3.2.4 Neutralizing antibody treatment	39
3.2.5 Histological evaluation	40
3.2.6 Cell imaging and quantification	40
3.2.7 Protein extraction from tissue sections	40
3.2.8 Protein array analysis.....	41

3.2.9 Cancer cell migration imaging.....	42
3.2.10 Statistical analyses.....	42
3.3 Results	42
3.3.1 Molecular pathway associated with inflammation-mediated cancer migration	42
3.3.2 Involvement of inflammatory cytokines in inflammation-associated cancer migration	48
3.3.3 Discovery of the role of RANTES in inflammation-mediated B16F10 melanoma migration	49
3.4 Discussion.....	54
3.5 Conclusion.....	57
4. STRATEGIES TO REDUCE CANCER PROGRESSION.....	58
4.1 Rationale	58
4.2 Materials and preparation	59
4.2.1 Materials.....	59
4.2.2 Preparation of chemokine-releasing PLGA scaffolds	59
4.2.3 Cancer cell type and culture condition	60
4.2.4 Scaffold implantation	60
4.2.5 Pharmaceutical treatment	60
4.2.6 Histological evaluation	61
4.2.7 Cell imaging and quantification	61
4.2.8 Cancer cell migration imaging.....	61
4.2.9 Statistical analyses.....	61
4.3 Results	61
4.3.1 Cancer cell recruitment to chemokine-releasing scaffolds	61
4.3.2 Substantial release of histamine from scaffold implants enhance cancer cell accumulation	65
4.3.3 Effectiveness of mast cell stabilizer on cancer cell extravasation	68

4.4 Discussion	69
4.5 Conclusion.....	71
5. SUMMARY AND FUTURE WORK	73
APPENDIX	
A. INFLAMMATORY CYTOKINE EXPRESSION PROFILE	76
REFERENCES.....	79
BIOGRAPHICAL INFORMATION	90

LIST OF ILLUSTRATIONS

Figure	Page
<p>1.1 Five basic steps involved in cancer metastasis. After primary tumor formation, cancer could progress via invasion, intravasation, survival in blood circulation, extravasation to the distal tumor site and finally colonize to form the secondary tumor. In our animal model, the research is focused on intravasation, circulation, and extravasation</p>	2
<p>2.1 Schematic procedure of induced subcutaneous inflammation in triggering migration of intraperitoneal transplanted cancer cells in C57BL/6J mice</p>	15
<p>2.2 Immunohistochemical staining of subcutaneous tissues surrounding the PLA microspheres with or without the treatment of dexamethasone (Dex). The accumulation of inflammatory cell (CD11b+) in tissue implanted with (a) PLA microspheres or (b) PLA microspheres soaked with dexamethasone can be observed (200X). The recruitment of melanoma cells (HMB45+) was also observed in tissues placed with (c) PLA microspheres or (d) dexamethasone soaked PLA microspheres (400X).....</p>	19
<p>2.3 Quantification of the numbers of inflammatory cells and melanoma cells in the subcutaneous tissues with/or without Dex treatments</p>	20
<p>2.4 Extent of foreign body responses and melanoma cell recruitment to different implants. (a, b, c) The degree of foreign body reactions and the accumulation of CD11b+ inflammatory cells and (d, e, f) HMB45+ melanoma cells surround the implant were quantified by immunohistochemistry. Materials tested are PLA, aluminum hydroxide and glass beads illustrated in the panels from top to the bottom.</p>	22
<p>2.5 Recruited melanoma cell number and CD11b positive cell number in surrounding tissue of implanted microspheres has a good linear correlation ($R^2=0.9197$).....</p>	23
<p>2.6 Fluorescence labeling of B16F10 cells with (a) X-Sight 761 Nanospheres, (b) Qtracker® 800 quantum dot or (c) nothing as negative control. Exposure condition based on manufacturer recommended condition</p>	24
<p>2.7 <i>In vitro</i> detection of X-Sight 761 Nanospheres-loaded B16F10 melanoma cells. Quantified fluorescence intensity values versus number of NIR probe labeled-cells per well. Error bars represent standard deviation for triplicate measurement</p>	25

2.8 <i>In vivo</i> detection of X-Sight 761 Nanospheres-primed B16F10 cells.	
(a) Intensity map of subcutaneously injected cells at four different concentrations.	
(b) Fluorescence intensity detected from each injection spot versus cell number.	
Error bars represent standard deviation for measurements made in three mice	26
2.9 (a) <i>In vivo</i> imaging detection on X-Sight labeled B16F10 cell migration	
in animals implanted with PLA microspheres for different implantation	
duration (1 day , 7days). (b) Confirmation of <i>in vivo</i> imaging detected	
X-Sight labeled B16F10 recruitment to the PLA microspheres implant	
for different duration by immunohistochemistry staining. (c) Quantification	
of <i>in vivo</i> imaging signal intensity detected was measured by ImageJ	
image processing program (left). HMB45 + cell quantification	
was illustrated (right). (n=1)	28
2.10 <i>Ex vivo</i> imaging of X-Sight-labeled B16F10 cell biodistribution	
in animal bearing with 1- day PLA implant.	
(a) Animal transplanted with B16F10 without labeling serves as a control.	
(b) Organs were positioned as illustration.	
P/MM represents pancreas and mesenteric membrane area	29
2.11 <i>Ex vivo</i> imaging of X-Sight-labeled B16F10 cell biodistribution	
in animal bearing with 7- day PLA implant.	
(a) Animal transplanted with B16F10 without labeling serves as a control.	
(b) Organs were positioned as illustration.	
P/MM represents pancreas and mesenteric membrane area	30
2.12 Lewis lung cancer cell (LLC) recruitment to the PLA implant area.	
Animal bearing PLA implant transplanted with non-labeling	
LLC cells served as control	31
2.13 Human prostate cancer cell (PC-3) recruitment to the PLA implant area.	
Animal bearing PLA implant transplanted with non-labeling	
PC-3 cells served as control	32
2.14 Rat prostate cancer cell (JHU-31) recruitment to the PLA implant area.	
Animal bearing PLA implant transplanted with non-labeling	
JHU-31 cells served as control	32
2.15 Human breast cancer cell (MDA-MB231) recruitment to the PLA implant area.	
Animal bearing PLA implant transplanted with non-labeling	
MDA-MB231 cells served as control	33
2.16 <i>Ex vivo</i> analysis of imaging intensity detected from each organ	
to illustrate biodistribution of different cancer cell types.	
LN represents 3 pairs of lymph nodes gathered from neck,	
axilla and inguinal regions. P/MM represents pancreas and	
mesenteric membrane regions. Cavity represents the signal	
detected from body cavity which was removed with internal organs. (n=3)	35
3.1 Treatment of AMD3100, antagonist of SDF-1 α receptor-	
CXCR4 treatment drastically reduced the recruitment of	
both melanoma cells and inflammatory cells to the	

subcutaneous PLA microsphere implantation sites. (n=4, *p<0.05, t-test)	44
3.2 Treatment of AMD3100 exerted no effect on the accumulation of melanoma cells in axillary lymph nodes	45
3.3 Treatment of CCL21 neutralizing antibody to block CCR7/CCL21 pathway drastically reduce the presence of B6F10 melanoma in axillary lymph nodes. (n=4, *p<0.05, t-test)	46
3.4 Treatment of CCL21 neutralizing antibody had no effect on the number of tumor cells migration to microsphere implantation site	47
3.5 (a) Effect of RANTES neutralizing antibody treatments on the recruitment of B16F10 melanoma to the microsphere implantation site by <i>in vivo</i> imaging. (b) The quantified intensity signals detected in RANTES neutralizing antibody treated animals are reduced by 2-fold. (n=2)	51
3.6 Quantification of HMB45+ B16F10 melanoma cells accumulated surround PLA implant area using immunohistochemistry staining. Blockage of RANTES expression diminished cancer cell recruitment to the inflamed area by 2-fold. (n=2)	52
3.7 Quantification of CD3+ lymphocytes recruited to PLA implant area using immunohistochemistry staining. Blockage of RANTES expression diminished lymphocyte accumulation to the inflamed area by 2-fold. (n=2)	53
4.1 Effect of localized release of SDF-1 α and EPO on cancer cell recruitment. Following transplantation for 24 hours, the distribution of X-Sight-labeled B16F10 cells was then monitored using whole-body imaging system. B16F10 cells were recruited to the variously treated scaffolds. (n=2).....	62
4.2 Effect of localized release of SDF-1 α and EPO on cancer cell recruitment. Following transplantation for 24 hours, the distribution of X-Sight-labeled B16F10 cells was then monitored using whole-body imaging system. B16F10 cells were recruited to the variously treated scaffolds. The implant-associated fluorescence intensities were then quantified using by ImageJ software. (n=2)	63
4.3 The survival duration of animals implanted with EPO-releasing, SDF-1 α -releasing, or control scaffolds. EPO group not only attract more cancer cell recruitment but also maintain the survival days and even last slightly longer than the control group. On the other hand, SDF-1 α group had shorter period of survival days. (n=3)	64
4.4 Histamine-releasing scaffolds significantly enhanced the recruitment of B16F10 melanoma cells to the implant area at different time points as shown in images.....	65

4.5 Histamine-releasing scaffolds significantly enhanced the recruitment of B16F10 melanoma cells to the implant area at different time points as shown in images. The signals were quantified to express the magnitude of recruitment as compare to control group. (n=2)	66
4.6 Localized release of histamine slightly reduces the survival of cancer cell bearing mice by compared with mice with control PLGA scaffold. (n=3)	67
4.7 Cromolyn treatment reduced about 30% B16F10 melanoma recruitment to the implant site. <i>In vivo</i> imaging was detected and the images were quantified by ImageJ processing program	68
5.1 General view of mechanisms involved in inflammation-mediated cancer metastasis. B16F10 melanoma cells may migrate through lymphatic system via CCR7/CCL21 pathway. Cancer cells then may go from lymphatic system to the blood circulation and reach to the implant area. On the other hand, CXCR4/CXCL12 pathway is involved in cell migration from peritoneal cavity to the implant site. Furthermore, lymphocyte plays a role in assisting cancer cell migration in response to inflammatory stimulus. Finally, RANTES secreted from implant site is related to lymphocyte associated cancer cell migration while other cytokines expressed from implant site such as MIP-1 α , MCP-5, IL-12p40/p70, IL-17, and eotaxin may be potent chemokines to affect cancer cell migration.....	75

LIST OF TABLES

Table	Page
1.1 Relative inflammatory cytokine expression in biomaterial-mediated inflammation	48

CHAPTER 1

INTRODUCTION

1.1 Cancer metastasis

Cancer metastasis is the major cause of lethality in cancer patients. Cancer develops when abnormal cells divide without appropriate control and further progress to invade other tissues. These cells can sometimes spread out from the primary site to distal organs through lymphatic systems and/or blood circulation. They frequently spread to regional lymph nodes near the primary tumor. This phenomenon of spreading to certain parts of the body is a characteristic feature of malignant cancers. For instance, breast cancer commonly spreads to the bones, lungs, liver, or brain while lung cancer tends to metastasize to the brain or bones (1-3). Current treatments include chemotherapy, radiation therapy, biological therapy, hormone therapy, surgery or a combination of those listed above. The treatment usually depends on the type and size of cancer, metastasis condition, related age and the types of treatments the patient has had in the past (4-6).

1.1.1. Mechanisms of cancer metastasis

Since the majority of cancer mortality is attributed to the cancer metastasis rather than the primary tumor, the understanding of cancer metastasis is critically important for clinical management of cancer (7-11). Despite intensive research efforts, the detailed mechanism of cancer metastasis is not totally understood. According to National Cancer Institute, metastasis is defined as the spread of cancer from one area of the body to another. Cancer metastasis is considered deadly, mainly because it leaves almost no chance for surgical interception of cancer progression and very commonly multiple organ are involved (12). Many factors including inflammation, reactive oxygen species, angiogenesis and even genes have shown to be related

to cancer metastasis (9, 13-15). Metastasis is a sequence of the events which can be roughly divided into five consecutive steps: local invasion, intravasation, survival in the circulation, extravasation and colonization in distal tissue/organs (9, 16, 17) (Figure 1.1).

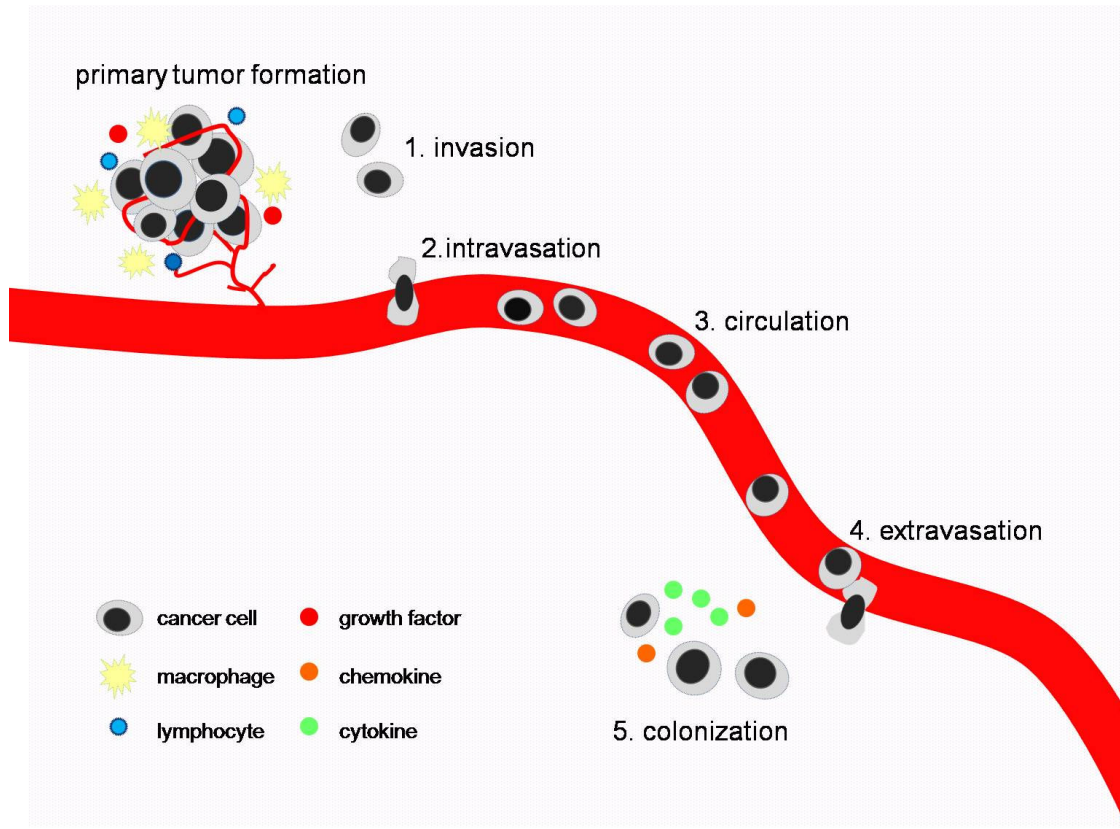


Figure 1.1 Five basic steps involved in cancer metastasis. After primary tumor formation, cancer could progress via invasion, intravasation, survival in blood circulation, extravasation to the distal tumor site and finally colonize to form the secondary tumor. In our animal model, the research is focused on intravasation, circulation, and extravasation

After infiltrating into distal organs, surviving cancer cells will form an aggressive colony and then damage the physiological function of organ. Thus, primary tumor cells must accomplish infiltration and colonization so as to metastasize to distant organs. The composition of each organ and the barriers against infiltration are unique. This is the reason why different tumor types may cause various organ metastases since infiltration and colonization functions

are acquired over variable periods of time (9). In light of cancer metastasis studies, the sentinel lymph node, also known as the first lymph node(s), is responsible for collecting lymphatic drainage from the site of the primary tumor. It is also the place where immunoreactive lymphocytes come in contact with cancer antigens and develop anti-cancer immunity. A growing body of evidence has supported the correlation of sentinel lymph node micrometastasis with a variety of solid tumors. Recent studies have shown that cancers not only induce lymphangiogenesis but also promote sentinel lymph node metastasis (18). The immune suppression of the sentinel lymph node may cause failure to prevent or eradicate tumor metastasis (18), since immunosuppression of a subset of T cells: regulatory T cells (Tregs) may impair their anti-tumor immunity (19).

1.1.2. Roles of inflammatory responses on cancer metastasis

It has been recognized for decades that there are strong associations between chronic inflammatory conditions and tumorigenesis (20, 21). Many recent works also implicate inflammatory products in the promotion of cellular changes leading to the uncontrolled growth of cancer cells (21-23). In addition, inflammatory stimuli have been shown to facilitate the escape of metastatic cells from the original tumor and aid in the spread to new tissue sites (21- 23). These implications are supported by many recent observations that infiltration with inflammatory cells and macrophages promotes both the development of breast cancers and their eventual spread to other sites in the body (24). Furthermore, an increasing body of evidence suggests that inflammatory responses play an important role in tumor development and progression (11, 21, 22, 25-27). For example, inflammatory chemokines, such as CXCR4/CXCL12, CCR7/CCL21, MIP-1 α /CCL3, IL-8/CXCL8 and RANTES/CCL5, have been associated with metastasis of breast cancer, melanoma, myeloma, colorectal carcinoma, ovarian carcinoma and non small cell lung cancer (28-33). Human and murine tumors are also found to secrete various inflammatory cytokines, CXC chemokines and their receptors (32, 34-37). Expression of inflammatory chemokine receptors such as CXCR4 and CCR7 are commonly found in human

breast cancer (38). CCR7 has also been demonstrated to dramatically increase metastasis of B16 murine melanoma to regional lymph nodes (39). Colorectal cancer cells are found to express chemokine receptor/ ligand such as CCR6/CCL20 and respond to chemokine gradients similar to leukocyte and monocytes inflammatory cells (40). Interestingly, many chemokine ligands, such as CXCL12 for SDF-1 and CCL21 for SLC (secondary lymphoid tissue chemokine), are highly expressed in the target organs of breast cancer metastasis (31, 38, 41, 42). Furthermore, recent studies have demonstrated that lymphocytes may play contradictory roles in tumor progression. Tumor-specific cytotoxic T cells may eliminate tumor cells by direct or antibody-dependent cell killing. On the other hand, the recruited regulatory T cells have been shown to mitigate the cytolytic ability of cytotoxic T cells so as to blunt the immune response (43, 44). During the development of breast cancer, increased leukocytes in neoplastic stroma were associated with tumor progression. It was demonstrated that IL-4-expressing CD4+ T lymphocytes promote mammary adenocarcinoma invasion and metastasis (45). However, the effect of T lymphocyte on the inflammation-induced cancer migration is still not clear. Part of this research effort is to determine the potential role of T lymphocytes on cancer metastasis. In addition, non-steroidal anti-inflammatory drugs were demonstrated to reduce both the chance of cancer development and mortality (46). Hence, the interplay of the inflammatory response on cancer metastasis is critically important.

1.1.3 Animal models of human cancer metastasis

Several *in vitro* and *in vivo* models have been used to assess human cancer metastasis. Animal tests are the gold standard for examining tumor progression due to the simplicity and ineffectiveness of *in vitro* model in studying the entire metastatic process. The majority of metastasis studies have been carried out in rodents with tumor xenograft (47-50). Typically, a tumor cell line known to metastasize *in vivo* is manipulated to change the expression or mutation status of a single gene. This in turn determines the manipulated gene function in the process of metastasis (51-53). Various animal models, such as

intravenous/intracardiac models, subcutaneous models and orthotopic implantation models are commonly used for these studies. Intravenous/ intracardiac routes were used to directly introduce cancer cells to tested animals. Subsequent metastasis evaluation was then conducted by quantifying tumor growth in vital organs following the injection of tumor cells into the bloodstream (54-56). However, the first three steps of metastasis could not be examined in these methods. In addition, intravenous/intracardiac administration of a large amount of cancer cells all at once is not similar to the flow of the metastatic cancer cells disseminating slightly but continually (57). On the contrary, subcutaneous and orthotopic models are more accurate at imitating all the five processes of cancer metastasis. Although these assays measure the whole metastatic processes, the methods are usually qualitative and time consuming (58, 59). Apart from the methods described above, it should also be noted that several transgenic mouse strains have been used to study primary tumorigenesis and spontaneous metastases (59-62). A significant disadvantage of these systems, however, is the time, cost, and lack of versatility. Therefore, a new animal model is needed to quantitatively analyze the migration/metastasis of cancer cells in vivo. Another goal of this project is to develop a precise, accurate and quantitative method portraying the steps of cancer metastasis.

1.2 Biomaterials-triggered inflammatory responses

Shortly after implantation, medical devices are often surrounded with substantial numbers of phagocytes. The interaction between phagocytes and biomaterials activate adherent phagocytes and may lead to chronic inflammation and fibrotic reactions (63-65). Before the arrival of inflammatory cells, biomaterial implants very quickly acquire a layer of host proteins. Thus, it is widely accepted that phagocytes interact with the spontaneously adsorbed proteins (63, 65, 66). Studies have shown that adsorbed fibrinogen is primarily responsible for the accumulation of phagocytes on implant surfaces (66). In fact, later studies have revealed that adsorbed fibrinogen resembles fibrin and phagocytes recognize the biomaterial implant as

a fibrin clot (63). In the process of foreign body reactions, many pro-inflammatory cytokines and chemokines, including TNF- α , IL-6, IL-1, MIP-1 α , and MCP-1 β , are secreted (63, 67). The release of these chemokines/cytokines may modulate phagocyte and other cellular responses.

1.2.1 Mechanisms

Biomaterials implanted into the body elicit a sequence of localized inflammatory and immune responses surrounding the implant. Within a few hours after implantation, most biomaterials cause accumulation of leukocytes on implant surfaces. Various leukocytes, such as monocyte, macrophages, polymorphonuclear leukocytes (PMN), and lymphocytes participate in host inflammatory and immune responses (68). Activated macrophages could produce a variety of inflammatory cytokines such as tumor necrosis factor- α (TNF- α), interleukin 1 β (IL-1 β), macrophage inflammatory protein-1 α (MIP-1 α), monocyte chemoattractant protein 1 (MCP-1), interleukin-6 (IL-6), and interleukin-8 (IL-8) (69). These inflammatory factors prompt the recruitment of inflammatory cells which are critical to the long term reactions of biomaterial implants (63, 67). The mechanisms of biomaterial-mediated inflammatory responses were divided into three events including: (i) phagocyte transmigration through the endothelial barrier, (ii) chemotaxis toward the implant, and (iii) phagocyte adherence to implant surfaces (70). Earlier results have shown that interaction between the phagocyte integrin, Mac-1, and surface fibrinogen is critical for phagocyte adherence to implants. Adsorbed fibrinogen on the biomaterial surface is primarily responsible for the accumulation of phagocytes surrounding the implant. Phagocytes may recognize fibrinogen adherent to medical implants as fibrin and respond by launching a series of inflammatory and wound healing responses commonly initiated by fibrin clot formation (71). In addition, mast cells and released histamine are also shown to be important to the recruitment of inflammatory cells during biomaterial-mediated inflammatory responses (70). In many circumstances, adhesion molecule receptors in circulating leukocytes up-regulated during inflammatory responses allow leukocyte binding to

endothelial adhesion molecules. Ligands such as the integrin Mac-1 (CD11b/CD18) which recognize intercellular adhesion molecule-1 (ICAM-1) on the endothelial surface are exposed at the surface of phagocytes (68).

1.2.2 Property of biomaterials affects inflammatory responses

Early studies have indicated that surface chemistry, topography and even the degradation products released from biomaterials affect tissue responses (72-74). Increasing efforts have been made to modify material surfaces for better biocompatibility. Techniques such as physical/chemical modifications and radiation have been developed to modify material surface properties (74). Surface wettability is one of the important parameters affecting protein-surface interactions. It is well established that hydrophobic surfaces tend to increase protein adsorption and denaturation. In turn surface wettability mediates adsorption kinetics and binding strengths, as well as subsequent protein activity (75-78). Denatured proteins (especially fibrinogen) subsequently trigger inflammatory cell adhesion and activation (71, 79, 80). It is generally believed that the hydrophobic properties of polymers are responsible for protein denaturation and subsequent cellular responses (71, 81). To increase surface hydrophilicity, polyethylene glycol (PEG), poly (2-hydroxyethyl methacrylate), poly (N-isopropyl acrylamide), poly (acrylamide), and phosphoryl choline-based polymers were thus invented and shown to resist protein adsorption. Despite the intensive studies on the effects of wettability exerted on biocompatibility, the development of hydrophilic surface coating techniques has not led to production of biocompatible medical implants (80, 82, 83). Other parameters such as surface topography have similarly been shown to affect implant performance. Surface topography is known as one of the major determinants that influence cell behavior in various ways including cell adhesion, selection, mechanical interlocking, topographic guidance, tissue organization and production of growth factors and cytokines (84, 85). In addition, wear fragments or degraded products released from biodegradable polymers also affect the tissue reaction to the implant.

For example, the number of poly-L-lactic acid (PLA) microspheres and monomers degraded from a biomaterial *in vivo* correlate with the degree of the inflammatory response. Both soluble and insoluble material fragments were indicated to influence subsequent adverse cellular reactions (73).

1.3 *In vivo* tracking of cancer cell migration

Many imaging methods have been developed recently to study cancer growth and metastasis in animals and humans. Imaging tools such as magnetic resonance imaging (MRI), ultrasonography, nuclear imaging, microtomography and optical imaging using fluorescence and bioluminescence can be used for tumor related studies (86). Among these methods, optical imaging draws particular attention to the cancer metastasis field. This method allows for effective detection of endogenously produced fluorescence and bioluminescence from animals *in vivo*, as well as being cost-effective and time-efficient (87). It also allows longitudinal monitoring in a single animal and thus reduces the number of experimental animals without compromising statistical significance (88). With the advances in cancer imaging, part of this research effort was devoted to develop an imaging method to quantitatively monitor cancer migration under inflammatory induction.

1.3.1 Overview of in vivo imaging

Several conventional imaging utilities such as magnetic resonance imaging (MRI), computed tomography (CT), and photon emission tomography (PET) were designed and fully developed for clinical application (89). In cancer research, it is necessary to combine different technologies from both molecular and optical imaging to determine the effects of newly found genes or developed intervention on cancer progression. Methods such as flat-panel volumetric computed tomography (fpVCT) are utilized in preclinical cancer research for the noninvasive study of tumor growth, vascularization, and metastasis screening. Using this technology, targets

tagged by molecular probes can be observed on the cellular and subcellular level and analyzed using near infrared laser based total body scanners. However, the resolution of these established methods are not high enough to visualize very small vessels, supplying the tumor. Other complementary near infrared based techniques and related fluorochromes/ dyes are now available to study molecular pathways or pharmacological treatments on cancer study (90, 91). Near infrared based animal imaging detection relies on nonionizing radiation (typically a low-intensity laser) which causes the tissue to emit a signal captured by a high-sensitivity photon detector in combination with a CCD camera-based setup. The advantage of this imaging system is a more accurate measurement of the effect of intervention, disease progression, and outcomes *in vivo* (91). For the purpose of cell tracking *in vivo*, optical imaging is also an appealing system with minimal fluorescence background in the near-infrared (NIR) range yielding excellent signal-to-noise ratios compared to other fluorescence based imaging. With advancing developments in optical imaging techniques now range from fluorescence reflectance imaging to fluorescence-mediated tomography approaches (92). Compared to NIR fluorescence, bioluminescence imaging eliminates background signal from the animal tissues and exhibits very specific signals originated from the targets. Recently, a new generation of firefly (*Photinus pyralis*) luciferase was engineered to deliver more than a four-fold increase in light emission (93, 95). Cancer cells genetically engineered with this type of luciferase reporter can be effectively used to screen for agents against metastasis in orthotopic tumor models. For quantification purposes, tumor growth has been assessed traditionally by calipers for subcutaneous tumors growth in animals (94, 95). However, this measurement method is only for palpable tumors found subcutaneously in the animals. Other tumor masses tested in different locations are not amenable to direct physical measurements. Therefore, application of the bioluminescence reporter approach for tumor growth detection in real-time may be a simple and effective solution to the problem addressed above. Overall, the rapid development of optical imaging technologies is likely to greatly facilitate both cancer research and therapy (95).

1.3.2 Limitation of monitoring cancer cell migration

There are many limitations associated with *in vivo* cancer imaging. First, some imaging technologies (such as flat-panel volumetric computed tomography, MRI) cannot be used for long term cancer monitoring due to the toxicity of contrast media used in those analyses (91). Second, despite of recent progress, little has been done to create an *in vivo* imaging system to monitor and quantify cancer metastasis. To fill this gap, one of the research goals is to establish a systemic analysis to mend the unresolved issues in evaluation of cancer migration *in vivo*. Based on the knowledge gained from these research results, we were able to develop novel anti-cancer treatments so as to enhance the survival rate in metastasized cancer patients.

1.4 Overview of research project

Based on the results of recent studies, we have hypothesized that localized inflammatory responses may prompt the recruitment of cancer cells to the implantation site. To test this hypothesis, we carried out three series of studies. Specifically,

Study 1 - Influence of localized inflammatory responses on cancer recruitment. Using biomaterials that prompt different extents of inflammatory responses, the influence of implant-associated inflammatory responses was studied. The migration of various cancer cells, including B16F10 melanoma cells, Lewis lung carcinoma cell line (LLC), rat prostate cancer cell line (JHU-31), human prostate adenocarcinoma (PC-3), and human breast cancer cell line (MDA-MB231) were determined. Using various cell-labeling agents, luciferase gene-transduced cells, and whole body imaging system, studies were designed to visualize the sequence of events during cancer cell migration in response to subcutaneous foreign body reactions.

Study 2 - Role of cytokines/chemokines on cancer metastasis. Using various biomaterials, drugs, antagonists, antibodies, cancer cell lines and animal breeds with different immunity status, studies were carried out to identify the possible candidate molecules and cell types involved in cancer metastasis.

Study 3 - Development of novel strategies for reducing cancer metastasis. Based on the results from above studies, different strategies and agents were tested to reduce cancer metastasis.

1.4.1 Innovative aspects

There are several novel methods developed in this project. The first novel achievement is the development of an animal model for inflammation-related metastasis study by biomaterial application. The second innovation is the establishment of an optical detection method to monitor cancer cell migration. The third innovative aspect is the discovery of chemokine-related pathways in our animal model through establishment of inflammatory chemokine expression profiles. The fourth novel aspect is the application of factor -releasing scaffolds for the treatment of cancer metastasis. These novel aspects provide a new window for both basic cancer research and pharmaceutical screening.

1.4.2 Successful outcome of the project

A successful outcome of the project is to provide a new method to study inflammatory vs. immunity balance on cancer progression. Imaging detection systems based on this project could be used for other disease models. Results from chemokine-releasing scaffolds may lead to the development of novel cancer treatment(s).

CHAPTER 2
INFLUENCE OF LOCALIZED INFLAMMATORY RESPONSES
ON CANCER CELL MIGRATION

2.1 Rationale

Previous results have indicated that inflammatory responses promote cancer cell migration (96). Our preliminary results support this statement showing that biomaterial-mediated inflammatory responses prompt cancer cell migration similar to cancer metastasis. However, whether cancer cells preferentially migrate to the implant area and the possible pathways involved in the process were not clear. For the further investigation, three series of studies were proposed. First, we tested the influence of inflammatory products on the recruitment of B16F10 cancer cells. Second, using materials with different proinflammatory properties, we examined the influence of inflammatory responses on the degree of cancer cell immigration. Finally, different types of cancer cells were used to test whether this metastasis model can be used to study the metastasis of different cancers. With application of *in vivo* imaging technology, cancer cell migration was also monitored to illustrate a general blueprint of cancer cell migration under inflammation stimulation.

2.2 Materials and preparation

2.2.1 Materials

Dulbecco's modified Eagle's media (DMEM), bovine serum albumin, dexamethasone (Dex) and diaminobenzidine (DAB) enhanced liquid substrate system were purchased from Sigma Aldrich (St. Louis, MO). Fetal calf serum (FCS) was purchased from Atlanta Biologicals (Lawrenceville, GA). Mouse monoclonal antibodies against melanoma HMB45 was purchased from Abcam (Cambridge, MA). Rat anti-mouse CD11b antibody was obtained from Serotec Inc.

(Raleigh, NC). Secondary antibodies goat-anti-mouse (HRP-conjugate) was obtained from Jackson ImmunoResearch Laboratories (West Grove, PA). Kodak X-Sight 761 Nanosphere was purchased from Carestream Health Inc. (New Haven, CT). Poly (D, L-lactic-co-glycolic acid) (75:25) with a molecular weight of 113 kDa was purchased from Medisorb (Lakeshore Biomaterials, Birmingham, AL). The solvent dichloromethane was purchased from EMD Chemicals Inc. (Gibbstown, NJ). The surfactant poly vinyl alcohol was purchased from Sigma Aldrich (St. Louis, MO). Aluminum hydroxide (Alhydrogel 85), acquired from the Superfos Biosector A/S Corporation, with an average diameter of 10 micrometers. Glasperlen glass beads with an average diameter of 0.45-0.50 mm were purchased from the B. Braun Melsungen Corporation (Melsungen, Germany).

2.2.2 PLA microsphere preparation

To prompt various degrees of foreign body reactions, microspheres were used in the study. Aluminum hydroxide (Alhydrogel 85, average size: 10 μ m in diameter, Superfos Biosector A/S Corporation, Kvistgaard, Denmark) and glass beads (Glasperlen®, average size: 450-500 μ m in diameter, B. Braun Melsungen Corporation, Melsungen, Germany) were commercially available whereas PLA microspheres were synthesized according to a modified precipitation method (97, 98). In brief, 0.45 g of PLA was dissolved in 3 mL of dichloromethane to which 0.3 ml deionized water was added. The solution was vortexed for about 15 minutes to form the primary emulsion. Then, the primary emulsion was poured in to 6 ml of 2 % poly vinyl alcohol solution and vortexed to form the secondary emulsion. This secondary emulsion was then poured into a beaker containing 150 ml deionized water and stirred at room temperature. The PLA microspheres (average size: 6.07 \pm 2.12 μ m in diameter) were formed after solvent evaporation and washed twice by centrifugation. Finally, microspheres were freeze-dried and stored in dry form refrigerated (4 °C) until implantation. All microspheres were sterilized with 70% ethanol and then transferred to phosphate buffered saline (PBS, 100 mM, pH 7.4) prior to

experiments. For the dexamethasone treatment, PLA microspheres were soaked with the anti-inflammatory agent, dexamethasone (0.1 mg drug/0.5 ml microsphere suspension) prior to administration.

2.2.3 Cancer cell types and culture condition

B16F10 melanoma cells, Lewis Lung carcinoma (LLC) cells, rat prostate cancer cell line (JHU-31), human prostate adenocarcinoma (PC-3), and human breast cancer cell line (MDA-MB231) used in this investigation were purchased from American Type Culture Collection (ATCC) (Manassas, Virginia, USA). B16F10 melanoma cells are skin melanoma cell lines isolated from C57BL/6J mice. LLC cells isolated from C57BL/6J mice are widely used as a model for cancer metastasis. JHU-31 are derived from rat and exhibit a high rate of metastasis to the lung and lymph nodes (>75%). PC-3 cells originate from a 62-year-old male Caucasian with bone metastatic prostate adenocarcinoma. MDA-MB231 are derived from breast adenocarcinoma metastasized pleural effusion. All cell types were maintained in DMEM supplemented with 10% heat inactivated fetal bovine serum at 37°C, 5% CO₂ humidified environment.

2.2.4 Animal implantation

As an *in vivo* model to assess biomaterial-mediated inflammation and cancer metastasis (Figure 2.1), subcutaneous microsphere implants (75 mg/0.5 mL/animal) were injected in C57BL/6J mice (The Jackson Laboratory, Bar Harbor, ME) via 18 gauge needle under inhalation anesthesia with isoflurane (Abbott Laboratories, North Chicago, IL) (1-3%). To trigger varying extent of biomaterial-mediated inflammatory responses, animals were implanted with PLA microspheres for different periods of time (6 hours, 12 hours, 24 hours, 2 days, 1 week, and 2 weeks). Animals were intraperitoneally transplanted with cancer cells (5×10^6 /0.2

ml/animal) under anesthesia with isoflurane inhalation. At the end of the studies, animals were sacrificed, followed by isolation of implant and surrounding tissues for histological evaluation.

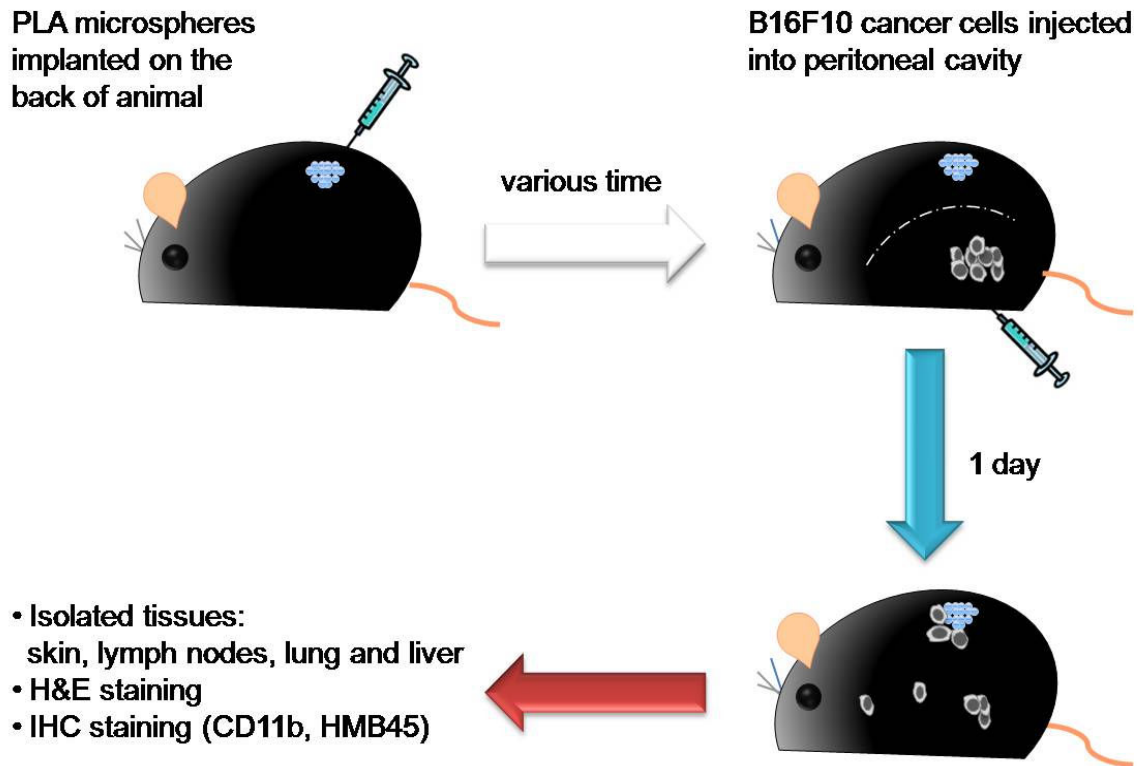


Figure 2.1 Schematic procedure of induced subcutaneous inflammation in triggering migration of intraperitoneal transplanted cancer cells in C57BL/6J mice.

2.2.5 Histological evaluation

To examine the recruitment of cancer cells and inflammatory cells to the implant area, tissues harvested from experiments were immediately embedded and sectioned for histological evaluation (H&E and immunohistochemistry staining). H&E staining was used for observing the biomaterial-mediated inflammation process. Immunohistological analyses for inflammatory cells and melanoma cells were carried out to assess the degree of implant-mediated inflammatory responses and cancer cell migration, respectively. Briefly, tissue sections were fixed in ice cold acetone (5 minutes), washed in PBS three times, and then dipped for 30 minutes in 0.3% hydrogen peroxide in phosphate-buffered saline (PBS) to quench endogenous peroxidase activity, washed twice for 5 minutes with PBS and incubated in 10% goat serum for 1 hour at room temperature. The sectioned tissues were then incubated with the primary anti-melanoma antibody (HMB45, 1:50 dilution, Abcam, Cambridge, MA, USA) or anti-mouse CD11b antibody (1:1000 dilution, Serotec Inc., Raleigh, NC, USA) for 1 hour at 37°C. After being washed thrice with PBS 5 minutes each, the slides were then incubated with HRP-conjugated secondary antibody (1:500 dilution ratios, Jackson ImmunoResearch Laboratories, West Grove, Pennsylvania, USA) for 1 hour at 37°C. HRP-conjugated antibody incubated sections were developed with a DAB liquid Substrate System (Sigma-Aldrich Inc., St. Louis, MO, USA). Counterstaining was performed with Mayer's hematoxylin. Control staining was performed by omission of the primary antibody and substitution with nonspecific serum at the same dilution.

To quantify cell recruitment, tissue section images were taken using a Leica fluorescence microscope (Leica Microsystems Wetzlar GmbH, Wetzlar, Germany) equipped with a QImaging Retiga-EXi CCD camera (QImaging, Surrey, BC, Canada). The tissue section images at a magnification of 400X (viewing area 0.24 mm²) were then used to quantify the cell numbers per view field by cell counter plugin of ImageJ processing program.

2.2.6 Cancer cell labeling for cell tracking

Three different bioluminescence or fluorescence-labeled cells were used in this investigation. For fluorescence detection method, cancer cells were labeled with Qtracker® 800 quantum dots (Invitrogen Corporation, Carlsbad, CA) or X-Sight 761 Nanospheres (Carestream Health Inc, New Haven, CT) according to the user manual and protocol listed in previous literature (67). Specifically, to label cells with Qtracker® 800, 10 nM labeling solution was made by pre-mixing 5 µL each of Qtracker® Component A and Component B and incubating the solution for 5 minutes at room temperature. Immediately, 1 mL of fresh complete medium was added to the labeling solution and vortexed for 30 seconds. 5×10^6 cells were then added to the labeling solution and incubated at 37°C for 45-60 minutes. After labeling, cells were washed twice with complete growth medium before imaging (excitation wavelength at 470 nm, emission wavelength at 790 nm, f-stop: 2.5, 120 mm field of view). In a separate study, cancer cells were labeled with Kodak X-Sight 761 Nanospheres according to the manufacture instructions (67). In brief, cancer cells at a state of ~60% confluence were incubated with complete medium with 5 µM of Kodak X-Sight 761 Nanospheres at 37 °C for 24 hours. Cells are then trypsinized and washed twice with PBS to remove excess nanospheres. Subsequently, cells at density of 5×10^6 cells/ 0.2 mL were detected at 760 nm excitation, 830 nm emission, 30 seconds exposure, f-stop 2.5, 120 mm field of view) to ensure cell labeling was successful for cell transplantation.

2.2.7 Cancer cell migration imaging

Before imaging detection, C57BL/6J black mice were depilated with hair removal lotion. Animals were placed in supine or prone position under anesthesia with isoflurane (1-3 %) inhalation. To demonstrate cell tracking using Qtracker® 800, *in vivo* imaging was configured at 470 nm excitation, 790 nm emission, exposure time 60 seconds, f-stop 2.5 and field of view (FOV) 120 mm by using Kodak In-Vivo Imaging System FX Pro (Carestream Health Inc, New Haven, CT). When imaging animal transplanted with X-Sight labeled cancer cells, the detection

was configured at 760 nm excitation, 830 nm emission, 60 seconds exposure, 4 × 4 binning, f-stop 2.5, and 120 mm FOV.

2.2.8 Statistical analyses

Statistical comparisons between different groups were carried out using Student t- test or one-way ANOVA. Differences were considered statistically significant when $p < 0.05$.

2.3 Results

2.3.1 Reduced inflammation decreases tumor cell immigration

To verify the importance of inflammatory responses in triggering cancer cell immigration, subcutaneous PLA microsphere implantations were carried out in the presence or absence of anti-inflammatory agent, dexamethasone. As expected, dexamethasone-incubated microspheres prompt substantially less inflammatory cell (CD11b+) recruitment than saline-incubated microsphere controls (Figure 2.2a, b). Coincidentally, the recruitment of B16F10 melanoma cells was also diminished with the treatment of dexamethasone (Figure 2.2c, d). The effects of locally released dexamethasone on the reduction of inflammatory cells and B16F10 melanoma cells are statistically significant (Figure 2.3). These results demonstrate and support the claim that inflammatory reactions are essential to initiating the cancer cell migration from the peritoneal cavity to the subcutaneous microsphere implantation sites.

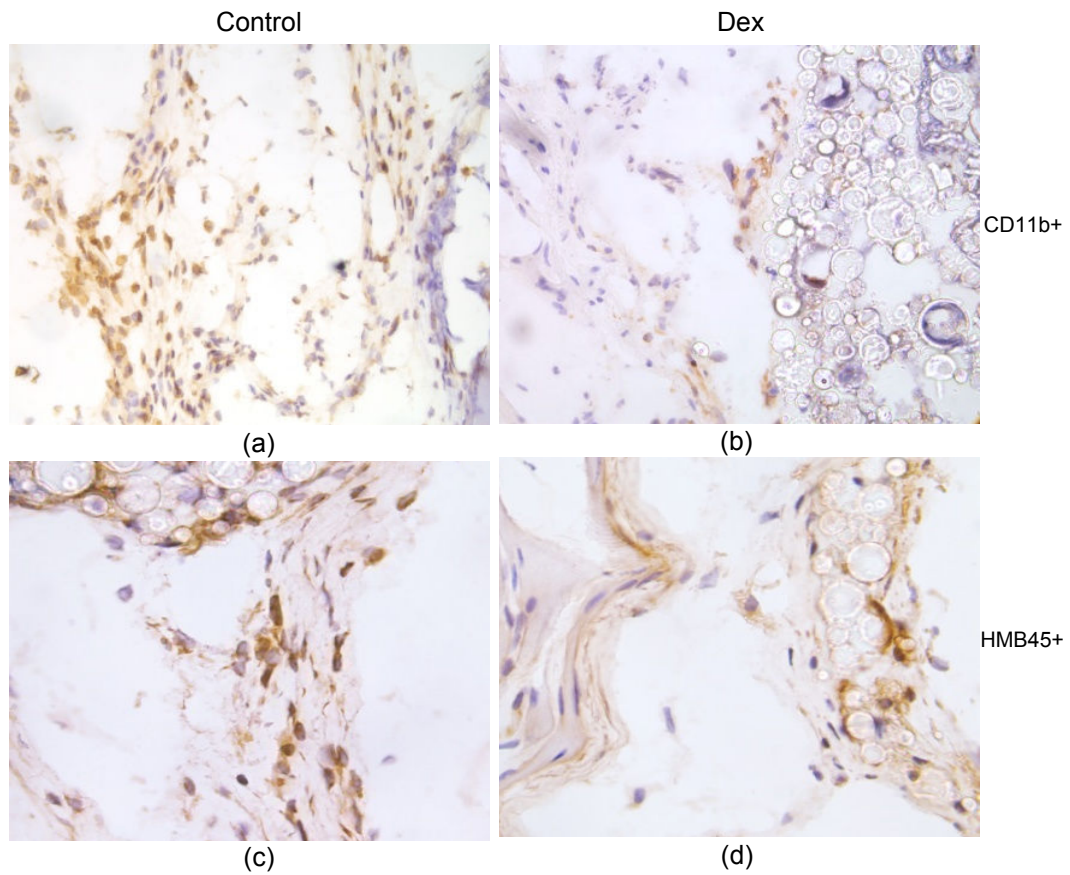


Figure 2.2 Immunohistochemical staining of subcutaneous tissues surrounding the PLA microspheres with or without the treatment of dexamethasone (Dex). The accumulation of inflammatory cell (CD11b+) in tissue implanted with (a) PLA microspheres or (b) PLA microspheres soaked with dexamethasone can be observed (200X). The recruitment of melanoma cells (HMB45+) was also observed in tissues placed with (c) PLA microspheres or (d) dexamethasone soaked PLA microspheres (400X).

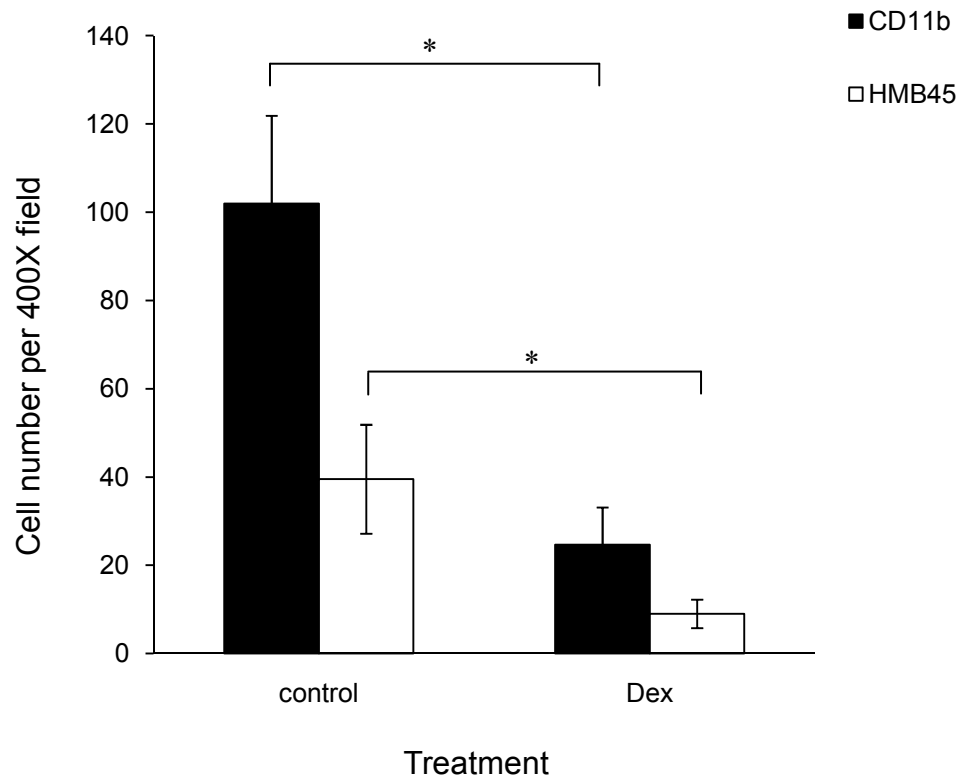


Figure 2.3 Quantification of the numbers of inflammatory cells and melanoma cells in the subcutaneous tissues with/or without Dex treatments.

2.3.2 Material tissue reactivity dictates the degree of cancer cell recruitment

Since biomaterial-mediated inflammatory responses affect cancer cell migration and various materials prompt different degrees of inflammatory reactions, it is likely that microspheres with different tissue biocompatibility will greatly influence melanoma cell recruitment. To test this hypothesis, microspheres made of poly L-lactide (PLA), aluminum hydroxide, and glass were tested. After implantation of the different microspheres for 24 hours, B16F10 cells were transplanted in the peritonea. Twenty four hours later, the microsphere implant and surrounding tissues were isolated and analyzed. As expected, these implanted microspheres trigger a different extent of inflammatory response and melanoma cell recruitment (Figure 2.4a, b, c). PLA microspheres were found to trigger more inflammatory cell and melanoma cell accumulation than microspheres made of aluminum hydroxide and glass materials (Figure 2.4d, e, f). By comparing the numbers of both cell types, our results show that there is a good correlation ($R^2=0.9197$) between the extent of inflammatory reactions (reflected by the accumulation of CD11b+ cells) and melanoma cell recruitment (Figure 2.5). These results lent strong support to our hypothesis that inflammatory responses play an important role in melanoma cell migration and, perhaps, metastasis.

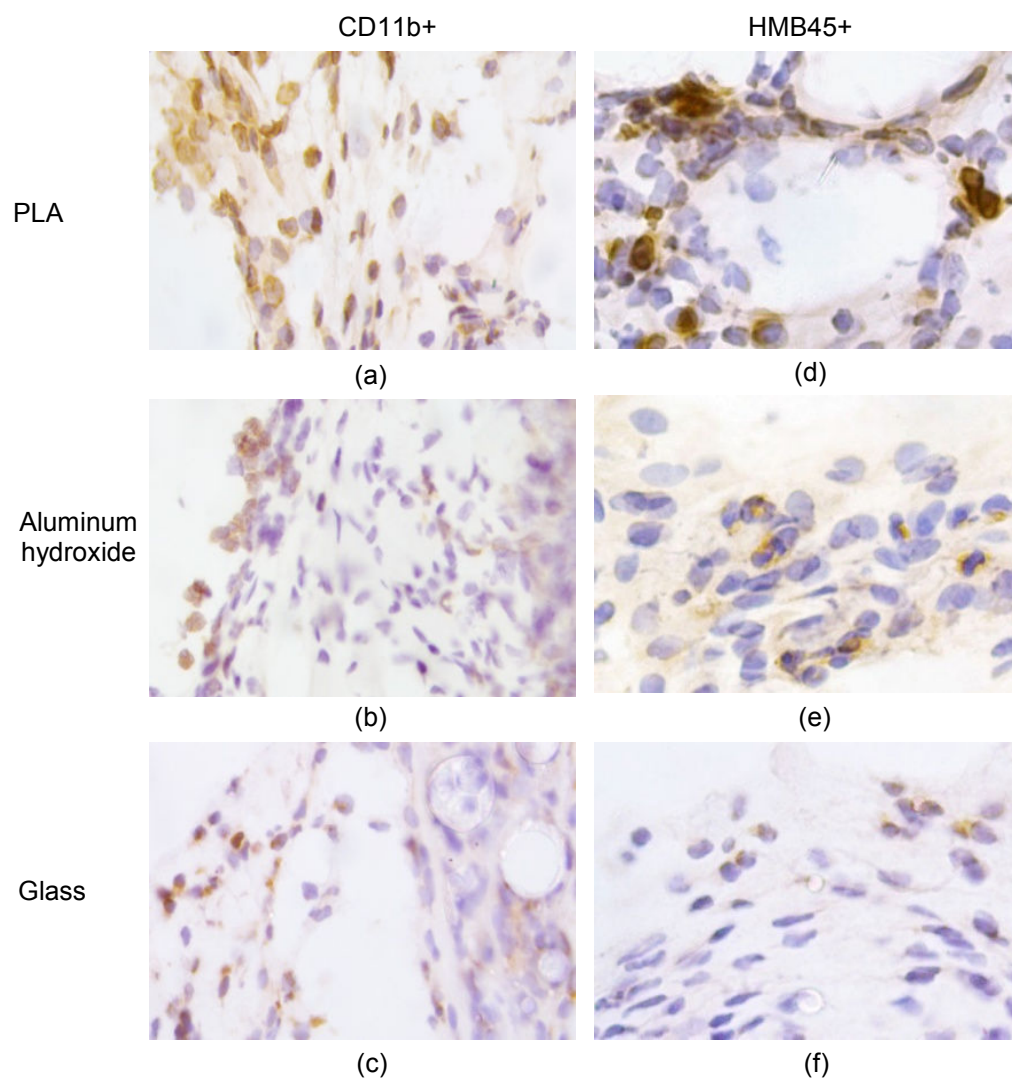


Figure 2.4 Extent of foreign body responses and melanoma cell recruitment to different implants. (a, b, c) The degree of foreign body reactions and the accumulation of CD11b+ inflammatory cells and (d, e, f) HMB45+ melanoma cells surround the implant were quantified by immunohistochemistry. Materials tested are PLA, aluminum hydroxide and glass beads illustrated in the panels from top to the bottom.

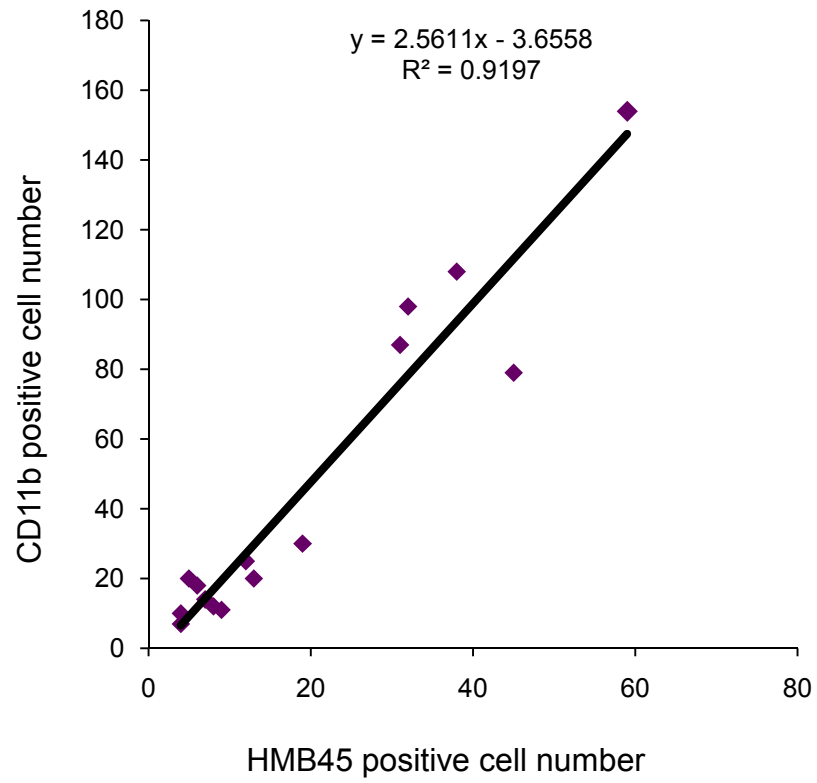


Figure 2.5 Recruited melanoma cell number and CD11b positive cell number in surrounding tissue of implanted microspheres has a good linear correlation ($R^2=0.9197$).

2.3.3. Tumor cells preferentially accumulated in the inflamed tissue

Although our histological results support the claim that localized inflammatory responses attract melanoma cell migration from the peritoneal cavity to the subcutaneous implantation site, it is not clear whether the inflamed tissue/microsphere implantation site is the only target for the immigrating melanoma cells. To confirm our previous results, we carried out two sets of studies, including whole body imaging and cancer cell biodistribution. Two near infrared agents, Kodak X-Sight 761 Nanospheres and Qtracker 800 were used to label cancer cells. Our studies have found that both agents are equally effective in labeling cells under Kodak In-Vivo Imaging System FX Pro detection (Figure 2.6). In addition, there is a linear relationship between cell numbers and fluorescence intensity *in vitro* (Figure 2.7). Furthermore, the relationship between fluorescence intensity and cell number was determined *in vivo*. For that, different numbers of cells were injected into the subcutaneous space of mice and then imaged to determine the fluorescence intensities. As expected, we found that there is an excellent linear relationship between cell numbers (1×10^4 - 1×10^5 cells) and fluorescence intensities (Figure 2.8). These results suggested that this *in vivo* imaging system can be used to quantify the number of recruited cancer cells in mice.

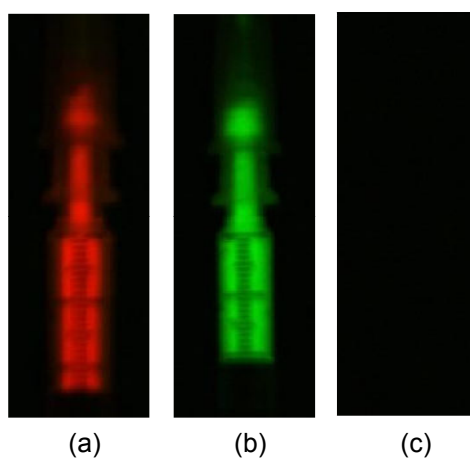


Figure 2.6 Fluorescence labeling of B16F10 cells with (a) X-Sight 761 Nanospheres, (b) Qtracker® 800 quantum dot or (c) nothing as negative control. Exposure condition based on manufacturer recommended condition.

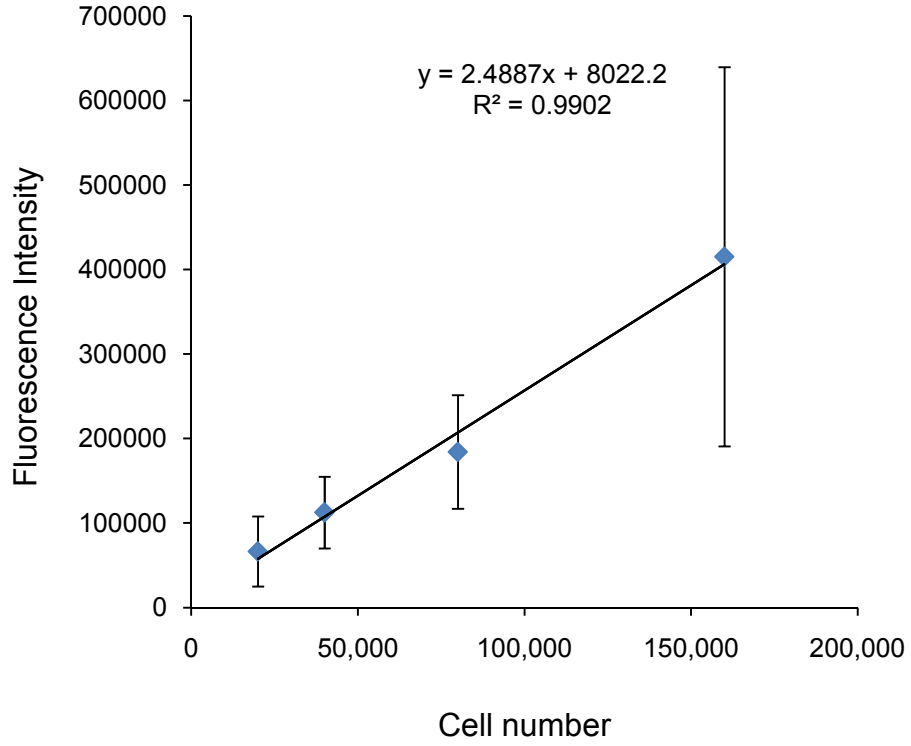


Figure 2.7 *In vitro* detection of X-Sight 761 Nanospheres-loaded B16F10 melanoma cells. Quantified fluorescence intensity values versus number of NIR probe labeled-cells per well. Error bars represent standard deviation for triplicate measurement.

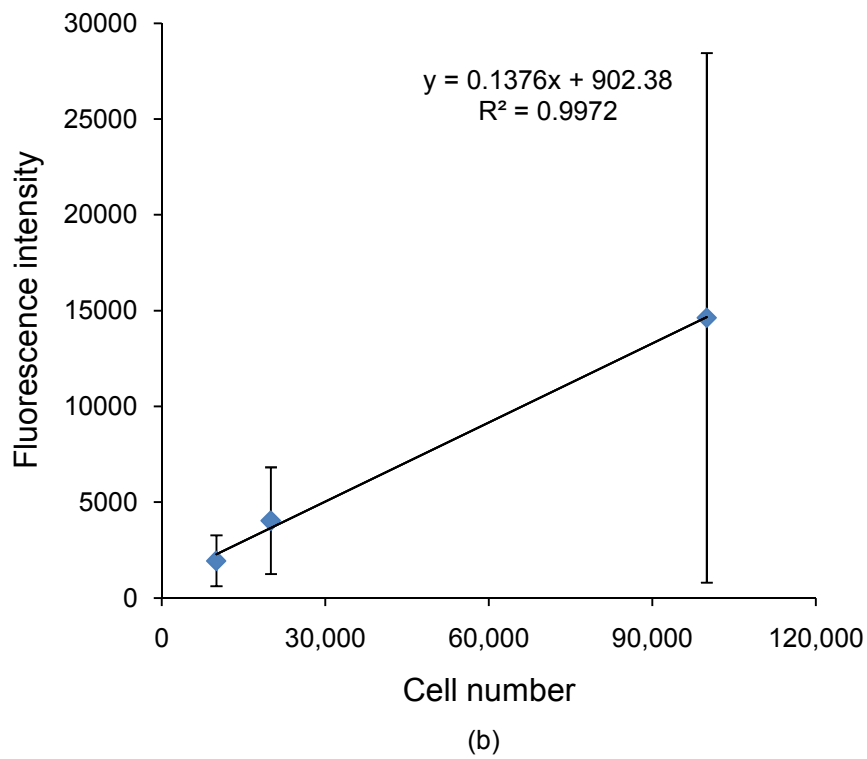
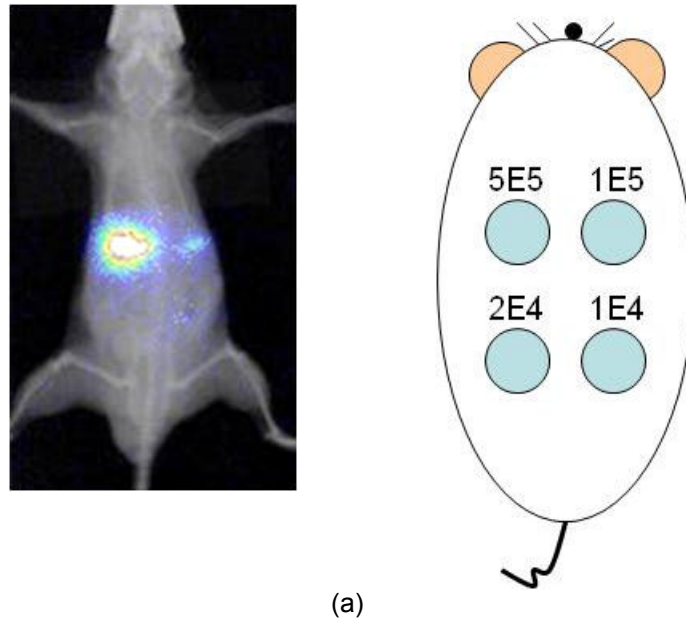


Figure 2.8 *In vivo* detection of X-Sight 761 Nanospheres-primed B16F10 cells. (a) Intensity map of subcutaneously injected cells at four different concentrations. (b) Fluorescence intensity detected from each injection spot versus cell number. Error bars represent standard deviation for measurements made in three mice.

Our previous studies revealed that 1-day implants are often accompanied with maximal inflammatory cell recruitment while 7-day implants often associated with substantially diminished inflammatory responses. To study the degree of inflammatory responses on cancer cell migration, subsequent studies were carried out to transplant X-Sight labeled B16F10 melanoma cells in mice bearing 1-day and 7-day PLA microsphere implants. After cell transplantation for 24 hours, the distribution of melanoma cells was determined using Kodak In-Vivo Imaging Systems. In support of our previous observations, we find that the majority of the fluorescence signal appears in the area of the 1-day implant, but not in the area of the 7-day implant (Figure 2.9a). Based on *ex vivo* intensity measurements, we estimated that the number of melanoma cells surrounding 1-day implant is 4-fold more than those surrounding 7-day implant (Figure 2.9c). Implant tissue collected from the study were sectioned for immunohistochemistry evaluation (Figure 2.9b). There was 2-fold of HMB45 positive cell recruitment in acute treatment (1-day implantation) (Figure 2.9d). The biodistribution in each organ is easily observed over the varying degree of inflammatory responses by performing *ex vivo* imaging (Figure 2.10) (Figure 2.11). B16F10 melanoma cells tended to spread out to each organ under acute inflammatory stimulus. Specifically, higher signals were detected in liver, and spleen areas while cells in response to chronic inflammation tended to accumulate in pancreas/mesenteric membrane and body cavity.

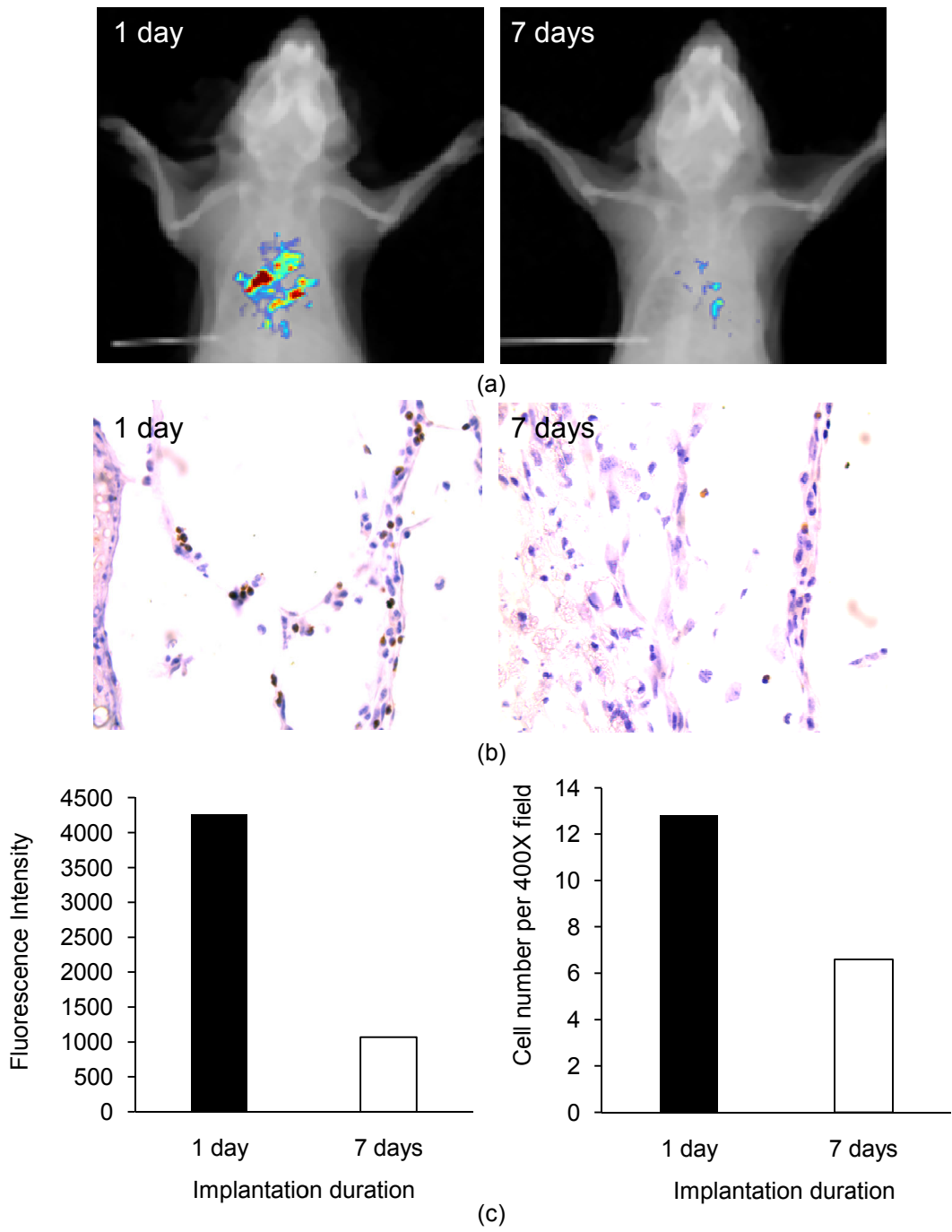


Figure 2.9 (a) *In vivo* imaging detection on X-Sight labeled B16F10 cell migration in animals implanted with PLA microspheres for different implantation duration (1 day , 7days). (b) Confirmation of *in vivo* imaging detected X-Sight labeled B16F10 recruitment to the PLA microspheres implant for different duration by immunohistochemistry staining. (c) Quantification of *in vivo* imaging signal intensity detected was measured by ImageJ image processing program (left). HMB45 + cell quantification was illustrated (right). (n=1)

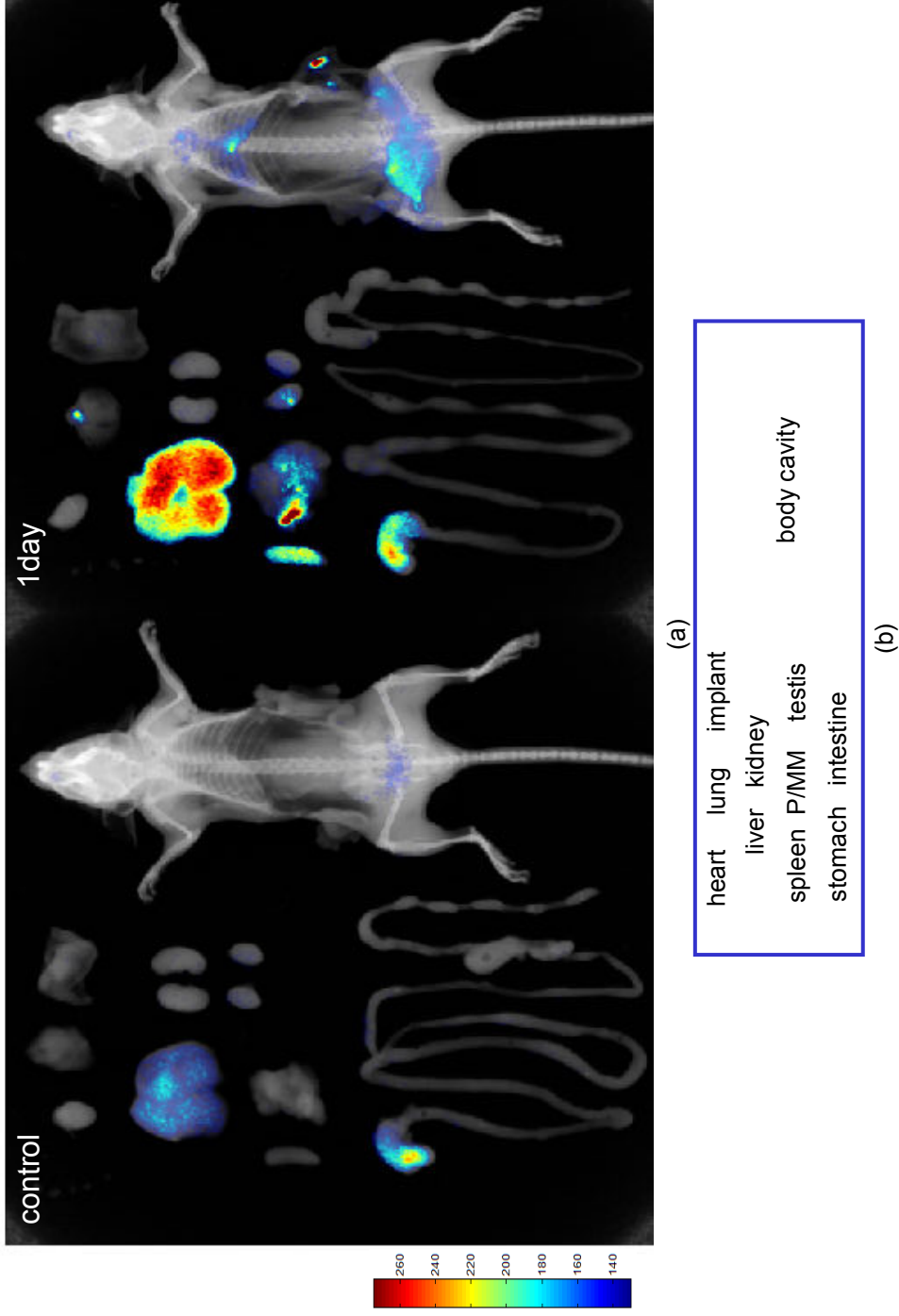


Figure 2.10 Ex vivo imaging of X-Sight-labeled B16F10 cell biotribution in animals bearing with 1- day PLA implant. (a) Animal transplanted with B16F10 without labeling serves as a control. (b) Organs were positioned as illustration. P/MM represents pancreas and mesenteric membrane area.

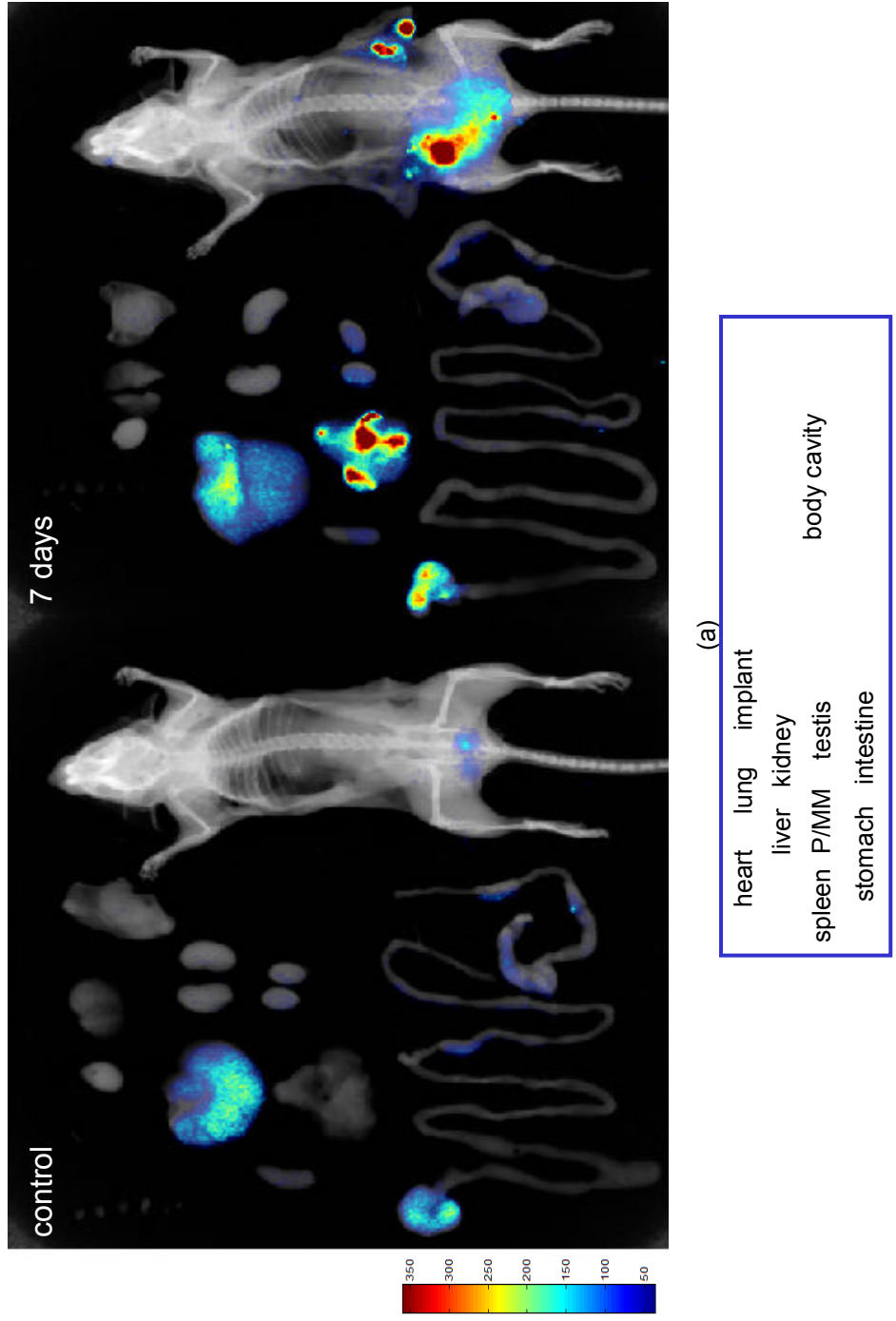


Figure 2.11 Ex vivo imaging of X-Sight-labeled B16F10 cell biodistribution in animals bearing with 7- day PLA implant. (a) Animal transplanted with B16F10 without labeling serves as a control. (b) Organs were positioned as illustration. P/MM represents pancreas and mesenteric membrane area.

2.3.4 In vivo biodistribution of different types of cancer cells

Although our results so far support the hypothesis that inflammatory stimulation would cause B16F10 melanoma cell migration to the inflamed area, it is not clear whether inflammatory responses also influence the migration of other types of cancer cells. By labeling several cancer cells (B16F10 melanoma, Lewis lung cancer, human MDA-MB231 breast cancer, human PC-3 prostate cancer, rat and JHU-31 prostate cancer) originating from different species with a near infrared (NIR) probe, the same animal model (Figure 2.1) was tested. Interestingly, we find that all cancer cells migrated to the subcutaneous implantation sites, although the extent of cancer cell migration varies between different types of cancer cells (Figure 2.12-2.15).

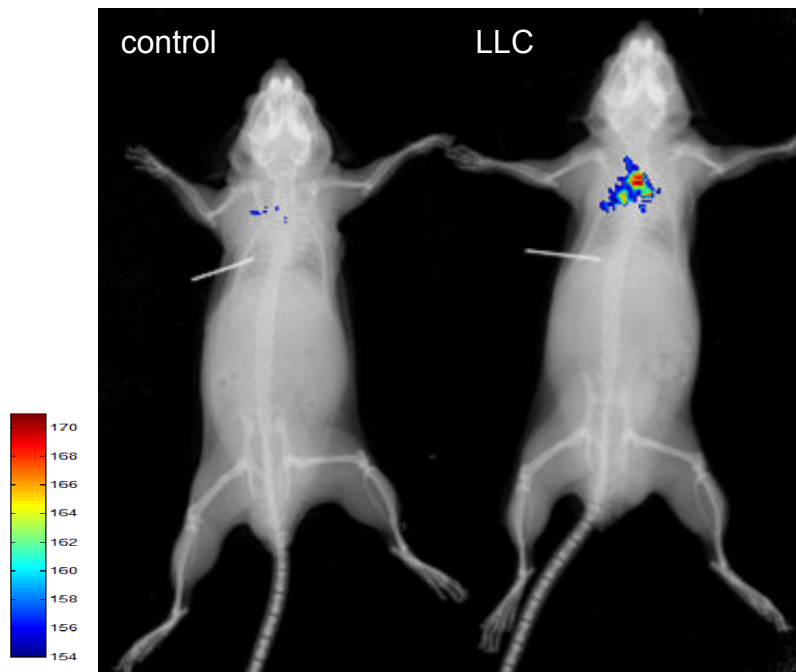


Figure 2.12 Lewis lung cancer cell (LLC) recruitment to the PLA implant area. Animal bearing PLA implant transplanted with non-labeling LLC cells served as control.

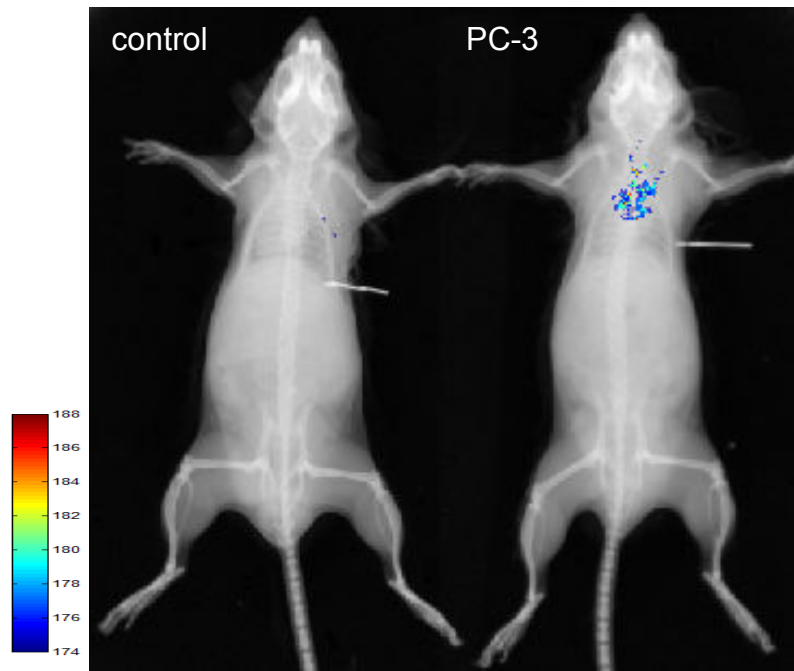


Figure 2.13 Human prostate cancer cell (PC-3) recruitment to the PLA implant area. Animal bearing PLA implant transplanted with non-labeling PC-3 cells served as control.

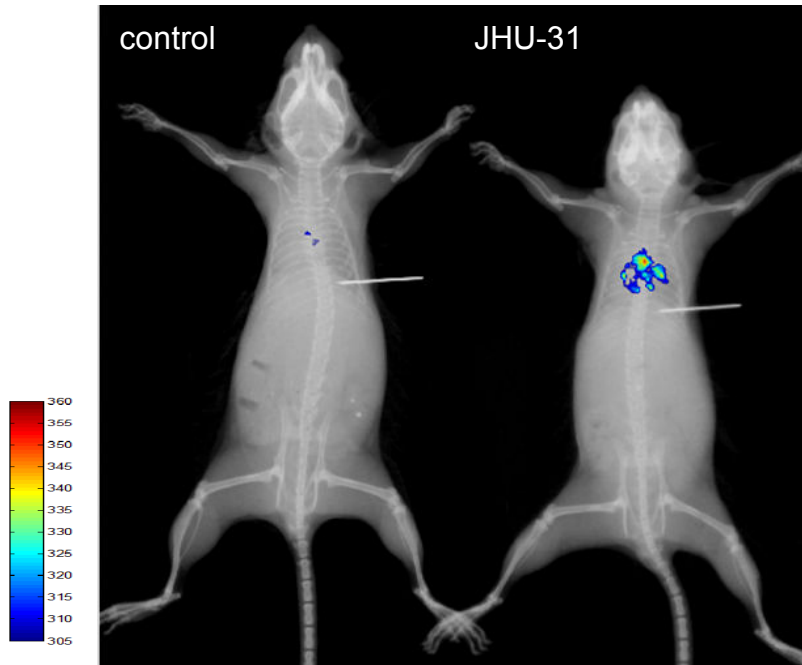


Figure 2.14 Rat prostate cancer cell (JHU-31) recruitment to the PLA implant area. Animal bearing PLA implant transplanted with non-labeling JHU-31 cells served as control.

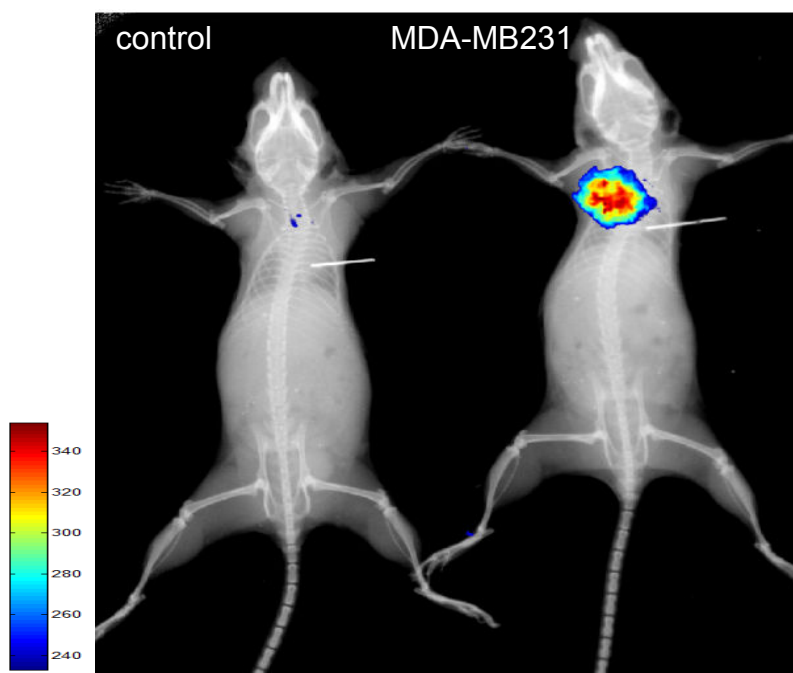


Figure 2.15 Human breast cancer cell (MDA-MB231) recruitment to the PLA implant area. Animal bearing PLA implant transplanted with non-labeling MDA-MB231 cells served as control.

Many recent results suggest that different types of cancer cells respond to inflammatory stimuli differently (99, 100). Subsequent studies were carried out to determine the biodistribution of transplanted cells. Following transplantation for 24 hours, animals were sacrificed and all internal organs were recovered for *ex vivo* imaging. Percentage of biodistribution was determined by dividing the fluorescence intensity measured from each organ with the sum intensity resulted from internal organs and body cavity. As anticipated, we found a significantly different distribution of cancer cells, with all types tested, in the target organs. Specifically, rat JHU-31 cell line showed a higher tendency to accumulate in testis over PC-3 cell line. Instead of staying in body cavity region, some population of B16F10 cell accumulated in testis region. However, most of the cancer cell lines tend to stay in the mesenteric membrane/pancreas and peritoneal cavity areas while the liver tends to be one organ populated with much more cancer

cells. These cell lines did not show any preference to populate in other particular organs (Figure 2.16).

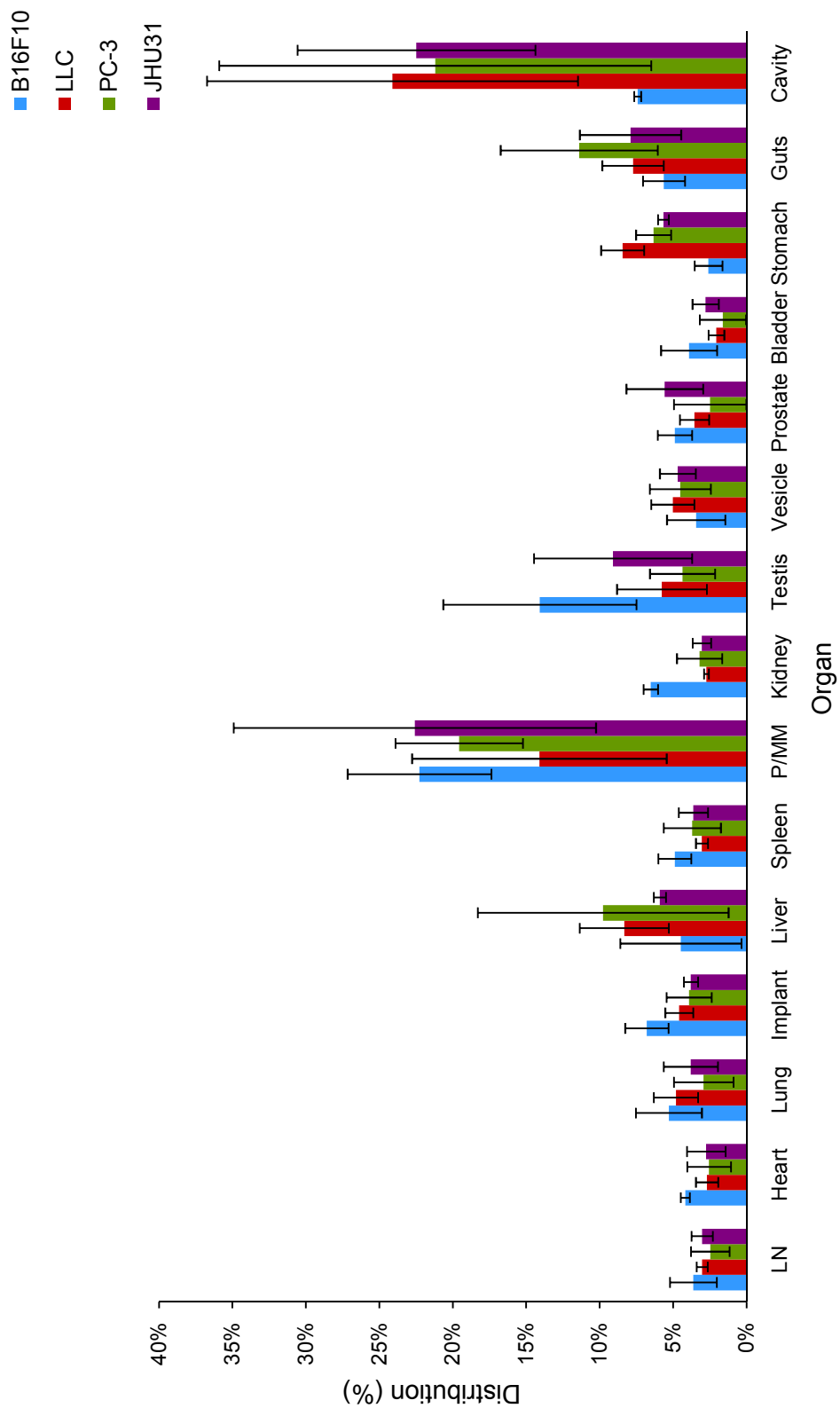


Figure 2.16 *Ex vivo* analysis of imaging intensity detected from each organ to illustrate biodistribution of different cancer cell types. LN represents 3 pairs of lymph nodes gathered from neck, axilla and inguinal regions. P/MM represents pancreas and mesenteric membrane regions. Cavity represents the signal detected from body cavity which was removed with internal organs. (n=3)

2.4 Discussion

The majority of the work proposed is based on a new animal model. The creation of this new animal model was intended to study the mechanism(s) governing cancer metastasis *in vivo*. Biomaterial particles have been found to trigger various degrees of inflammatory reactions. We are aware that many other proinflammatory agents are available for triggering different inflammatory diseases, such as cytosine-phosphorothioate-guanine (CpG), and lipopolysaccharide (LPS) (101, 102). These agents tend to prompt broad area or even systemic inflammatory reactions. In order to limit the area of inflamed tissue, we used microsphere implants that were found to perfectly suite this purpose. The reason for including additional four cancer cell lines in the study is to discuss if the phenomena observed in B16F10 migration can be applied and generalized to other cancer cells under inflammation induction. It is our belief that the inflammatory response attracts the cancer cell migration because cancer cells generally share similar inflammatory chemokine receptors with leukocytes. However, the characteristics of cancer cell migration with cancer cell lines originating from various species may need to be further confirmed by using a spontaneous metastasis model. SCID or nude mice may also be considered as the host to verify tumor xenograft metastasis. Different implantation sites may be needed to simulate cancer migration directly from tumors. Since mice have been used to study the metastasis processes of these cancer cells, we believe that our new imaging system should improve our current understanding of cancer metastasis. Our animal model holds several advantages compared with other existing models. First, our animal model is set to include a start point (peritoneal cavity) and a targeted destination (inflamed area) to evaluate cancer cell migration in a controllable time frame. Second, is the idea of isolating two different body cavities to investigate both the routes of blood circulation and lymphatic system as they are involved in cancer cell migration. Third, rather than traditional immunohistochemistry quantification, our newly established *in vivo* imaging detection provides useful and quick evaluation for cell recruitment quantification in the implant area and even the biodistribution in each organ. This

method provides more general and complete information on the cell migration. Finally, promising results demonstrated by several cancer cell lines showed the capability of our model to investigate the general phenomenon of inflammation-related cancer metastasis. An additional beneficial aspect of our model is to figure out possible mechanisms used by various cancer cell types within 24- 48 hours. This is not only time saving but also allows us to discuss the phenomenon obtained from the cell lines with different species origins with less consideration of the immune rejection issue. In addition to the advantages mentioned above, our *in vivo* imaging detection methods provide specific signal detection in the inflamed area for cancer cell tracking. Further, the fluorescence system established here may be beneficial for additional research into the fields of study such as stem cell recruitment, which is also investigated in our laboratory. We look forward to determining additional applications in combining both our *in vivo* imaging methods and metastasis model towards the development of clinical relevant treatments for cancer.

2.5 Conclusion

A novel animal model for studying inflammation-mediated cancer metastasis was developed by the application of biomaterial-induced foreign body reaction. By a newly established *in vivo* imaging system, further evaluation of the pharmaceutical effects on the cancer cell migration in response to inflammatory stimulation is feasible to achieve. Through in depth understanding of the metastasis process our model may be able to provide a new research direction to manipulating the balance between inflammation and immune responses for more effective cancer therapies.

CHAPTER 3

ROLE OF CYTOKINES/CHEMOKINES ON CANCER METASTASIS

3.1. Rationale

Intensive research efforts have been done in the past to uncover the factor(s) responsible for cancer metastasis. Based on recent observations, we believe that several factors participate in cancer cell migration *in vivo*. Specifically, CXCR4/CXCL12 and CCR7/CCL21 pathways have been shown to participate in many types of cancer metastasis including human breast cancer and murine melanoma (28-31). Studies have indicated that lymph nodes are very important in mediating cancer progression (103). Interestingly, the role of lymphocytes on cancer migration and growth is rather controversial. Although many studies indicate that lymphocytes could suppress cancer invasion (104-106), some recent studies have uncovered that subtypes of lymphocytes may assist cancer metastasis (19, 105, 107). The overall goal of this proposal is to test the potential role of these chemokines and lymphocytes in inflammatory responses-mediated cancer metastasis.

3.2 Materials and methods

3.2.1 Materials

Dulbecco's modified Eagle's media (DMEM), bovine serum albumin, and AMD3100 were purchased from Sigma Aldrich (St. Louis, MO). Fetal calf serum (FCS) was purchased from Atlanta Biologicals (Lawrenceville, GA). Mouse monoclonal antibodies against melanoma HMB45 was purchased from Abcam (Cambridge, MA). Rat anti-mouse CD11b antibody was obtained from Serotec Inc. (Raleigh, NC). Rat anti- mouse CD3 antibody was purchased from BD Sciences (Franklin Lakes, NJ). CCL21 neutralizing antibody and recombinant mouse RANTES was purchased from R&D Systems Inc (Minneapolis, MN). Diaminobenzine (DAB)

enhanced liquid Substrate system was purchased from Sigma (St Louis, MO). Secondary antibodies goat-anti-mouse (HRP-conjugate) was obtained from Jackson ImmunoResearch Laboratories (West Grove, PA). B16F10 melanoma cell line was purchased from American Type Culture Collection (ATCC) (Manassas, Virginia, USA). Kodak X-Sight 761 Nanosphere was purchased from Carestream Health Inc. (New Haven, CT). Poly (D, L-lactic-co-glycolic acid) (75:25) with a molecular weight of 113 kDa was purchased from Medisorb (Lakeshore Biomaterials, Birmingham, AL) and high-molecular weight poly (L-lactic acid) (PLLA, 137 kDa), was purchased from Birmingham Polymers (Birmingham, AL, USA). The solvent dichloromethane was purchased from EMD Chemicals Inc. (Gibbstown, NJ). The surfactant Poly vinyl alcohol was purchased from Sigma Aldrich (St. Louis, MO).

3.2.2 Fabrication of PLA microspheres

The PLA microspheres were manufactured using identical procedure as listed in 2.2.2.

3.2.3 Cancer cell type and culture

B16F10 melanoma cells were maintained following the same procedure as described in 2.2.3.

3.2.4 Neutralizing antibody treatment

To trigger localized inflammatory responses, PLA microspheres were implanted in animal subcutaneously as described in 2.3.3. After implantation for 24 hours, B16F10 melanoma cells were transplanted in the peritonea. To determine the mechanism(s) underlying cancer cell migration *in vivo*, AMD3100 and CCL21 neutralizing antibody were used to block CXCR4/CXCL12 and CCR7/CCL21 pathways, respectively. Specifically, PLA microspheres-implanted animals were administered intraperitoneally with either AMD3100 (250 µg/0.1 ml/mouse) or CCL21 neutralizing antibody (10 µg/0.1 ml/mouse) 1 hour prior to and 12 hours

post cancer cell transplantation. PLA microspheres-implanted animals administered with PBS serve as controls. Twenty-four hours following cell transplantation, the PLA microsphere implants and surrounding tissue were isolated for histological analyses as described in 2.2.5.

3.2.5 Histological evaluation

To examine the effect of blocking CXCR4/CXCL12 or CCR7/CCL21 pathways on the recruitments of cancer cells to the implant area, tissues harvested from experiments were immediately embedded and sectioned for histological evaluation (H&E and immunohistochemistry staining) as listed in 2.2.5.

3.2.6 Cell imaging and quantification

All tissue section images were captured using a Leica fluorescence microscope (Leica Microsystems Wetzlar GmbH, Wetzlar, Germany) equipped with a QImaging Retiga-EXi CCD camera (QImaging, Surrey, BC, Canada). The images at a magnification of 400X (viewing area 0.24 mm²) were then used to quantify the cell numbers per field of view.

3.2.7 Protein extraction from tissue sections

Tissue samples harvested from implant area were sectioned at 10 µm thickness and 30 slices were collected for protein extraction. Samples were subjected to 3 cycles of freezing and thawing after adding 100µl of protein extraction buffer with proteinase inhibitor (Sigma-Aldrich, St, Louis, MO). Protein extracts were collected by 14,000 rpm centrifugation for 10 minutes to discard suspension. The final volume of protein extracts were then reconstituted in 100 µl PBS with proteinase inhibitor added.

Total protein concentration of samples extracted from implant tissues were evaluated by using Pierce® BCA Protein Assay kit (Thermo Fisher Scientific Inc., Waltham, MA). The measurement was performed according to manufacturer's instruction. Briefly, three replications

of diluted albumin (BSA) standards were prepared. Series of BSA dilution, 0 µg/ml, 5 µg/ml, 25 µg/ml, 50 µg/ml, 125 µg/ml, 250 µg/ml, 500 µg/ml, 1000 µg/ml were made. Protein samples were then 10X diluted in PBS for later measurement. In this method, BCA working reagent was used for the colorimetric detection and quantification of total protein. Basically, 50 parts of BCA Reagent A were mixed with 1 part of BCA Reagent B (50:1). 25 µl of each standard or sample replicate were added to microplate well which contains 200 µl of the BCA working reagent. After thoroughly mixing, microplate was incubated at 37°C for 30 minutes. Once temperature of the plate goes back to room temperature, the absorbance was measured at or near 562 nm on a plate reader. Unknown protein sample concentration could be estimated according to the BSA standard.

3.2.8 Protein array analysis

Mouse cytokine antibody array III (Raybiotech, Norcross, GA) was used. The analysis was according to the manufacturer's instructions. In general, array slides were blocked for 30 minutes and incubated with 100 µL of mouse skin homogenate for 2 hours at room temperature. Samples were then decanted from each chamber, and the slides were washed 3 times with 1× wash buffer I, followed by two washes with of 1 x wash buffer II at room temperature with gentle shaking. Glass slides were then incubated in biotin-conjugated anti-cytokines antibodies at room temperature for 2 hours and washed as described above before incubation in fluorescent-dye conjugated streptavidin. After incubation in fluorescent-dye conjugated streptavidin for 60 minutes, slides were washed thoroughly and extra buffer droplets were removed by centrifugation at 1,000 rpm for 3 minutes. The slides were then dried completely in air at least 20 minutes (protect from light) for image analysis by Axon GenePix 4000B microarray scanner (Molecular Devices, Sunnyvale, CA) using Cy3 channel. The fluorescence intensity readout collected from the protein array analyses was processed by calculating the ratio of relative

expression after subtraction of the background intensity and comparison with the internal positive controls.

3.2.9 Cancer cell migration imaging

Following the same procedure described in 2.3.6, X-Sight labeled cells were transplanted in the animals. At the end of the study, animals were placed in supine or prone position under anesthesia with Isoflurane (1-3 %) inhalation. *In vivo* imaging system was configured at 760 nm excitation, 830 nm emission, 60 seconds exposure, 4 × 4 binning, f-stop 2.5, and 120 mm FOV by using Kodak In-Vivo Imaging System FX Pro (Carestream Health Inc, New Haven, CT). X-ray imaging was captured for anatomical identification. The numbers of recruited cells were then quantified based on standard curves established in 2.3.3.

3.2.10 Statistical analyses

Statistical comparison between different groups will be carried out using Student t- test or one-way ANOVA. Differences will be considered statistically significant when $p < 0.05$.

3.3 Results

3.3.1 Molecular pathway associated with inflammation-mediated cancer migration

Our recent studies have uncovered that a large number of cancer cells was recruited to microsphere implantation sites. However, the molecular processes governing the foreign body reactions-mediated cancer cell migration is mostly undetermined. Since both CXCR4/CXCL12 and CCR7/CCL21 pathways have been shown to play an important role in cancer metastasis, the potential role of both pathways in foreign body reaction-mediated cancer migration was assessed.

We first investigate the potential role of CXCR4/CXCL12 axis in the migration of melanoma cells to the inflamed area. We find that the treatment of AMD3100, antagonist of

SDF-1 α receptor - CXCR4, drastically reduced the recruitment of both melanoma cells and inflammatory cells to the subcutaneous microsphere implantation sites (Figure 3.1). On the other hand, AMD3100 treatment exerted no effect on the accumulation of melanoma cells in lymph node (Figure 3.2). These results confirmed that SDF-1 α /CXCR4 pathway may participate in the migration of melanoma cells into inflamed tissue. Since our recent *in vivo* studies have shown that microsphere-mediated acute inflammatory responses triggered the production of SDF-1 α in tissue, it is possible that subcutaneous SDF-1 α gradient in the inflamed tissue is essential for cancer cell immigration to the implantation sites.

Further studies were done to assess the importance of CCR7/CCL21 pathway in B16F10 melanoma cell accumulation in the inflamed sites. For that, microsphere-bearing mice were treated with either CCL21 neutralizing antibody or phosphate buffered saline (as control) prior to B16F10 melanoma cell transplantation. As expected, CCL21 neutralizing antibody treatment dramatically diminished the presence of B16F10 melanoma cells in the lymph node (Figure 3.3). However, the number of tumor cells migrating to microsphere implantation site was not affected by the treatment of CCL21 neutralizing antibody (Figure 3.4). These results have shown that CCR7/CCL21 pathway is critical to melanoma migration through lymphatic system, but not responsible for cell immigration into the subcutaneous implantation site.

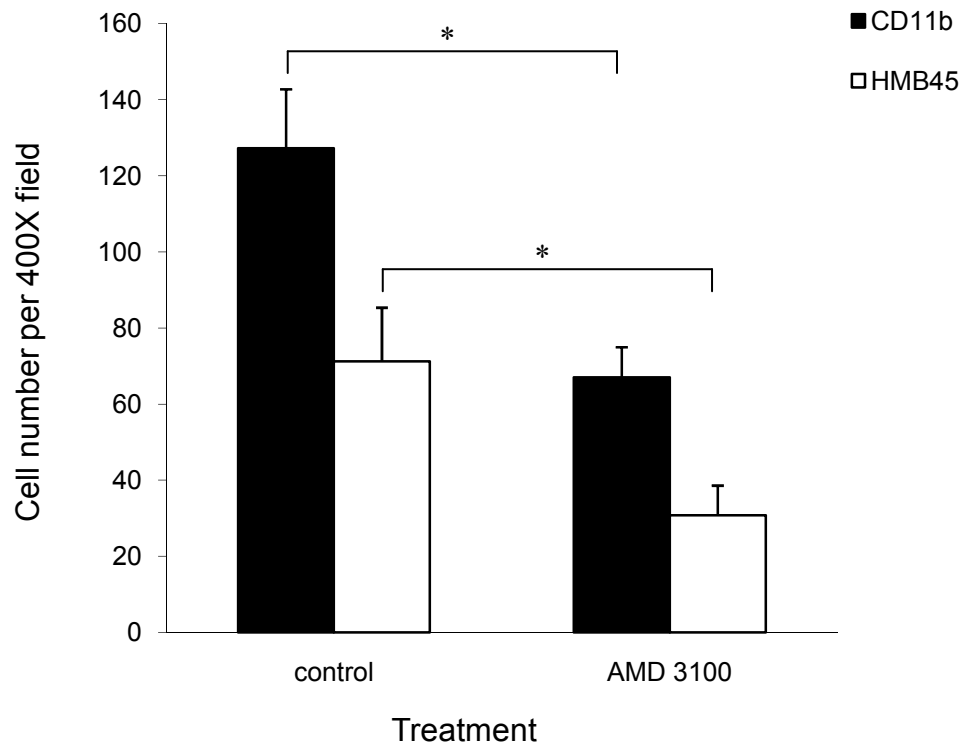


Figure 3.1 Treatment of AMD3100, antagonist of SDF-1 α receptor- CXCR4 treatment drastically reduced the recruitment of both melanoma cells and inflammatory cells to the subcutaneous PLA microsphere implantation sites. (n=4, *p<0.05, t-test)

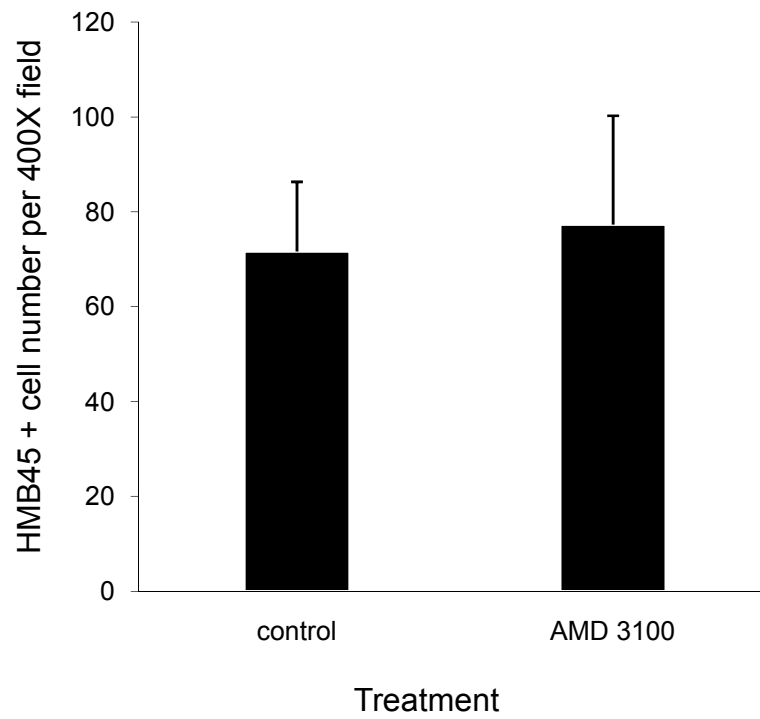


Figure 3.2 Treatment of AMD3100 exerted no effect on the accumulation of melanoma cells in axillary lymph nodes.

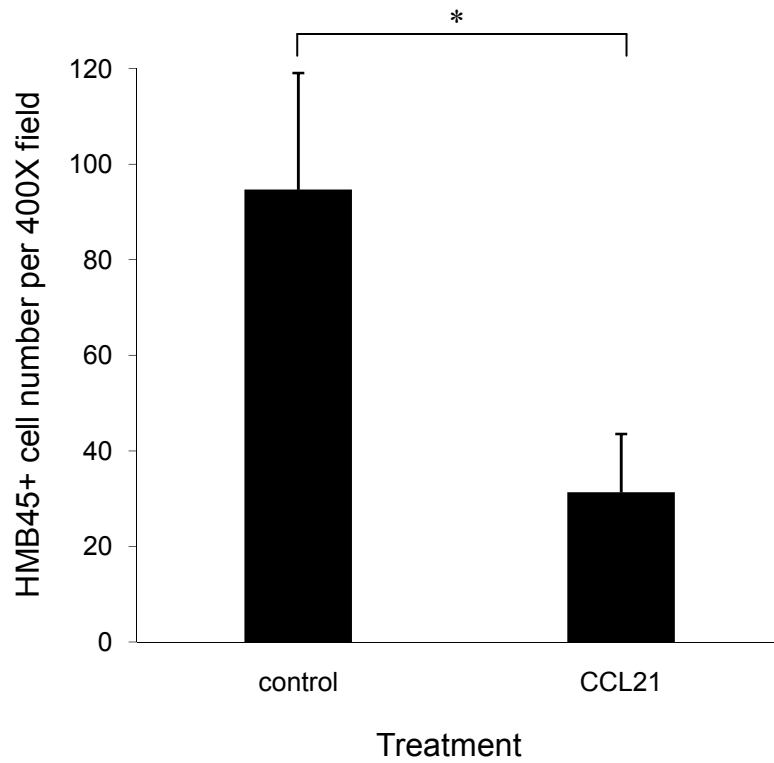


Figure 3.3 Treatment of CCL21 neutralizing antibody to block CCR7/CCL21 pathway drastically reduce the presence of B16F10 melanoma in axillary lymph nodes. (n=4, *p<0.05, t-test)

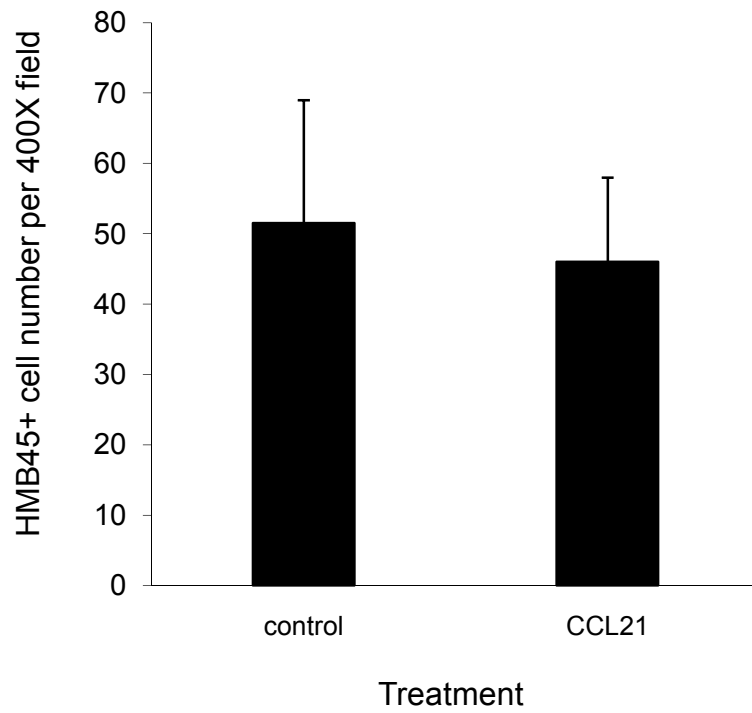


Figure 3.4 Treatment of CCL21 neutralizing antibody had no effect on the number of tumor cells migration to microsphere implantation site.

3.3.2 Involvement of inflammatory cytokines in inflammation-associated cancer migration

Our previous studies have shown that some of the proinflammatory cytokine/chemokines play an important role in cancer cell migration. To determine the profile of inflammatory cytokines in implant-surrounding tissue, proteins were extracted from tissue sections and then assayed for a panel of inflammatory cytokines. Our results show that many proinflammatory cytokines are up-regulated during inflammatory responses as compared with protein expression profile of implant tissues harvested from severe combined immunodeficient (SCID) mice (Table 1.1) (The completed data is attached in Appendix A). These cytokines include RANTES, MIP-1 α , Eotaxin, IL-17, IL-12 p40/p70, and MCP-5.

Table 1.1 Relative inflammatory cytokine expression in biomaterial-mediated inflammation

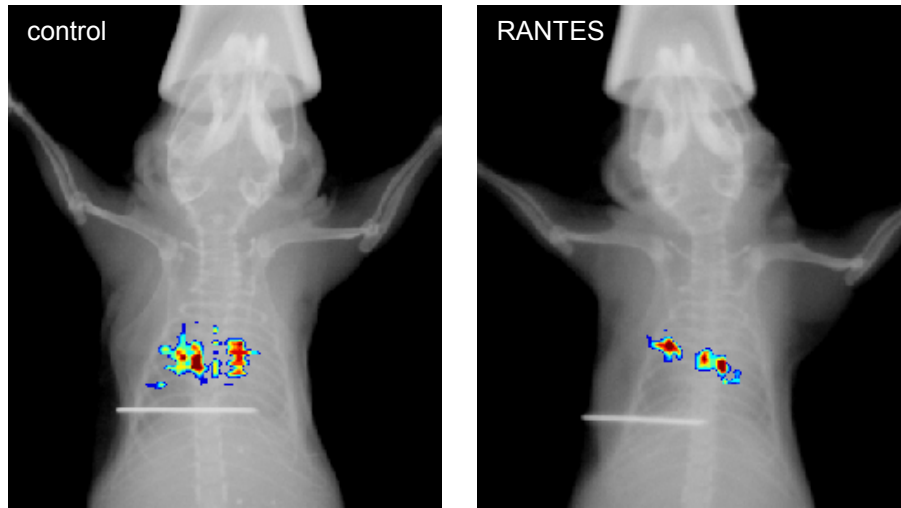
Cytokine	Balb/c mice	SCID mice	Fold Change (Balb/c/SCID)
IL-1 α	15057.50	17417.34	0.86
IL-6	405.00	502.79	0.81
IL-10	257.00	230.11	1.12
IL-2	245.00	157.63	1.55
IL-4	265.50	180.73	1.47
SDF-1 α	118.00	106.90	1.10
TNF α	232.00	289.44	0.80
P-Selectin	2730.00	2626.28	1.04
VCAM-1	5843.00	5501.69	1.06
IL-17	291.50	124.11	2.35
IL-12 p40/p70	1016.00	449.34	2.26
Eotaxin	814.50	327.04	2.49
MCP-5	292.00	142.68	2.05
MIP-1 α	4435.50	1178.61	3.76
RANTES	1406.00	343.35	4.09

These cytokines have different potential functions in mediating immune responses. RANTES and MIP-1 α are known to attract monocytes/ macrophages to the biomaterial surface during foreign body formation process (63, 69). Eotaxin is thought to be a very selective and potent chemokine for eosinophils (108), and it has been demonstrated later that Eotaxin together with Th2 type cytokines (IL-13 and IL-4) is important for inflammatory response, cell recruitment and tissue damage (109). IL-17 is mainly secreted from CD4 +T cells and other T cell subpopulations such as CD8+ T cells, natural killer (NK) T cells and $\gamma\delta$ T cells (110-112). IL-17 is quite proinflammatory in character. It increases the production of other chemokines such as IL-8 (113,114), monocyte chemoattractant protein-1 (MCP-1), and Growth regulated oncogene-alpha (Gro α) to promote monocytes and neutrophils recruitments (115). Further, it stimulates IL-6 and PGE2 production to enhance the local inflammatory environment (116). In addition, IL-17 also mediates T-cell responses (117). IL12 p40/p70 is expressed by activated macrophages that serve as an essential inducer of Th1 cells development (118). MCP-5 can be induced in macrophages. It specifically attracts eosinophils, monocytes and lymphocytes (119). Though the functions of these screened cytokines on the inflammation-associated cancer metastasis is not clear, it is intriguing that protein array analyses provide us directions for further investigate the potential roles of those cytokine candidates played in relation to the lymphocyte functions exerted in our model.

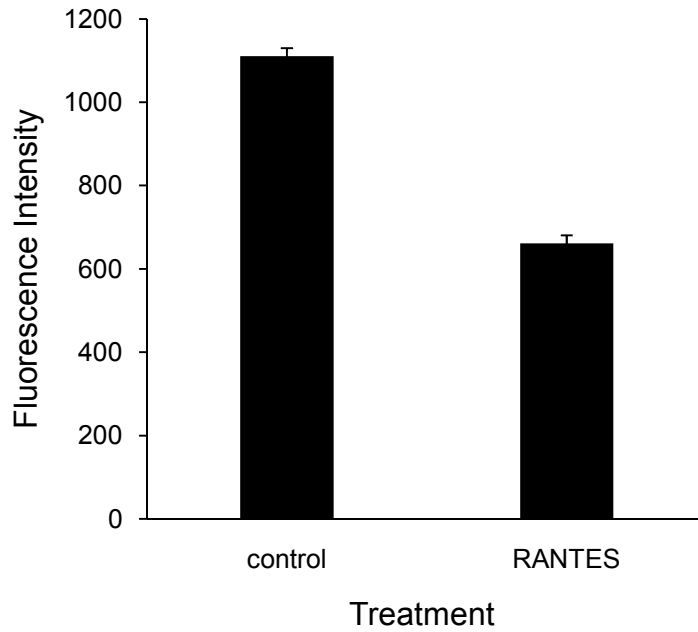
3.3.3 Discovery of the role of RANTES in inflammation-mediated B16F10 melanoma migration

RANTES was selected as a potential culprit based on the published results (120-125). Specifically, it is linked to systemic malignancies with different diseases. It has been shown that RANTES expression in biopsy specimens is correlated with tumor progression in breast cancer (120). Recently, it was reported that gastric cancer patients in stage IV have significantly higher RANTES concentration in serum compared to patients at earlier stages (121). Gastric cancer cells could stimulate secretion of RANTES from CD4+ lymphocytes and also induce Fas-FasL-

mediated apoptosis of CD8+ lymphocytes by RANTES (122). Further, a previous study has indicated that RANTES+ activated cytotoxic T cells play important roles in the active inflammatory process of chronic gastritis (123). It is also believed that altered RANTES expression of T lymphocytes infected with human T-cell leukemia viruses may be involved in the pathogenesis of adult T-cell leukemia (124, 125). These findings support our hypothesis that RANTES expression is associated with lymphocyte to assist cancer cell migration in response to biomaterial-induced inflammation. To test this hypothesis, neutralizing antibody against RANTES was used to determine its role in cancer cell migration. As expected, treatment with RANTES neutralizing antibody treatment substantially reduced the recruitment of cancer cells to the microsphere implantation site as depicted by the *in vivo* imaging system (Figure 3.5a). Based on the fluorescence intensity measurement, it was estimated that the numbers of recruited cells are reduced for about 2-fold (Figure 3.5b). Such cell reduction effect is also confirmed with immunohistochemistry analyses in which the cell accumulation surround the implant area also decreased by about 2-fold of change (Figure 3.6). Further, we also detected CD3 + cell recruitment in response to RANTES neutralizing antibody treatment by immunohistochemical staining. It is interesting that CD3+ lymphocyte recruitment to the PLA microsphere implant reduced by 2-fold in RANTES neutralizing antibody treated animals (Figure 3.7).



(a)



(b)

Figure 3.5 (a) Effect of RANTES neutralizing antibody treatments on the recruitment of B16F10 melanoma to the microsphere implantation site by *in vivo* imaging. (b) The quantified intensity signals detected in RANTES neutralizing antibody treated animals are reduced by 2-fold. (n=2)

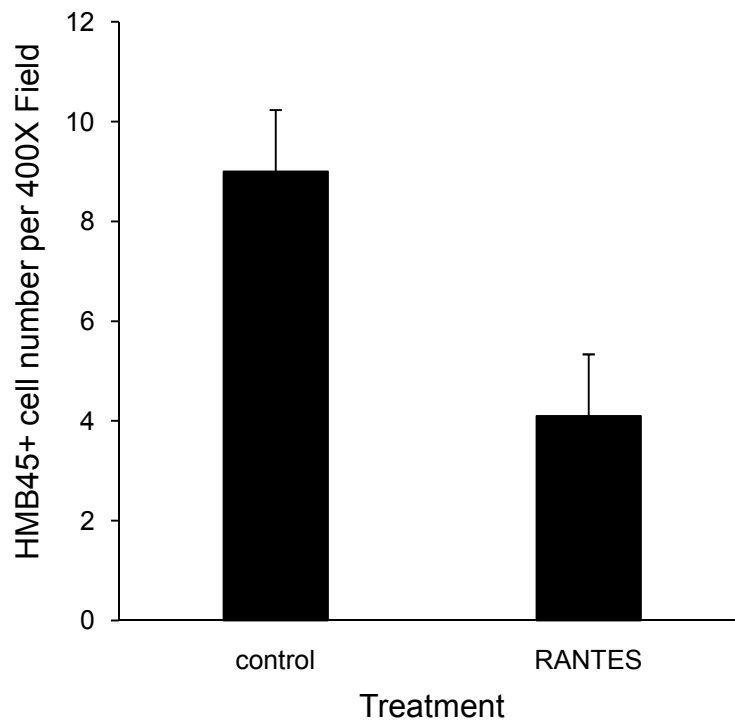


Figure 3.6 Quantification of HMB45+ B16F10 melanoma cells accumulated surround PLA implant area using immunohistochemistry staining. Blockage of RANTES expression diminished cancer cell recruitment to the inflamed area by 2- fold. (n=2)

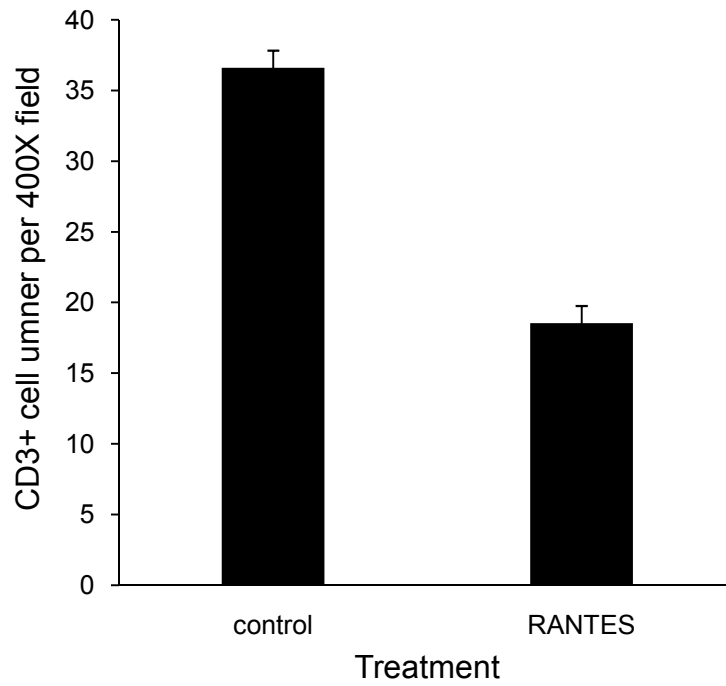


Figure 3.7 Quantification of CD3+ lymphocytes recruited to PLA implant area using immunohistochemistry staining. Blockage of RANTES expression diminished lymphocyte accumulation to the inflamed area by 2-fold. (n=2)

3.4 Discussion

Tumorigenesis, tumor metastasis and immune response are complex processes and interactions between tumor cells and immune cells. Both SDF-1 α /CXCR4 and CCR7/CCL21 pathways were tested for their participation in inflammation-associated cancer metastasis, since both pathways have been shown in previous studies to be critical to the migration of cancer cells, especially B16F10 cells (31, 39). It is possible that different metastasis pathways may be responsible for the migration of different cancer cells. Specifically, colorectal cancer cells are also found to express chemokine receptor/ ligand such as CCR6/CCL20 and respond to chemokine gradients similar to leukocyte and monocytes inflammatory cells (40). CXCR2 is important in regulating the IL-8-mediated invasion and migration of human melanoma (126). Other chemokine axis, such as CXCR3 with its ligands is responsible for metastases of melanoma and colon cancer into lymph nodes, as well as breast cancer metastasis to lungs where the CXCR3 ligands, CXCL9, CXCL10 or CXCL11, are expressed (127, 128). The primary focus of this investigation is to uncover the mechanism critical to B16F10 cell migration. Based on the results from many previous works including those from our laboratory (129-132), the migration of cancer cells from peritoneal transplantation sites to the subcutaneous microsphere implantation sites can be categorized into at least three consecutive steps: cancer cell invasion into capillary possibly via lymph node, cancer cell migration via circulation, and extravasation of cancer cells into the subcutaneous implantation sites (129). The components/factors participating in different steps of the cell migration are discussed in the following paragraphs.

Since cancer cells such as breast cancer, ovarian cancer, melanoma and prostate cancer are found to highly express CXCR4 and metastatic organs (such as lymph nodes, lungs, liver and bones) release a high concentration of SDF-1 α , CXCR4/ SDF-1 α (CXCL12) pathway is believed to participate in cancer metastasis (31). Interestingly, the treatment with CXCR4 antagonist AMD3100 substantially reduces the accumulation of cancer cells in the subcutaneous PLA microsphere implantation sites. These results are in good agreement with

recent observations that CXCR4/CXCL12 axis is essential to some types of cancer cells with different organ metastases (133,134). It should be noted that CXCR4/CXCL12 axis may also play a role in mediating cancer cell migration through blood circulation. A recent study had demonstrated that CXCR4/CXCL12 interactions promote early extravasation in liver metastatic epithelial cancer cells (135). Transendothelial/stromal cell migration affected by impairing CXCR4 suggests a pivotal role of the CXCR4-CXCL12/SDF-1 α in tumor extra- and intravasation (136). Therefore further studies are needed to examine the relationship between CXCR4/SDF-1 α axis, cancer migration and inflammatory responses in our model.

For cancer cell invasion into capillary possibly via lymph node, our study also showed that CCR7 expression is essential to B16F10 melanoma cells accumulation in lymph node. Neutralization of CCL21 reduced the accumulation of melanoma cells in lymph node. These findings are in agreement with many recent observations that CCR7/CCL21 pathway is important for cancer cell trafficking through lymph node. First, many study results have demonstrated that lymph nodes play an important role in metastasis of many tumor cells, including melanoma, breast cancer, prostate, colon, and gastric cancer (137). Second, lymph node metastasis is associated strongly with clinically poor prognosis in many tumors, such as melanoma, breast cancer and colon cancer etc. (138-141). Third, the enhanced CCR7 expression may promote B16 melanoma cells metastasis to draining lymph nodes (142). Finally, CCL21 induces CCR7 expression and associated Ca²⁺ flux in lymphatic endothelial cells (143). However, the reduction of B16F10 congregation in lymph node has insignificant influence on cancer cell accumulation in subcutaneous implantation site. These results suggest that, during cancer metastasis, cancer cells may enter blood circulation through the invasion of either capillary directly or lymphatic system/capillary combination as suggested earlier (129, 144-146). Since lymphatic pathway is critical to our model and some of our preliminary data (data is not shown in our study) have also shown that the same animal model carried out in severe combined immunodeficiency mice (SCID) did not support the hypothesis that less

immune response enhances cancer cell migration in response to inflammatory response. On the contrary, less extent of cancer cell recruitment was observed in SCID animals carried out by metastasis study. These pieces of evidences suggest a new hypothesis that lymphocytes somehow play a role in mediating cancer cell migration. To find the answer, protein array analyses were performed by collecting implant samples from both Balb/c and SCID with similar genetic background. Interestingly, several inflammatory cytokines expression such as RANTES, MIP-1 α , eotaxin, IL-17, IL- 12 p40/p70, and MCP-5 are higher in normal animals. In the progression of foreign body reaction, monocytes/macrophages are recruited to the implant site by extravasation and migration. Once monocytes/macrophages are attracted to the inflamed area by blood-material interaction and under effect of mast cell degranulation, macrophage production of cytokines may lead more cells to the implant area (79). Chemokines such as CCL2 (Monocyte chemotactic protein, MCP-1) along with RANTES (CCL5), CCL3 (macrophage inflammatory protein, MIP- 1 α), CCL4 (MIP-1 β), CCL7 (MCP-3), CCL8 (MCP-2), and CCL13 (MCP-4) are known to attract monocytes/ macrophages to the implant area (63, 69). As for eotaxin, IL-17, IL-12p40/p70, and MCP-5, their roles in foreign body reaction are still not studied.

It is possible that these biomaterial-mediated inflammatory signals also participate in cancer cell migration. To test the hypothesis, we determine the role of various chemokines in prompting cancer cell migration. We first hypothesized that RANTES is involved in lymphocyte-mediated cancer cell migration. First, many studies demonstrated the potential role of tumor-infiltrating lymphocytes in relation to favorable outcome in cancers. (147-149). Second, chemokines are known to direct specific T cells toward the tumor and induce tumor cell proliferation, angiogenesis, or matrix metalloproteinase expression (150,151). Third, it has been reported that CCL5/RANTES plays an important role in inflammatory diseases and cancers (120). Finally, study has shown that gastric cancer cells stimulate CD4+ lymphocytes to secrete RANTES and Fas-FasL-induced apoptosis of CD8+ lymphocytes may also be mediated by

RANTES (122). To test the potential of RANTES on inflammation-mediated cancer cell migration, we used RANTES neutralizing antibody. We found that the treatment of RANTES neutralizing antibody significantly reduced the recruitment of B16F10 melanoma cells to the implant area. Further, by examining CD3+ lymphocyte recruitment to PLA microsphere implant, it was surprising that CD3+ lymphocytes accumulation was reduced in RANTES neutralizing antibody treated group. Our findings support that RANTES plays a pivotal role in mediating B16F10 cancer cell and lymphocyte migration in response to distal inflammatory stimulation. However, it is not clear how RANTES pathway affect cancer cell interaction with lymphocytes.

3.5 Conclusion

Using biomaterial-induced inflammation as an application is our idea to establish such a quick and controllable method for studying inflammation-mediated cancer metastasis. Our studies determined that, in inflammation-mediated cancer migration model, B16F10 melanoma cell migration to the inflamed area is mediated through CXCR4/CXCL12 axis while CCR7/CCL21 axis is important to mediate lymphatic pathway for B16F10 melanoma cell migration. Our results also revealed that lymphocytes play an important role in cancer cell migration. To search for the potential link between lymphocyte responses and cancer cell migration, we found that RANTES is highly produced in the inflamed tissue and the neutralization of RANTES substantially reduces the recruitment of melanoma cells and lymphocytes to the PLA microsphere implantation site. Our preliminary results also demonstrated that RANTES neutralizing antibody treatment reduced HMB45+ cell accumulation in the axillary lymph nodes. Furthermore, the effect of silencing lymphocyte derived chemokines on the balance of immunity and inflammation in response to external stimuli will be an interesting direction for metastasis study by using our model.

CHAPTER 4

STRATEGIES TO REDUCE CANCER PROGRESSION

4.1 Rationale

Our results have shown that biomaterial-induced inflammation trigger cancer cell recruitment. It is possible that, by varying inflammatory stimuli, the recruitment of cancer cells can be hindered or diverted to reduce cancer metastasis. To test this general hypothesis, three strategies were carried out to test their ability to affect cancer metastasis.

First, it is well established that cytokines such as stromal cell-derived factor-1 alpha (SDF-1 α) and erythropoietin (EPO) have been shown to promote cancer cell migration (152,153). It is possible that, by recruiting cancer cells to the subcutaneous space with locally release of chemokines may reduce the number of circulating cancer cells in the blood circulation and thus reduce the potential cancer cell spreading.

Mast cell activation and associated histamine release have been found to be critical to triggering inflammatory responses (154, 155). Since inflammatory responses promote cancer cell migration, the extent of cancer cell recruitment may be diminished by reducing mast cell activation or blocking histamine-associated cellular responses. The second strategy involves the use of mast cell stabilizer and histamine receptor antagonists to reduce cancer intravasation from the cell transplantation site to the blood stream.

Since inflammatory responses have been shown to influence cancer cell migration, we have thus assumed that degree of inflammatory responses may affect tumor growth. By triggering different extent of distal inflammatory responses, the third approach investigates the influence of distal inflammatory responses on tumor growth.

4.2 Materials and preparation

4.2.1 Materials

Poly (D, L-lactic-co-glycolic acid) (75:25) with a molecular weight of 113 kDa was purchased from Medisorb (Lakeshore Biomaterials, Birmingham, AL). The solvent 1, 4-dioxane was obtained from Aldrich (Milwaukee, WI). BSA, histamine, pyrilamine, famotidine, and cromolyn were bought from Sigma (St Louis, MO). SDF-1 α , and Erythropoietin was obtained from ProSpec (Rehovot, Israel) and Cell Sciences (Canton, MA) respectively. Dulbecco's modified Eagle's media (DMEM), RPMI1640, bovine serum albumin, and AMD3100 were purchased from Sigma Aldrich (St. Louis, MO). Fetal calf serum (FCS) was purchased from Atlanta Biologicals (Lawrenceville, GA). Mouse monoclonal antibodies against melanoma HMB45 was purchased from Abcam (Cambridge, MA). Rat anti-mouse CD11b antibody was obtained from Serotec Inc. (Raleigh, NC). CCL21 neutralizing antibody and recombinant mouse RANTES was purchased from R&D Systems Inc (Minneapolis, MN). DAB enhanced liquid Substrate system was purchased from Sigma (St Louis, MO). Secondary antibodies goat-anti-mouse (HRP-conjugate) was obtained from Jackson ImmunoResearch Laboratories (West Grove, PA). Kodak X-Sight 761 Nanosphere was purchased from Carestream Health Inc. (New Haven, CT).

4.2.2 Preparation of chemokine-releasing PLGA scaffolds

BSA microbubble PLGA scaffolds were used in the study based on our published procedure (156). This scaffold fabrication method, invented by our laboratory, provides a versatile tool to create cytokines/chemokine -releasing scaffolds for a period of 7-10 days (156). For this work, SDF-1 α (1 μ g/mL), erythropoietin (EPO) (100 IU/mL), histamine (20 mg/ mL) releasing scaffolds were produced based on published procedure (156) (Briefly, drug-loaded microbubbles (500 ng/mL) solution was mixed with BSA solution before sonication under nitrogen gas at 20 kHz for 10 seconds. 5% w/v of BSA microbubbles were then be added into

7.5% w/v PLGA polymer solution (1:1 ratio). After gentle agitation for 3 min at room temperature, the polymer solution mixture in glass Petri dishes (5 cm diameter) was quenched in liquid nitrogen to induce phase separation. The solidified scaffolds were lyophilized for 72 hours at 0.03 mbar vacuum in a Freezone 12 lyophilizer (Labconco, Kansas City, MO). The scaffolds were fabricated in a sterilized environment and all components were pyrogen-free.

4.2.3 Cancer cell type and culture condition

B16F10 melanoma cells were used for transplantation in this study. The specific cell culture condition and procedure are listed in 2.2.3.

4.2.4 Scaffold implantation

For implantation, mice were anesthetized with isoflurane inhalation, a 1 cm mid-dorsal longitudinal incision was made and drug-releasing scaffolds implanted subcutaneously. The incision was closed with 4-0 black braided suture to eliminate nonspecific signal detection by *in vivo* imaging system. Two days after scaffold implantation, animals were intraperitoneally transplanted with cancer cells (5×10^6 / 0.2 ml/animal) under anesthesia with isoflurane inhalation (1-3%). At the end of the studies, animals were sacrificed and implant along with surrounding tissues isolated for histological evaluation.

4.2.5 Pharmaceutical treatment

Mast cell stabilizer- cromolyn (50 mg/kg) were administered to animal by intraperitoneal injection one hour prior to PLA microparticles implantation and boosted with this agent every 6 hours to maintain the efficacy.

4.2.6 Histological evaluation

To examine the effect of pharmaceutical treatments on the recruitments of cancer cells to the implant area, and animal survival, tissues harvested from experiments were immediately embedded and sectioned for histological evaluation (H&E and immunohistochemistry staining). The detailed procedure is listed in 2.2.5.

4.2.7 Cell imaging and quantification

All tissue sections were imaged following the procedures listed in 2.2.5.

4.2.8 Cancer cell migration imaging

Cancer cells with exogenous X-Sight 761 labeling could be detected by methods listed in 2.2.7.

4.2.9 Statistical analyses

Statistical comparison between different groups was carried out using Student t- test or one-way ANOVA. Differences were considered statistically significant when $p < 0.05$.

4.3 Results

4.3.1 Cancer cell recruitment to chemokine-releasing scaffolds

Animals implanted with either SDF-1 α -releasing or EPO-releasing PLGA scaffolds were detected by *in vivo* imaging while animals implanted with PLGA scaffold alone served as control group to evaluate the cancer cell recruitment. Among these groups, localized release of EPO prompted the most cancer cell recruitment to the implant area as compared to the signal detected from animals implanted with SDF-1 α -releasing scaffolds and PLGA control scaffold (Figure 4.1). On the other hand, there was no apparent difference in implant-associated fluorescence intensity between SDF-1 α -releasing scaffolds and control scaffolds. The

fluorescence intensities were quantified by using Image J software to compare the gray value of region of interest (ROI) (Figure 4.2).

Our assumption was that, by increasing localized recruitment of cancer cells, the circulating stem cells would be reduced and the life span of the cancer cell-bearing mice would be extended. To test the hypothesis, the survival duration of scaffold-bearing animals were also evaluated after completion of the *in vivo* imaging detection. Since the cell number of melanoma transplantation was high at 5×10^6 cells/ mouse, all the animals were developed massive tumors in the peritoneal cavity and died from the tumor development. Endpoint assessment of animal was determined based on the clinical signs observed from animals including unkempt haircoat, abdominal distention that impedes movement, labored breathing, abnormal posture, dehydration, and weight loss. From the survival observation, animals that received EPO scaffold implantation seemed to have longer survival while mice implanted with SDF-1 α scaffold stayed with shorter period of survival (Figure 4.3).

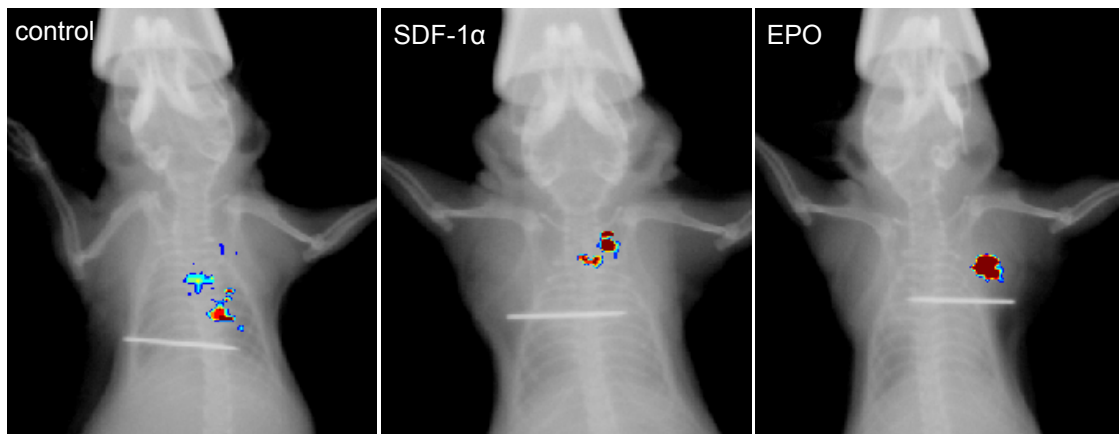


Figure 4.1 Effect of localized release of SDF-1 α and EPO on cancer cell recruitment. Following transplantation for 24 hours, the distribution of X-Sight-labeled B16F10 cells was then monitored using whole-body imaging system. B16F10 cells were recruited to the variously treated scaffolds. (n=2)

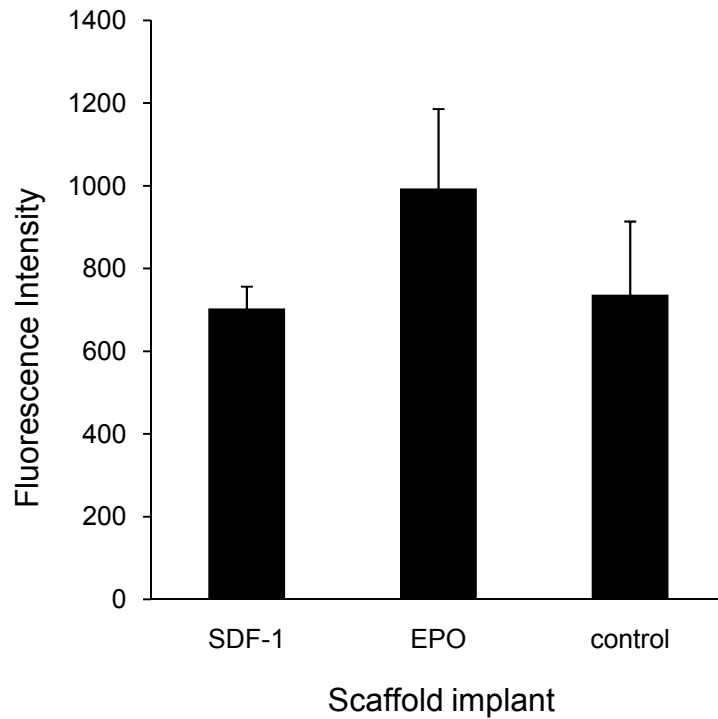


Figure 4.2 Effect of localized release of SDF-1 α and EPO on cancer cell recruitment. Following transplantation for 24 hours, the distribution of X-Sight-labeled B16F10 cells was then monitored using whole-body imaging system. B16F10 cells were recruited to the variously treated scaffolds. The implant-associated fluorescence intensities were then quantified using by ImageJ software. (n=2)

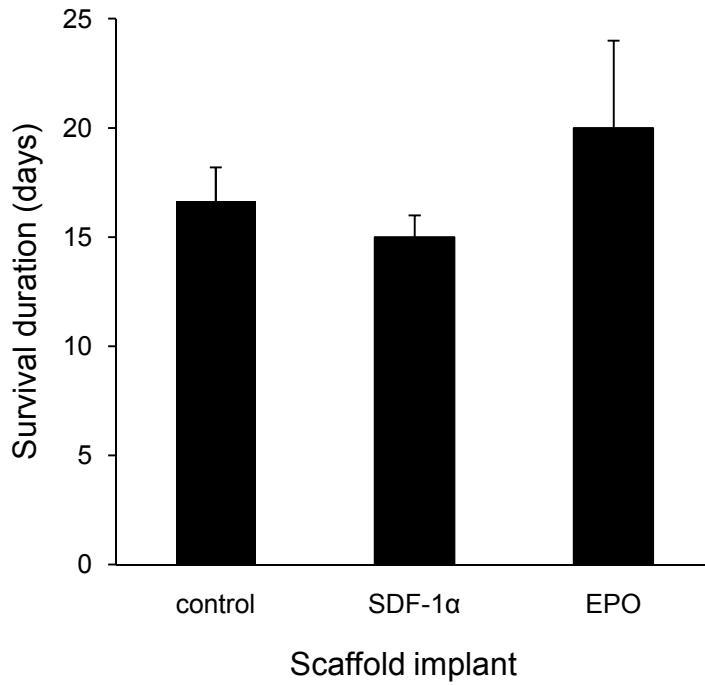


Figure 4.3 The survival duration of animals implanted with EPO-releasing, SDF-1 α -releasing, or control scaffolds. EPO group not only attract more cancer cell recruitment but also maintain the survival days and even last slightly longer than the control group. On the other hand, SDF-1 α group had shorter period of survival days. (n=3)

4.3.2 Substantial release of histamine from scaffold implants enhance cancer cell accumulation

A previous study had shown that biomaterial-mediated acute inflammatory responses are both histamine and mast cell dependent (70). Direct administration of histamine led to vasodilation, increased vascular permeability, and localized edema. Since cancer cells are recruited by inflammatory responses, it is possible that mast cell activation and histamine release are responsible to cancer cell recruitment. In this study, we implanted histamine-releasing scaffolds to create localized histaminic responses. Interestingly, this approach tremendously enhanced cell recruitment to the implant area. *In vivo* imaging detection showed very intense signal as compared with control animals implanted with PLGA scaffold (Figure 4.4). The signals were quantified by ImageJ image processing program (Figure 4.5). Moreover, in comparison of the survival period between both histamine group and control group, animals treated with histamine scaffold implantation had a trend of shorter survival period (Figure 4.6).

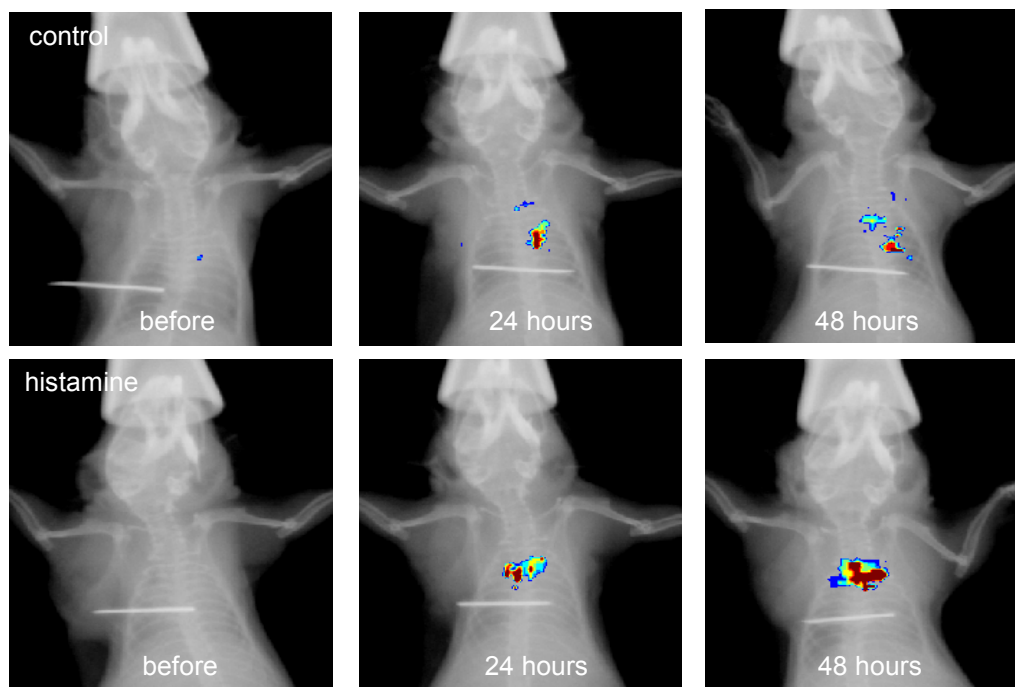


Figure 4.4 Histamine-releasing scaffolds significantly enhanced the recruitment of B16F10 melanoma cells to the implant area at different time points as shown in images.

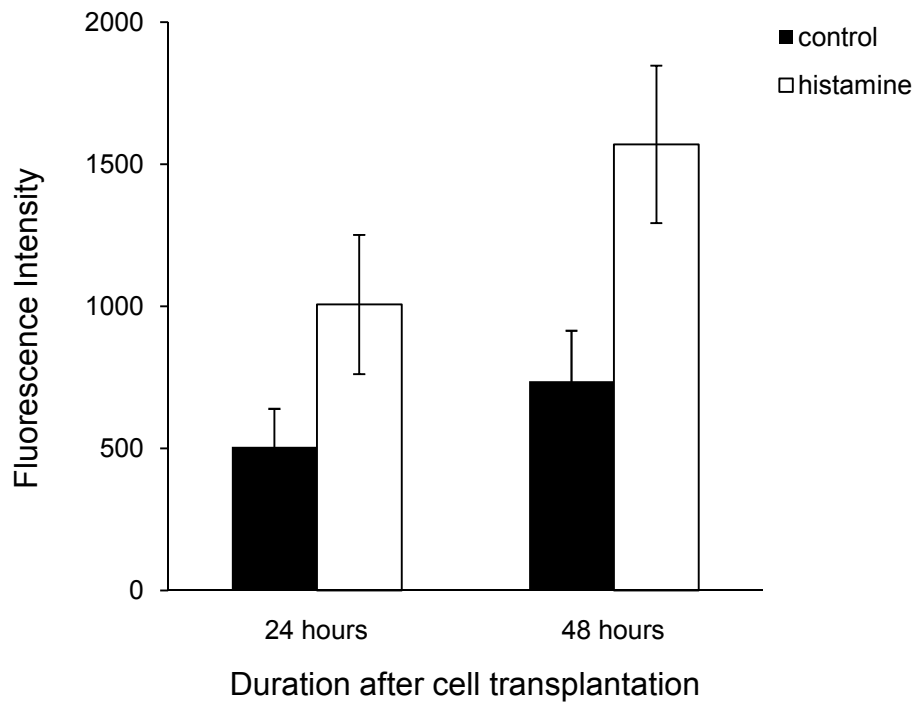


Figure 4.5 Histamine-releasing scaffolds significantly enhanced the recruitment of B16F10 melanoma cells to the implant area at different time points as shown in images. The signals were quantified to express the magnitude of recruitment as compare to control group. (n=2)

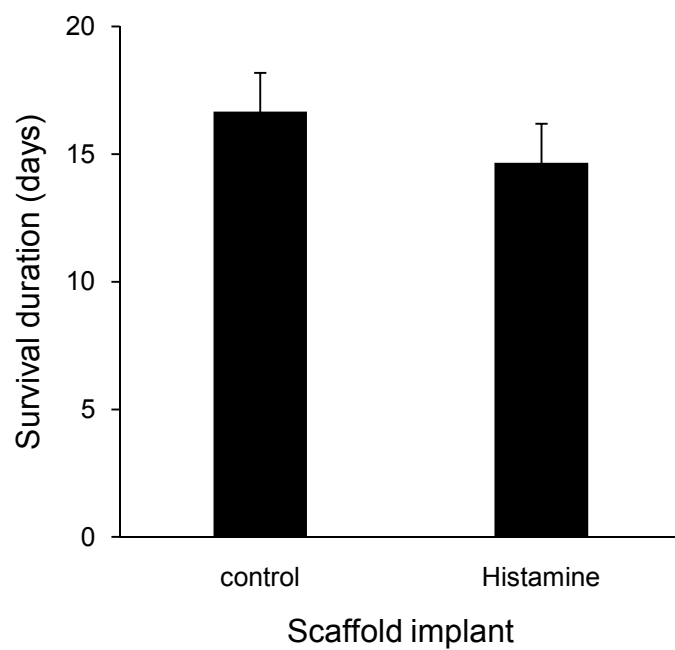


Figure 4.6 Localized release of histamine slightly reduces the survival of cancer cell bearing mice by compared with mice implanted with control PLGA scaffold. (n=3)

4.3.3 Effectiveness of mast cell stabilizer on cancer cell extravasation

Since mast cells are the major source of tissue histamine during inflammatory responses, it is likely that mast cell activation is responsible for histamine release and the inflammation-mediated cancer cell recruitment. To test this hypothesis, mast cell stabilizer-Cromolyn was tested to evaluate its pharmaceutical effects of reducing B16F10 melanoma cell recruitment. To maintain the therapeutic efficacies of cromolyn, animals were administered the drug one hour before cell transplantation and boosted with these agents every 6 hours. Cromolyn treatment exerted only mild effect on reducing B16F10 melanoma recruitment by *in vivo* imaging detection (Figure 4.7).

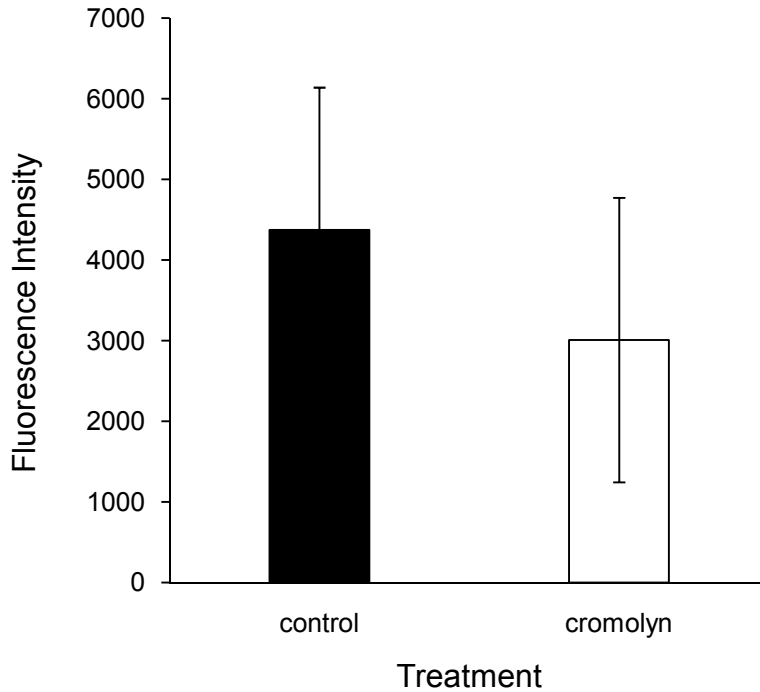


Figure 4.7 Cromolyn treatment reduces about 30% of B16F10 melanoma recruitment to the implant site. *In vivo* imaging was detected and the images were quantified by ImageJ image processing program.

4.4 Discussion

EPO scaffold was shown to induce more melanoma recruitment to the implant site while SDF-1 α did not exert influence on cancer cell migration as compared to the control signal. It is interesting that EPO scaffold not only prompts more cell migration but also extended the lifespan of animals beyond the controls. *In vivo*, EPO is naturally produced by the kidney and is regulated under hypoxia conditions. It is known to elicit proliferation, maturation, and differentiation of red blood cells. Recent studies demonstrated that high levels of EPO and EPO receptor expression are found in many different cell types, including cancer cells such as breast, head-and-neck tumors, colon, lung, prostate and melanoma (157-159). EPO/EPO receptors are known to induce proliferation, chemotaxis, and angiogenesis, and inhibit apoptosis (160, 161). Pretreating some cancer cell lines with EPO causes them less responsive to the chemotherapy drug, cisplatin (162). However, the degree of influence of EPO pathway in different cancer types is highly variable. The biological influence of EPO on cancers is still not clear. Based on what we have found here, EPO may play a role in immunomodulation (163). EPO have shown to antagonize proinflammatory cytokines and promotes wound healing following injury (164). On the other hand, it was demonstrated in murine model that EPO mediates an augmented B cell response. These studies along with our findings point to potential therapeutic applications of EPO scaffold for possible cancer vaccine design (165).

Though the result of applying SDF-1 α -releasing scaffold for distracting cancer cells from circulation to localized inflammation site was not as we expected, the survival duration of SDF-1 α treated group provide useful information. Our results indicated B16F10 melanoma may require CXCR4/SDF-1 α axis for recruitment. However, continuous release of SDF-1 α at higher concentration may repel T lymphocytes migration and cause impaired immune reaction to the animals (166-168). This may explain why SDF-1 α group had shorter survival period due to impaired immunity induced from animals to loss protection from massive tumor growth. In addition, the cell recruitment to the SDF-1 α releasing scaffold without enhancement may due to

localized release of SDF-1 α causing reduced inflammatory responses and cytokines which are required for triggering cancer cell migration (169-171).

We are surprised to find that localized delivery of histamine showed intense signal detection by *in vivo* imaging system. Although it is well established that mast cells are required for inflammatory responses to biomaterial implants, the potential role of histamine and mast cells in cancer cell migrations has not been determined yet. However, there are several pieces of information to support this observation. First, it has been shown that mast cell accumulation surrounding the tumor contributes to a permissive microenvironment for carcinogenesis and metastasis (172-174). Second, mast cells recruited by tumor-derived chemoattractants selectively secrete factors such as histamine, heparin, VEGF as well as proteases that facilitate new blood vessel formation and metastases. In addition, mast cell mediators could also promote brain metastases by regulating the permeability of the blood-brain-barrier (173, 175, 176). Further, histamine was demonstrated to have influence on the invasive and metastatic phenotype of colorectal cancer cells (177).

Our results showed that the release of histamine not only promotes cancer cell migration but also reduce the lifespan of the cancer cell-transplanted animals. It may be due to the continuous release of histamine which alters Th1/Th2 balance which then promotes tumor progression in the animals (178). However, this study still offer a new direction for us to explore potential application of using appropriate amount of histamine for develop advance cancer trap. To determined how mast cell activation affect cancer cell migration, mast cell function-related pharmaceutical agents, such as mast cell stabilizer- cromolyn was tested. Cromolyn treatment seemed to slightly reduce melanoma migration to the inflamed area. This drug is known as a mast cell stabilizer that prevents the release of inflammatory chemicals such as histamine from mast cells (179). The mechanism of cromolyn action is not fully understood. It is shown to inhibit chloride channels and may thus inhibit the exaggerated neuronal reflexes triggered by irritant receptors that are stimulated on sensory nerve endings. This causes the release of preformed

cytokines from T cells, and eosinophils in allergen-induced asthma (181). The possible mechanisms of our treatment of cromolyn in the inflammation-mediated cancer migration are: (i) dose frequency issue, (ii) mast cell activation was not fully antagonized or (iii) the influence of mast cells in assisting melanoma cell migration in our model is not high. Further studies are needed to determine the potential mechanisms.

4.5 Conclusion

It is intriguing that biomaterial-induced cancer metastasis model could be used not only for the exploration of inflammation-mediated migration mechanism but also to the discovery of pharmaceutical effects of drug screened for inflammation-induced cancer migration and tumor progression. EPO-releasing scaffold draws our attention to further apply its immunomodulation and chemoattractant characteristics to the possibility of cancer vaccine development. The strategy of releasing chemokines for cancer therapy under metastasis condition should be taken into serious consideration. Incorrect usage of this strategy could worsen cancer cell dissemination and thus enhance the mortality rate. Further, localized release of histamine is potent enough to enhance B16F10 melanoma cell immigration to the implant site. Increased vasculature permeability at the inflamed area did correlate with enhanced cancer cell accumulation. However, the substantial delivery of histamine at the implant site also shortens the survival periods of animals. We are still optimistic of further manipulating the release profile of histamine for the purpose of designing implantable cancer traps. Since mast cell is indicated to play a role in biomaterial-mediated inflammatory response and cancer progression (70, 175), mast cell-related pharmaceutical agent- mast stabilizer (cromolyn) was tested. Cromolyn showed a trend in reducing melanoma cell migration. It was recently shown using cromolyn, and mast cell deficient mice that mast cells are required for the development of pancreatic islet tumors (181). Our novel inflammation-induced cancer metastasis model along with *in vivo* imaging systems using either exogenous or endogenous labeling methods should be able to

provide platforms to perform high through output of list of different categorized anti-inflammatory drugs for the treatment of cancer therapy.

CHAPTER 5

SUMMARY AND FUTURE WORK

The potential role of inflammatory responses in cancer metastasis has not yet been fully determined mostly due to the lack of quantifiable animal models. Taking advantage of the nature of localized foreign body reactions, we have established an animal model in which cancer cells migrated from the intraperitoneal transplantation sites to the subcutaneous biomaterial microsphere implantation area. This animal model allows us to study the potential cellular and molecular mechanism of cancer cell migrations. We have also incorporated this animal model with whole body imaging technique. The combination systems can be used to monitor cancer migration in real time.

We further investigated the mechanism governing the inflammation-mediated cancer metastasis (Figure 5.1). Our results support that B16F10 melanoma cell migration to the inflamed area was mediated through CXCR4/CXCL12 axis while CCR7/CCL21 is important to mediate lymphatic pathway for B16F10 melanoma cell migration. Surprisingly, we find that T-lymphocytes play a critical role in cancer cell migration. Although the interaction between T-lymphocytes and cancer cell migration has yet to be determined, further study has revealed that lymphocyte-associated RANTES release is essential to cancer cell trafficking.

In an effort to develop novel treatments to combat cancer metastasis, several lines of studies were carried out and many interesting results were obtained from these works. First, EPO-releasing scaffolds were found to prolong lifespan of animals. However, the strategy of releasing chemokines for cancer therapy under metastasis condition should be taken into serious consideration. Incorrect condition could worsen cancer cell dissemination and thus increase the mortality rate. Second, we find that localized release of histamine is powerful to enhance B16F10 melanoma cell immigration to the implant site. However, the substantial

delivery of histamine at the implant site also shortens the survival periods of animals. Advanced manipulation of histamine releasing profile for the purpose of implantable cancer trap design is still possible. Third, mast cell-related pharmaceutical agent, mast stabilizer (cromolyn) was tested. Cromolyn showed a trend in reducing melanoma cell migration. The evaluation of over-the-counter drugs, including Aspirin, Tylenol Severe Allergy and Claritin, on the tumor progression under inflammatory stimuli could be also tested in the future. Finally, it is also our interests to establish a 3D image model and cell multi-labeling system which would allow us to illustrate cancer cell migration and the cell-cell interaction in real-time manner so as to further investigate the mechanisms involved inflammation-mediated cancer metastasis.

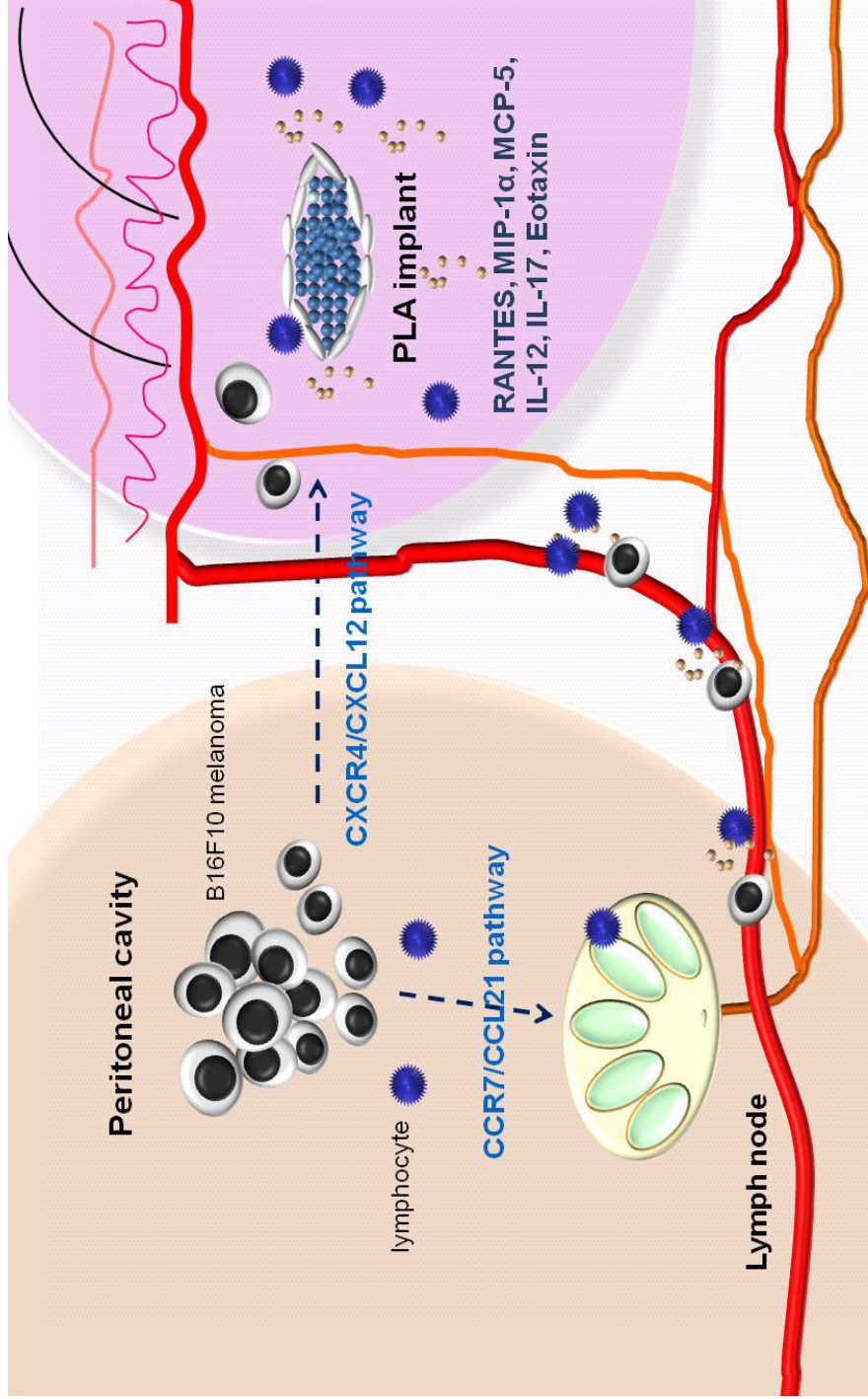


Figure 5.1 General view of mechanisms involved in inflammation-mediated cancer metastasis. B16F10 melanoma cells may migrate through lymphatic system via CCR7/CCL21 pathway. Cancer cells then may go from lymphatic system to the blood circulation and reach to the implant area. On the other hand, CXCR4/CXCL12 pathway is involved in cell migration from peritoneal cavity to the implant site. Furthermore, lymphocyte plays a role in assisting cancer cell migration in response to inflammatory stimulus. Finally, RANTES secreted from implant site is related to lymphocyte associated cancer cell migration while other cytokines expressed from implant site such as MIP-1 α , MCP-5, IL-12p40/p70, IL-17, and eotaxin may be potent chemokines to affect cancer cell migration.

APPENDIX A
RELATIVE CYTOKINE LEVELS
IN BIOMATERIALS-MEDIATED INFLAMMATORY RESPONSES

Cytokine	Balb/c mice	SCID mice	Fold Change (Balb/c/SCID)
Axl	1041.00	1047.25	0.99
BLC	370.50	232.37	1.59
CD30	220.50	140.87	1.57
CD30 L	155.50	130.00	1.20
CD40	4209.50	3974.30	1.06
CRG-2	150.00	107.81	1.39
CTACK	451.50	519.10	0.87
CXCL16	1752.00	1657.39	1.06
Eotaxin	814.50	327.04	2.49
Eotaxin-2	971.50	890.53	1.09
Fas Ligand	107.00	64.32	1.66
Fractalkine	358.00	645.93	0.55
GCSF	135.00	272.23	0.50
GM-CSF	339.00	540.39	0.63
IFN γ	173.50	446.17	0.39
IGFBP-3	509.00	346.52	1.47
IGFBP-5	1327.00	1040.00	1.28
IGFBP-6	268.00	158.08	1.70
IL-1 beta	164.50	1.00	N/A
IL-10	257.00	230.11	1.12
IL-12 p40/p70	1016.00	449.34	2.26
IL-12 p70	252.50	230.56	1.10
IL-13	102.50	67.94	1.51
IL-17	291.50	124.11	2.35
IL-1 α	15057.50	17417.34	0.86
IL-2	245.00	157.63	1.55
IL-3	1.00	1.00	N/A
IL-3 R β	216.00	214.25	1.01
IL-4	265.50	180.73	1.47
IL-5	276.00	228.75	1.21
IL-6	405.00	502.79	0.81

Cytokine	Balb/c mice	SCID mice	Fold Change (Balb/c/SCID)
IL-9	1026.00	896.87	1.14
KC	258.00	369.17	0.70
Leptin	123.00	103.73	1.19
Leptin R	126.00	91.05	1.38
LIX	259.50	219.69	1.18
L-Selectin	181.50	128.64	1.41
Lymphotactin	381.50	288.99	1.32
MCP1	22038.50	12724.19	1.73
MCP-5	292.00	142.68	2.05
M-CSF	1728.50	966.62	1.79
MIG	121.50	211.53	0.57
MIP-1 α	4435.50	1178.61	3.76
MIP-1 γ	19518.50	19548.99	1.00
MIP-2	16345.00	9269.44	1.76
MIP-3 β	116.50	85.16	1.37
MIP-3 α	186.00	147.67	1.26
PF-4	2825.00	2901.68	0.97
P-Selectin	2730.00	2626.28	1.04
RANTES	1406.00	343.35	4.09
SCF	222.50	254.57	0.87
SDF-1 α	118.00	106.90	1.10
sTNF RI	13673.50	11681.47	1.17
sTNF RII	9142.50	6171.63	1.48
TARC	181.00	155.37	1.16
TCA-3	210.00	126.38	1.66
TECK	237.50	269.06	0.88
TIMP-1	3558.00	2422.90	1.47
TNF α	232.00	289.44	0.80
TPO	172.00	120.94	1.42
VCAM-1	5843.00	5501.69	1.06
VEGF	477.00	307.11	1.55

REFERENCES

1. Kang, Y. 2009. New tricks against an old foe: molecular dissection of metastasis tissue tropism in breast cancer. *Breast Dis.* 26:129-138.
2. Nguyen, D.X., Chiang, A.C., Zhang, X.H., Kim, J.Y., Kris, M.G., Ladanyi, M., Gerald, W.L., and Massagué, J. 2009. WNT/TCF signaling through LEF1 and HOXB9 mediates lung adenocarcinoma metastasis. *Cell.* 138(1):51-62.
3. Nguyen, D.X., Bos, P.D., and Massagué, J. 2009. Metastasis: from dissemination to organ-specific colonization. *Nat Rev Cancer.* 9(4):274-284.
4. Gien, L.T., Beauchemin, M.C., Thomas, G. 2010. Adenocarcinoma: A unique cervical cancer. *Gynecol Oncol.* 116(1):140-146.
5. Agarwal, M., Brahmanday, G., Chmielewski, G.W., Welsh, R.J., and Ravikrishnan, K.P. 2009. Age, tumor size, type of surgery, and gender predict survival in early stage (stage I and II) non-small cell lung cancer after surgical resection. *Lung Cancer.*
6. Scarpa, R. 2009. Surgical management of head and neck carcinoma. *Semin Oncol Nurs.* 25(3):172-182.
7. Liotta, L.A., and Stetler-Stevenson, W.G. 1993. Principles of molecular cell biology of cancer: cancer metastasis. In *Cancer: Principles & Practice of Oncology.* V. Devita, S. Hellman, and S.A. Rosenberg, editors. JB Lippincott Co. Philadelphia, USA. 134-149.
8. Klein, C.A. 2009. Parallel progression of primary tumours and metastases. *Nat Rev Cancer.* 9(4):302-312.
9. Nguyen, D.X., Bos, P.D., and Massagué, J. 2009. Metastasis: from dissemination to organ-specific colonization. *Nat Rev Cancer.* 9(4):274-284.
10. Clarke, N.W., Hart, C.A., and Brown, M.D. 2009. Molecular mechanisms of metastasis in prostate cancer. *Asian J Androl.* 11(1):57-67.
11. Melnikova, V.O., and Bar-Eli, M. 2009. Inflammation and melanoma metastasis. *Pigment Cell Melanoma Res.* 22(3):257-267.
12. Rusciano, D. 2000. Differentiation and metastasis in melanoma. *Crit Rev Oncog.* 11(2):147-163.
13. Wu, Y., and Zhou, B.P. 2009. Inflammation: A driving force speeds cancer metastasis. *Cell Cycle.* 8(20):3267-3273.
14. Weinberg, F., and Chandel, N.S. 2009. Reactive oxygen species-dependent signaling regulates cancer. *Cell Mol Life Sci.* 66(23):3663-3673.
15. Gómez-Raposo, C., Mendiola, M., Barriuso, J., Casado, E., Hardisson, D., and Redondo, A. 2009. Angiogenesis and ovarian cancer. *Clin Transl Oncol.* 11(9):564-571.
16. Folkman, J. 1992. The role of angiogenesis in tumor growth. *Semin Cancer Biol.* 3(2): 65-71.
17. Chambers, A.F., Groom, A.C., and MacDonald, I.C. 2002. Dissemination and growth of cancer cells in metastatic sites. *Nat Rev Cancer.* 2(8):563-572.
18. Takeuchi, H., Kitajima, M., and Kitagawa, Y. 2008. Sentinel lymph node as a target of molecular diagnosis of lymphatic micrometastasis and local immunoresponse to malignant cells. *Cancer Sci.* 99(3):441-450.
19. Vence, L., Palucka, A.K., Fay, J.W., Ito, T., Liu, Y.J., Banchereau, J., and Ueno, H. 2007. Circulating tumor antigen-specific regulatory T cells in patients with metastatic melanoma. *PNAS.* 104(52):20884-20889.
20. López-Novoa, J.M., and Nieto, M.A. 2009. Inflammation and EMT: an alliance towards organ fibrosis and cancer progression. *EMBO Mol Med.* 1(6-7):303-314.

21. Lu, H., Ouyang, W., and Huang, C. 2006. Inflammation, a key event in cancer development. *Mol Cancer Res.* 4(4):221-233.
22. Lorusso, G., and Rüegg, C. 2008. The tumor microenvironment and its contribution to tumor evolution toward metastasis. *Histochem Cell Biol.* 130(6):1091-1103.
23. Marx, J. 2004. Inflammation and cancer: the link grows stronger. *Science.* 306(5698): 966-968.
24. Pollard, J.W. 2004. Tumour-educated macrophages promote tumor progression and metastasis. *Nat Rev Cancer.* 4(1):71-78.
25. Aggarwal, B.B., Shishodia, S., Sandur, S.K, Pandey, M.K, and Sethi, G. 2006. Inflammation and cancer: how hot is the link? *Biochem Pharmacol.* 72(11): 1605-1621.
26. Arias, J.I., Aller, M.A., and Arias, J. 2007. Cancer cell: using inflammation to invade the host. *Mol Cancer.* 6:29.
27. Saha, A., Lee, Y.C., Zhang, Z., Chandra, G., Su, S.B., and Mukherjee, A.B. 2010. Lack of an endogenous anti-inflammatory protein in mice enhances colonization of B16F10 melanoma cells in the lungs. *J Biol Chem.* 285(14):10822-10831.
28. Shields, J.D., Emmett, M.S., Dunn D.B., Joory, K.D., Sage, L.M., Rigby, H., Mortimer, P.S., Orlando, A., Levick, J.R., and Bates, D.O. 2007. Chemokine-mediated migration of melanoma cells towards lymphatics - a mechanism contributing to metastasis. *Oncogene.* 26(21):2997-3005.
29. Opdenakker, G., and Van Damme, J. 2004. The countercurrent principle in invasion and metastasis of cancer cells. Recent insights on the roles of chemokines. *Int J Dev Biol.* 48(5-6):519-527.
30. Gomperts, B., and Strieter, R. 2006. Chemokine-directed metastasis. *Contrib Microbiol.* 13:170-190.
31. Kakinuma, T., and Hwang, S.T. 2006. Chemokines, chemokine receptors, and cancer metastasis. *J Leukoc Biol.* 79(4):639-651.
32. Ben-Baruch, A. 2006. The multifaceted roles of chemokines in malignancy. *Cancer Metastasis Rev.* 25(3):357-371.
33. Soria, G., and Ben-Baruch, A. 2008. The inflammatory chemokines CCL2 and CCL5 in breast cancer. *Cancer Lett.* 267(2):271-285.
34. Mantovani, A., Bottazzi, B., Colotta, F., Sozzani, S., and Ruco, L. 1992. The origin and function of tumor-associated macrophages, *Immunol Today.* 13(7):265-270.
35. Negus, R.P., Stamp, G.W., Relf, M.G., Burke, F., Malik, S.T., Bernasconi, S., Allavena, P., Sozzani, S., Mantovani, A., and Balkwill, F.R. 1995. The detection and localization of monocyte chemoattractant protein-1 (MCP-1) in human ovarian cancer. *J Clin Invest.* 95(5):2391-2396.
36. Luboshits, G., Shina, S., Kaplan, O., Engelberg, S., Nass, D., Lifshitz-Mercer, B., Chaitchik, S., Keydar, I., and Ben-Baruch, A. 1999. Elevated expression of the CC chemokine regulated on activation, normal T cell expressed and secreted (RANTES) in advanced breast carcinoma. *Cancer Res.* 59(18):4681-4687.
37. Germano, G., Allavena, P., and Mantovani, A. 2008. Cytokines as a key component of cancer-related inflammation. *Cytokine.* 43(3):374-379.
38. Müller, A., Homey, B., Soto, H., Ge, N., Catron, D., Buchanan, M.E., McClanahan, T., Murphy, E., Yuan, W., Wagner, S.N., Barrera, J.L., Mohar, A., Verástegui, E., and Zlotnik, A. 2001. Involvement of chemokine receptors in breast cancer metastases. *Nature.* 410(6824):50-56.
39. Murakami, T., Maki, W., Cardones, A.R., Fang, H., Tun Kyi, A., Nestle, F.O., and Hwang, S.T. 2002. Expression of CXC chemokine receptor-4 enhances the pulmonary metastatic potential of murine B16 melanoma cells. *Cancer Res.* 62(24):7328-7334.
40. Ghadjar, P., Coupland, S.E., Na, I.K., Noutsias, M., Letsch, A., Stroux, A., Bauer, S., Buhr, H.J., Thiel, E., Scheibenbogen, C., and Keilholz, U. 2006. Chemokine receptor

- CCR6 expression level and liver metastases in colorectal cancer. *J Clin Oncol*. 24(12):1910-1916.
41. Hassan, S., Baccarelli, A., Salvucci, O., and Basik, M. 2008. Plasma stromal cell-derived factor-1: host derived marker predictive of distant metastasis in breast cancer. *Clin Cancer Res*. 14(2):446-454.
 42. Bussard, K.M., Gay, C.V., and Mastro, A.M. 2008. The bone microenvironment in metastasis; what is special about bone? *Cancer Metastasis Rev*. 27(1):41-55.
 43. Le Bitoux, M.A., and Stamenkovic, I. Tumor-host interactions: the role of inflammation. 2008. *Histochem Cell Biol*. 130(6):1079-1090.
 44. Leffers, N., Gooden, M.J., de Jong, R.A., Hoogeboom, B.N., ten Hoor, K.A., Hollema, H., Boezen, H.M., van der Zee, A.G., Daemen, T., and Nijman, H.W. 2009. Prognostic significance of tumor-infiltrating T-lymphocytes in primary and metastatic lesions of advanced stage ovarian cancer. *Cancer Immunol Immunother*. 58(3):449-459.
 45. DeNardo DG, Barreto JB, Andreu P, Vazquez L, Tawfik D, Kolhatkar N, Coussens LM. 2009. CD4(+) T cells regulate pulmonary metastasis of mammary carcinomas by enhancing protumor properties of macrophages. *Cancer Cell*. 16(2):91-102.
 46. Mantovani, A., Allavena, P., Sica, A., and Balkwill, F. 2008. Cancer-related inflammation. *Nature*. 454(7203):436-444.
 47. Welch, D.R. 1997. Technical considerations for studying cancer metastasis in vivo. *Clin and Exp Metastasis*. 15(3):272-306.
 48. Gupta, G.P., Perk, J., Acharyya, S., de Candia, P., Mittal, V., Todorova-Manova, K., Gerald, W.L., Brogi, E., Benezra, R., and Massagué, J. 2007. ID genes mediate tumor reinitiation during breast cancer lung metastasis. *Proc Natl Acad Sci U S A*. 104(49):19506-19511.
 49. Lunt, S.J., Kalliomaki, T.M., Brown, A., Yang, V.X., Milosevic, M., and Hill, R.P. 2008. Interstitial fluid pressure, vascularity and metastasis in ectopic, orthotopic and spontaneous tumors. *BMC Cancer*. 8:2.
 50. Yamamoto, M., Kikuchi, H., Ohta, M., Kawabata, T., Hiramatsu, Y., Kondo, K., Baba, M., Kamiya, K., Tanaka, T., Kitagawa, M., and Konno, H. 2008. TSU68 prevents liver metastasis of colon cancer xenografts by modulating the premetastatic niche. *Cancer Res*. 68(23):9754-9762.
 51. Mehrotra, S., Languino, L.R., Raskett, C.M., Mercurio, A.M., Dohi, T., and Altieri, D.C. 2010. IAP regulation of metastasis. *Cancer Cell*. 17(1):53-64.
 52. Kaneda, T., Sonoda, Y., Ando, K., Suzuki, T., Sasaki, Y., Oshio, T., Tago, M., and Kasahara, T. 2008. Mutation of Y925F in focal adhesion kinase (FAK) suppresses melanoma cell proliferation and metastasis. *Cancer Lett*. 270(2):354-361.
 53. Tang, Z.Y., Ye, S.L., Liu, Y.K., Qin, L.X., Sun, H.C., Ye, Q.H., Wang, L., Zhou, J., Qiu, S.J., Li, Y., Ji, X.N., Liu, H., Xia, J.L., Wu, Z.Q., Fan, J., Ma, Z.C., Zhou, X.D., Lin, Z.Y., and Liu, K.D. 2004. A decade's studies on metastasis of hepatocellular carcinoma. *J Cancer Res Clin Oncol*. 130(4):187-196.
 54. Kawaguchi, T., Kawaguchi, M., Miner, K.M., Lembo, T.M., and Nicolson, G.L. 1983. Brain meninges tumor formation by in vivo-selected metastatic B16 melanoma variants in mice. *Clin Exp Metastasis*. 1(3):247-259.
 55. Wexler, H. 1966. Accurate identification of experimental pulmonary metastases *J Natl Cancer Inst*. 36(4):641-645.
 56. Power, C.A., Pwint, H., Chan, J., Cho, J., Yu, Y., Walsh, W., Russell, P.J. 2009. A novel model of bone-metastatic prostate cancer in immunocompetent mice. *Prostate*. 69(15):1613-1623.
 57. Wang, J., Xia, T.S., Liu, X.A., Ding, Q., Du, Q., Yin, H., and Wang, S. 2010. A novel orthotopic and metastatic mouse model of breast cancer in human mammary microenvironment. *Breast Cancer Res Treat*. 120(2):337-344.

58. Céspedes, M.V., Casanova, I., Parreño, M., and Mangues, R. 2006. Mouse models in oncogenesis and cancer therapy. *Clin Transl Oncol.* 8(5):318-329.
59. Talmadge, J.E., Singh, R.K., Fidler, I.J., and Raz, A. 2007. Murine models to evaluate novel and conventional therapeutic strategies for cancer. *Am J Pathol.* 170(3):793-804.
60. Khanna, C., and Hunter, K. 2005. Modeling metastasis in vivo. *Carcinogenesis.* 26(3):513-523.
61. Schwertfeger, K.L., Xian, W., Kaplan, A.M., Burnett, S.H., Cohen, D.A., and Rosen, J.M. 2006. A critical role for the inflammatory response in a mouse model of preneoplastic progression. *Cancer Res.* 66(11):5676-5685.
62. Taketo, M.M., and Edelmann, W. 2009. Mouse models of colon cancer. *Gastroenterology.* 136(3):780-798.
63. Tang, L., and Eaton, J.W. 1999. Natural responses to unnatural materials: A molecular mechanism for foreign body reactions. *Molecular Medicine,* 5(6):351-358.
64. Tang, L., and Hu, W.J. 2005. Molecular deterrents of biocompatibility. *Expert Review of Medical Devices.* 2(4):493-500.
65. Eskin, S.G., Horbett, T.A., McIntire, L.V., Mitchell, R.N., Ratner, B.D., Schoen, F.J., and Yee, A. 2004. Some background concept. In *Biomaterials Science: An introduction to Materials in Medicine.* B.D. Ratner, A.S. Hoffman, F.J. Scheon, and J.E. Lemons, editor. Elsevier Academic Press. California, USA. 237-245.
66. Tang, L., and Eaton, J.W. 1993. Fibrin(ogen) mediates acute inflammatory responses to biomaterials. *J Exp Med.* 178(6):2147-2156.
67. Rodriguez, A., Meyerson, H., and Anderson, J.M. 2009. Quantitative in vivo cytokine analysis at synthetic biomaterial implant sites. *J Biomed Mater Res A.* 89(1):152-159.
68. Barbosa, J.N., Madureira, P., Barbosa, M.A., and Aguas, A.P. 2005. The attraction of Mac-1+ phagocytes during acute inflammation by methyl-coated self-assembled monolayers. *Biomaterials.* 26(16):3021-3027.
69. Chang, D.T., Colton, E., and Anderson, J.M. 2009. Paracrine and juxtacrine lymphocyte enhancement of adherent macrophage and foreign body giant cell activation. *J Biomed Mater Res A.* 89(2):490-498.
70. Tang, L., Jennings, T.A., and Eaton, J.W. 1998. Mast cells mediate acute inflammatory responses to implanted biomaterials. *Proc Natl Acad Sci U S A.* 95(15):8841-8846.
71. Hu, W.J., Eaton, J.W., Ugarova, T.P., and Tang, L. 2001. Molecular basis of biomaterial-mediated foreign body reactions. *Blood.* 98(4):1231-1238.
72. Allen, L.T., Tosetto, M., Miller, I.S., O'Connor, D.P., Penney, S.C., Lynch, I., Keenan, A.K., Pennington, S.R., Dawson, K.A., and Gallagher, W.M. 2006. Surface-induced changes in protein adsorption and implications for cellular phenotypic responses to surface interaction. *Biomaterials.* 27(16):3096-3108.
73. Jiang, W.W., Su, S.H., Eberhart, R.C., and Tang, L. 2007. Phagocyte responses to degradable polymers. *J Biomed Mater Res A.* 82(2):492-497.
74. Nair, A., Zou, L., Bhattacharyya, D., Timmons, R.B., and Tang, L. 2008. Species and density of implant surface chemistry affect the extent of foreign body reactions. *Langmuir.* 24(5):2015-2024.
75. Xu, L.C., and Siedlecki, C.A. 2007. Effects of surface wettability and contact time on protein adhesion to biomaterial surfaces. *Biomaterials.* 28(22):3273-3283.
76. Fang, F., Satulovsky, J., and Szleifer, I. 2005. Kinetics of protein adsorption and desorption on surfaces with grafted polymers. *Biophys J.* 89(3):1516-1533.
77. Agashe, M., Raut, V., Stuart, S.J., and Latour, R.A. 2005. Molecular simulation to characterize the adsorption behavior of a fibrinogen gamma-chain fragment. *Langmuir.* 21(3):1103-1117.

78. Hylton, D.M., Shalaby, S.W., and Latour, R.A. Jr. 2005. Direct correlation between adsorption-induced changes in protein structure and platelet adhesion. *J Biomed Mater Res A*. 73(3):349-358.
79. Anderson, J.M., Rodriguez, A., and Chang, D.T. 2008. Foreign body reaction to biomaterials. *Semin Immunol*. (2):86-100.
80. Bridges, A.W., and Garcia, A.J. 2008. Anti-inflammatory polymeric coatings for implantable biomaterials and devices. *J Diabetes Sci Technol*. 2(6):984-994.
81. Brodbeck, W.G., Voskerician, G., Ziats, N.P., Nakayama, Y., Matsuda, T., and Anderson, J.M. 2003. In vivo leukocyte cytokine mRNA responses to biomaterials are dependent on surface chemistry. *J Biomed Mater Res A*. 64(2):320-329.
82. Nolan, C.M., Reyes, C.D., Debord, J.D., Garcia AJ, Lyon LA. 2005. Phase transition behavior, protein adsorption, and cell adhesion resistance of poly(ethylene glycol) cross-linked microgel particles. *Biomacromolecules*. 6(4):2032-2039.
83. Goreish, H.H., Lewis, A.L., Rose, S., and Lloyd, A.W. 2004. The effect of phosphorylcholine-coated materials on the inflammatory response and fibrous capsule formation: in vitro and in vivo observations. *J Biomed Mater Res A*. 68(1):1-9.
84. Refai AK, Textor M, Brunette DM, Waterfield JD. 2004. Effect of titanium surface topography on macrophage activation and secretion of proinflammatory cytokines and chemokines. *J Biomed Mater Res A*. 70(2):194-205.
85. Soskolne, W.A., Cohen, S., Sennerby, L., Wennerberg, A., and Shapira, L. 2002. The effect of titanium surface roughness on the adhesion of monocytes and their secretion of TNF-alpha and PGE2. *Clin Oral Implants Res*. 13(1):86-93.
86. Cuénod, C.A., Fournier, L., Balvay, D., Pradel, C., Siauve, N., Clement, O., Vecchio, S., Salvatore, M., Law, B., and Tung, C.H, 2007. Tumor Imaging. In Textbook of in vivo Imaging in Vertebrates. V, Ntziachristos, A. Leroy-Willig, and B. Tavitian, editors. John Wiley & Sons, Ltd. 277-304. West Sussex, England.
87. Hanyu, A., Kojima, K., Hatake, K., Nomura, K., Murayama, H., Ishikawa, Y., Miyata, S., Ushijima, M., Matsuura, M., Ogata, E., Miyazawa, K., and Imamura, T. 2009. Functional in vivo optical imaging of tumor angiogenesis, growth, and metastasis prevented by administration of anti-human VEGF antibody in xenograft model of human fibrosarcoma HT1080 cells. *Cancer Sci*. 100(11):2085-2092.
88. Löwik, C.W., Kaijzel, E., Que, I., Vahrmeijer, A., Kuppen, P., Mieog, J., Van de Velde, C. 2009. Whole body optical imaging in small animals and its translation to the clinic: intra-operative optical imaging guided surgery. *Eur J Cancer*. Suppl 1:391-393.
89. Simpson DR, Lawson JD, Nath SK, Rose BS, Mundt AJ, Mell LK. 2009. Utilization of advanced imaging technologies for target delineation in radiation oncology. *J Am Coll Radiol*. 6(12):876-883.
90. Wu Y, Cai W, Chen X. 2006. Near-infrared fluorescence imaging of tumor integrin alpha v beta 3 expression with Cy7-labeled RGD multimers. *Mol Imaging Biol*. 8(4):226-236.
91. Wessels, J.T., Busse, A.C., Mahrt, J., Dullin, C., Grabbe, E., and Mueller, G.A. 2007. In vivo imaging in experimental preclinical tumor research--a review. *Cytometry A*. 71(8):542-549.
92. Eisenblätter, M., Ehrchen, J., Varga, G., Sunderkötter, C., Heindel, W., Roth, J., Bremer, C., and Wall, A. 2009. In vivo optical imaging of cellular inflammatory response in granuloma formation using fluorescence-labeled macrophages. *J Nucl Med*. 50(10):1676-1682.
93. Schorpp M, Jäger R, Schellander K, Schenkel J, Wagner EF, Weiher H, and Angel P. 1996. The human ubiquitin C promoter directs high ubiquitous expression of transgenes in mice. *Nucleic Acids Res*. 24(9):1787-1788.

94. Killion, J.J., Radinsky, R., and Fidler, I.J. 1998-1999. Orthotopic models are necessary to predict therapy of transplantable tumors in mice. *Cancer Metastasis Rev.* 17(3):279-284.
95. Kim, J.B., Urban, K., Cochran, E., Lee, S., Ang, A., Rice, B., Bata, A., Campbell, K., Coffee, R., Gorodinsky, A., Lu, Z., Zhou, H., Kishimoto, T.K., and Lassota, P. 2010. Non-invasive detection of a small number of bioluminescent cancer cells in vivo. *PLoS One.* 5(2):e9364.
96. Taranova, A.G., Maldonado, D. 3rd., Vachon, C.M., Jacobsen, E.A., Abdala-Valencia, H., McGarry, M.P., Ochkur, S.I., Protheroe, C.A., Doyle, A., Grant, C.S., Cook-Mills, J., Birnbaumer, L., Lee, N.A., and Lee, J.J. 2008. Allergic pulmonary inflammation promotes the recruitment of circulating tumor cells to the lung. *Cancer Res.* 68(20):8582-8589.
97. Weng, H., Zhou, J., Tang, L., and Hu, Z. 2004. Tissue responses to thermally responsive hydrogel nanoparticles. *J Biomater Sci Polym Ed.* 15(9):1167-1180.
98. Fessi, H., Puisieux, F., Devissaguet, J.P., Ammoury, N., and Benita, S. 1989. Nanocapsules formation by interfacial polymer deposition following solvent displacement. *Int J Pharm.* 55: R1-R4.
99. Koller, F.L., Hwang, D.G., Dozier, E.A., and Fingleton, B. 2010. Epithelial interleukin-4 receptor expression promotes colon tumour growth. *Carcinogenesis.*
100. Ikebe M, Kitaura Y, Nakamura M, Tanaka H, Yamasaki A, Nagai S, Wada J, Yanai K, Koga K, Sato N, Kubo M, Tanaka M, Onishi H, Katano M. 2009. Lipopolysaccharide (LPS) increases the invasive ability of pancreatic cancer cells through the TLR4/MyD88 signaling pathway. *J Surg Oncol.* 100(8):725-731.
101. Ueki, M., Taie, S., Chujo, K., Asaga, T., Iwanaga, Y., Ono, J., and Maekawa, N. 2007. Urinary trypsin inhibitor reduces inflammatory response in kidney induced by lipopolysaccharide. *J Biosci Bioeng.* 104(4):315-320.
102. Garbi, N., Arnold, B., Gordon, S., Hämmerling, G.J., and Ganss, R. 2004. CpG motifs as proinflammatory factors render autochthonous tumors permissive for infiltration and destruction. *J Immunol.* 172(10):5861-5869.
103. Lores, B., García-Estevez, J.M., and Arias, C. 1998. Lymph nodes and human tumors (review). *Int J Mol Med.* 1(4):729-733.
104. Koch, M., Beckhove, P., Op den Winkel, J., Autenrieth, D., Wagner, P., Nummer, D., Specht, S., Antolovic, D., Galindo, L., Schmitz-Winnenthal, F.H., Schirmacher, V., Büchler, M.W., and Weitz, J. 2006. Tumor infiltrating T lymphocytes in colorectal cancer: Tumor-selective activation and cytotoxic activity in situ. *Ann Surg.* 244(6):986-992.
105. Kim, J.H., Yu, C.H., Yhee, J.Y., Im, K.S., and Sur, J.H. 2010. Lymphocyte infiltration, expression of interleukin (IL) -1, IL-6 and expression of mutated breast cancer susceptibility gene-1 correlate with malignancy of canine mammary tumours. *J Comp Pathol.* 142(2-3):177-186.
106. Romero, P., Cerottini, J.C., and Speiser, D.E. 2006. The human T cell response to melanoma antigens. *Adv Immunol.* 92:187-224.
107. Cuff S, Dolton G, Matthews RJ, Gallimore A. 2010. Antigen specificity determines the pro- or antitumoral nature of CD8+ T cells. *J Immunol.* 184(2):607-614.
108. Ponath PD, Qin S, Ringler DJ, Clark-Lewis I, Wang J, Kassam N, Smith H, Shi X, Gonzalo JA, Newman W, Gutierrez-Ramos JC, Mackay CR. 1996. Cloning of the human eosinophil chemoattractant, eotaxin. Expression, receptor binding, and functional properties suggest a mechanism for the selective recruitment of eosinophils. *J Clin Invest.* 97(3):604-612.

109. Amerio, P., Frezzolini, A., Feliciani, C., Verdolini, R., Teofoli, P., De Pità, O., and Puddu, P. 2003. Eotaxins and CCR3 receptor in inflammatory and allergic skin diseases: therapeutical implications. *Curr Drug Targets Inflamm Allergy*. 2(1):81-94.
110. Sutton, C.E., Lalor, S.J., Sweeney, C.M., Brereton, C.F., Lavelle, E.C., and Mills, K.H. 2009. Interleukin-1 and IL-23 induce innate IL-17 production from gammadelta T cells, amplifying Th17 responses and autoimmunity. *Immunity*. 31(2):331-341.
111. Rachitskaya, A.V., Hansen, A.M., Horai, R., Li, Z., Villasmil, R., Luger, D., Nussenblatt, R.B., and Caspi, R.R. 2008. Cutting edge: NKT cells constitutively express IL-23 receptor and ROR γ and rapidly produce IL-17 upon receptor ligation in an IL-6-independent fashion. *J Immunol*. 180(8):5167-5171.
112. Liu, G., Zhang, L., and Zhao, Y. 2010. Modulation of immune responses through direct activation of Toll-like receptors to T cells. *Clin Exp Immunol*.
113. Fossiez, F., Banchereau, J., Murray, R., Van Kooten, C., Garrone, P., and Lebecque, S. 1998. Interleukin-17. *Int Rev Immunol*. 16(5-6):541-551.
114. Laan, M., Lötval, J., Chung, K.F., and Lindén, A. 2001. IL-17-induced cytokine release in human bronchial epithelial cells in vitro: role of mitogen-activated protein (MAP) kinases. *Br J Pharmacol*. 133(1):200-206.
115. Jovanovic, D.V., Di Battista, J.A., Martel-Pelletier, J., Reboul, P., He, Y., Jolicoeur, F.C., and Pelletier, J.P. 2001. Modulation of TIMP-1 synthesis by antiinflammatory cytokines and prostaglandin E2 in interleukin 17 stimulated human monocytes/macrophages. *J Rheumatol*. 28(4):712-718.
116. Yamamura, Y., Gupta, R., Morita, Y., He, X., Pai, R., Endres, J., Freiberg, A., Chung, K., and Fox, D.A. 2001. Effector function of resting T cells: activation of synovial fibroblasts. *J Immunol*. 166(4):2270-2275.
117. Aggarwal, S., and Gurney, A.L. 2002. IL-17: prototype member of an emerging cytokine family. *J Leukoc Biol*. 71(1):1-8.
118. Yamauchi, K., Shibata, Y., Kimura, T., Abe, S., Inoue, S., Osaka, D., Sato, M., Igarashi, A., and Kubota, I. 2009. Azithromycin suppresses interleukin-12p40 expression in lipopolysaccharide and interferon-gamma stimulated macrophages. *Int J Biol Sci*. 5(7):667-678.
119. Jia, G.Q., Gonzalo, J.A., Lloyd, C., Kremer, L., Lu, L., Martinez-A, C., Wershil, B.K., and Gutierrez-Ramos, J.C. 1996. Distinct expression and function of the novel mouse chemokine monocyte chemoattractant protein-5 in lung allergic inflammation. *J Exp Med*. 184(5):1939-1951.
120. Owen, J.L., Iragavarapu-Charyulu, V., and Lopez, D.M. 2004. T cell-derived matrix metalloproteinase-9 in breast cancer: friend or foe? *Breast Dis*. 20:145-153.
121. Kim, H.K., Song, K.S., Park, Y.S., Kang, Y.H., Lee, Y.J., Lee, K.R., Kim, H.K., Ryu, K.W., Bae, J.M., and Kim, S. 2003. Elevated levels of circulating platelet microparticles, VEGF, IL-6 and RANTES in patients with gastric cancer: possible role of a metastasis predictor. *Eur J Cancer*. 39(2):184-191.
122. Sugasawa, H., Ichikura, T., Kinoshita, M., Ono, S., Majima, T., Tsujimoto, H., Chochi, K., Hiroi, S., Takayama, E., Saitoh, D., Seki, S., and Mochizuki, H. 2008. Gastric cancer cells exploit CD4+ cell-derived CCL5 for their growth and prevention of CD8+ cell-involved tumor elimination. *Int J Cancer*. 122(11):2535-2541.
123. Ohtani, N., Ohtani, H., Nakayama, T., Naganuma, H., Sato, E., Imai, T., Nagura, H., and Yoshie, O. 2004. Infiltration of CD8+ T cells containing RANTES/CCL5+ cytoplasmic granules in actively inflammatory lesions of human chronic gastritis. *Lab Invest*. 84(3):368-375.
124. Kapoor, S. 2008. Association of chemokine CCL5 and systemic malignancies. *J Hum Genet*. 53(5):377-178.

125. Mori, N., Krensky, A.M., Ohshima, K., Tomita, M., Matsuda, T., Ohta, T., Yamada, Y., Tomonaga, M., Ikeda, S., and Yamamoto, N. 2004. Elevated expression of CCL5/RANTES in adult T-cell leukemia cells: possible transactivation of the CCL5 gene by human T-cell leukemia virus type I tax. *Int J Cancer*. 111(4):548-557.
126. Gabellini, C., Trisciuglio, D., Desideri, M., Candiloro, A., Ragazzoni, Y., Orlandi, A., Zupi, G., and Del Bufalo, D. 2009. Functional activity of CXCL8 receptors, CXCR1 and CXCR2, on human malignant melanoma progression. *Eur J Cancer*. 45(14):2618-2627.
127. Pradelli, E., Karimjee-Soilihi, B., Michiels, J.F., Ricci, J.E., Millet, M.A., Vandebos, F., Sullivan, T.J., Collins, T.L., Johnson, M.G., Medina, J.C., Kleinerman, E.S., Schmid-Alliana, A., and Schmid-Antomarchi, H. 2009. Antagonism of chemokine receptor CXCR3 inhibits osteosarcoma metastasis to lungs. *Int J Cancer*. 125(11):2586-2594.
128. Waiser, T.C., Rifat, S., Ma, X., Kundu, N., Ward, C., Goloubeva, O., Johnson, M.G., Medina, J.C., Collins, T.L., and Fulton, A.M. 2006. Antagonism of CXCR3 inhibits lung metastasis in a murine model of metastatic breast cancer. *Cancer Res*. 66(15):7701-7707.
129. Steeg, P.S. 2006. Tumor metastasis: mechanistic insights and clinical challenges. *Nat Med*. 12(8):895-904.
130. Wu, L.*, Ko, C.*, Tsai, Y., Lin, V., and Tang, L. 2010. Animal model to study tumor metastasis in responding to local inflammatory responses. *J Clin Invest.* (*in manuscript*). *Co-First Author.
131. Ko, C., Wu, L., and Tang, L. 2009. Novel animal model for studying cancer metastasis. 12th SCBA International Symposium. Taipei, Taiwan.
132. Wu, L., Ko, C., and Tang, L. 2009. Foreign Body Reactions-Induced Cancer Metastasis. Society for Biomaterials Annual Meeting and Exposition. San Antonio, TX.
133. Matsusue, R., Kubo, H., Hisamori, S., Okoshi, K., Takagi, H., Hida, K., Nakano, K., Itami, A., Kawada, K., Nagayama, S., and Sakai, Y. 2009. Hepatic stellate cells promote liver metastasis of colon cancer cells by the action of SDF-1/CXCR4 axis. *Ann Surg Oncol*. 16(9):2645-2653.
134. Saur, D., Seidler, B., Schneider, G., Algül, H., Beck, R., Senekowitsch-Schmidtke, R., Schwaiger, M., and Schmid, R.M. 2005. CXCR4 expression increases liver and lung metastasis in a mouse model of pancreatic cancer. *Gastroenterology*. 129(4):1237-1250.
135. Gassmann, P., Haier, J., Schlüter, K., Domikowsky, B., Wendel, C., Wiesner, U., Kubitzka, R., Engers, R., Schneider, S.W., Homey, B., and Müller, A. 2009. CXCR4 regulates the early extravasation of metastatic tumor cells in vivo. *Neoplasia*. 11(7):651-661.
136. Sun, Y.X., Schneider, A., Jung, Y., Wang, J., Dai, J., Wang, J., Cook, K., Osman, N.I., Koh-Paige, A.J., Shim, H., Pienta, K.J., Keller, E.T., McCauley, L.K., and Taichman, R.S. 2005. Skeletal localization and neutralization of the SDF-1(CXCL12)/CXCR4 axis blocks prostate cancer metastasis and growth in osseous sites in vivo. *J Bone Miner Res*. 20(2):318-329.
137. Das, S., and Skobe, M. 2008. Lymphatic vessel activation in cancer. *Ann N Y Acad Sci*. 1131:235-241
138. Balch, C.M., Soong, S.J., Gershenwald, J.E., Thompson, J.F., Reintgen, D.S., Cascinelli, N., Urist, M., McMasters, K.M., Ross, M.I., Kirkwood, J.M., Atkins, M.B., Thompson, J.A., Coit, D.G., Byrd, D., Desmond, R., Zhang, Y., Liu, P.Y., Lyman, G.H., and Morabito, A. 2001. Prognostic factors analysis of 17,600 melanoma patients: validation of the American Joint Committee on cancer melanoma staging system. *J Clin Oncol*. 19(16):3622-3634.

139. Uharcek, P. 2008. Prognostic factors in endometrial carcinoma. *J Obstet Gynaecol Res.* 34(5):776-783.
140. Darling, G. 2009. The role of lymphadenectomy in esophageal cancer. *J Surg Oncol.* 99(4):189-193.
141. Pugliese, M.S., Beatty, J.D., Tickman, R.J., Allison, K.H., Atwood, M.K., Szymonifka, J., Arthurs, Z.M., Huynh, P.P., and Dawson, J.H. 2009. Impact and outcomes of routine microstaging of sentinel lymph nodes in breast cancer: significance of the pN0(i+) and pN1mi categories. *Ann Surg Oncol.* 16(1):113-120.
142. Wiley, H.E., Gonzalez, E.B., Maki, W., Wu, M.T., and Hwang, S.T. 2001. Expression of CC chemokine receptor-7 and regional lymph node metastasis of B16 murine melanoma. *J Natl Cancer Inst.* 93(21):1638-1643.
143. Saeki, H., Moore, A.M., Brown, M.J., and Hwang, S.T. 1999. Cutting edge: secondary lymphoid-tissue chemokine (SLC) and CC chemokine receptor 7 (CCR7) participate in the emigration pathway of mature dendritic cells from the skin to regional lymph nodes. *J Immunol.* 162(5):2472-2475.
144. Hippo, Y., Yashiro, M., Ishii, M., Taniguchi, H., Tsutsumi, S., Hirakawa, K., Kodama, T., and Aburatani, H. 2001. Differential gene expression profiles of scirrhous gastric cancer cells with high metastatic potential to peritoneum or lymph nodes. *Cancer Res.* 61(3):889-95.
145. Gerber, S.A., Rybalko, V.Y., Bigelow, C.E., Lugade, A.A., Foster, T.H., Frelinger, J.G., and Lord, E.M. 2006. Preferential attachment of peritoneal tumor metastases to omental immune aggregates and possible role of a unique vascular microenvironment in metastatic survival and growth. *Am J Pathol.* 169(5):1739-1752.
146. Carvalho, M.A., Zecchin, K.G., Seguin, F., Bastos, D.C., Agostini, M., Rangel, A.L., Veiga, S.S., Raposo, H.F., Oliveira, H.C., Loda, M., Coletta, R.D., and Graner, E. 2008. Fatty acid synthase inhibition with Orlistat promotes apoptosis and reduces cell growth and lymph node metastasis in a mouse melanoma model. *Int J Cancer.* 123(11):2557-2565.
147. Marrogi, A.J., Munshi, A., Merogi, A.J., Ohadike, Y., El-Habashi, A., Marrogi, O.L., and Freeman, S.M. 1997. Study of tumor infiltrating lymphocytes and transforming growth factor-beta as prognostic factors in breast carcinoma. *Int J Cancer.* 74(5):492-501.
148. Yigit, R., Massuger, L.F., Figdor, C.G., and Torensma, R. 2010. Ovarian cancer creates a suppressive microenvironment to escape immune elimination. *Gynecol Oncol.* 117(2):366-372.
149. Kilic, A., Landreneau, R.J., Luketich, J.D., Pennathur, A., and Schuchert, M.J. 2009. Density of tumor-infiltrating lymphocytes correlates with disease recurrence and survival in patients with large non-small-cell lung cancer tumors. *J Surg Res.*
150. Wang, J.M., Deng, X., Gong, W., and Su, S. 1998. Chemokines and their role in tumor growth and metastasis. *J Immunol Methods.* 220(1-2):1-17.
151. Rossi, D., and Zlotnik, A. 2000. The biology of chemokines and their receptors. *Annu Rev Immunol.* 18:217-242.
152. Hamadmad, S.N., and Hohl, R.J. 2008. Erythropoietin stimulates cancer cell migration and activates RhoA protein through a mitogen-activated protein kinase/extracellular signal-regulated kinase-dependent mechanism. *J Pharmacol Exp Ther.* 324(3):1227-1233.
153. Otsuka, S., and Bebb, G. 2008. The CXCR4/SDF-1 chemokine receptor axis: a new target therapeutics for non-small cell lung cancer. *J Thorac Oncol.* 3(12):1379-1383.
154. Reuter, S., Dehzad, N., Martin, H., Heinz, A., Castor, T., Sudowe, S., Reske-Kunz, A.B., Stassen, M., Buhl, R., and Taube, C. 2009. Mast Cells Induce Migration of Dendritic Cells in a Murine Model of Acute Allergic Airway Disease. *Int Arch Allergy Immunol.* 151(3):214-222.

155. Zdolsek, J., Eaton, J.W., and Tang, L. 2007. Histamine release and fibrinogen adsorption mediate acute inflammatory responses to biomaterial implants in humans. *J Transl Med.* 5:31.
156. Nair, A., Thevenot, P.T., Dey, J., Shen, J., Sun, M.W., Yang, J., and Tang, L. 2010. Novel Polymeric Scaffolds Using Protein Microbubbles as Porogen and Growth Factor Carriers. *Tissue Eng Part C Methods.* 16(1):23-32.
157. Henke, M., Laszig, R., Rube, C., Schäfer, U., Haase, K.D., Schilcher, B., Mose, S., Beer, K.T., Burger, U., Dougherty, C., and Frommhold, H. 2003. Erythropoietin to treat head and neck cancer patients with anaemia undergoing radiotherapy: randomised, double-blind, placebo-controlled trial. *Lancet.* 362(9392):1255-1260.
158. Arcasoy, M.O., Jiang, X., and Haroon, Z.A. 2003. Expression of erythropoietin receptor splice variants in human cancer. *Biochem Biophys Res Commun.* 307(4):999-1007.
159. Mirmohammadsadegh, A., Marini, A., Gustrau, A., Delia, D., Nambiar, S., Hassan, M., and Hengge, U.R. 2010. Role of erythropoietin receptor expression in malignant melanoma. *J Invest Dermatol.* 130(1):201-210.
160. Weiss, M.J. 2003. New insights into erythropoietin and epoetin alfa: mechanisms of action, target tissues, and clinical applications. *Oncologist.* Suppl 3:18-29.
161. Lappin, T.R., Maxwell, A.P., and Johnston, P.G. 2002. EPO's alter ego: erythropoietin has multiple actions. *Stem Cells.* 20(6):485-492.
162. Yasuda, Y., Fujita, Y., Matsuo, T., Koinuma, S., Hara, S., Tazaki, A., Onozaki, M., Hashimoto, M., Musha, T., Ogawa, K., Fujita, H., Nakamura, Y., Shiozaki, H., and Utsumi, H. 2003. Erythropoietin regulates tumour growth of human malignancies. *Carcinogenesis.* 24(6):1021-1029.
163. Yuan, R., Maeda, Y., Li, W., Lu, W., Cook, S., and Dowling, P. 2008. Erythropoietin: a potent inducer of peripheral immuno/inflammatory modulation in autoimmune EAE. *PLoS One.* 3(4):e1924.
164. Brines, M., and Cerami, A. 2008. Erythropoietin-mediated tissue protection: reducing collateral damage from the primary injury response. *J Intern Med.* 264(5):405-432.
165. Katz, O., Gil, L., Lifshitz, L., Prutchi-Sagiv, S., Gassmann, M., Mittelman, M., and Neumann, D. 2007. Erythropoietin enhances immune responses in mice. *Eur J Immunol.* 37(6):1584-1593.
166. Poznansky, M.C., Olszak, I.T., Foxall, R., Evans, R.H., Luster, A.D., and Scadden, D.T. 2000. Active movement of T cells away from a chemokine. *Nat Med.* 6(5):543-548.
167. Huttenlocher, A., and Poznansky, M.C. 2008. Reverse leukocyte migration can be attractive or repulsive. *Trends Cell Biol.* 18(6):298-306.
168. Vianello, F., Olszak, I.T., and Poznansky, M.C. 2005. Fugotaxis: active movement of leukocytes away from a chemokinetic agent. *J Mol Med.* 83(10):752-763.
169. Thevenot, P.T., Nair, A.M., Shen, J., Lotfi, P., Ko, C.Y., and Tang, L. 2010. The effect of incorporation of SDF-1alpha into PLGA scaffolds on stem cell recruitment and the inflammatory response. *Biomaterials.* 31(14): 3997-4008.
170. Wu, Y., and Zhou, B.P. 2010. TNF-alpha/NF-kappaB/Snail pathway in cancer cell migration and invasion. *Br J Cancer.* 102(4):639-644.
171. Yano, S., Nokihara, H., Yamamoto, A., Goto, H., Ogawa, H., Kanematsu, T., Miki, T., Uehara, H., Saijo, Y., Nukiwa, T., and Sone, S. 2003. Multifunctional interleukin-1beta promotes metastasis of human lung cancer cells in SCID mice via enhanced expression of adhesion-, invasion- and angiogenesis-related molecules. *Cancer Sci.* 94(3):244-252.
172. Coussens, L.M., and Werb, Z. 2001. Inflammatory cells and cancer: think different! *J Exp Med.* 193(6):F23-26.

173. Theoharides, T.C., and Conti, P. 2004. Mast cells: the Jekyll and Hyde of tumor growth. *Trends Immunol.* 25(5):235-241.
174. Ch'ng, S., Wallis, R.A., Yuan, L., Davis, P.F., and Tan, S.T. 2006. Mast cells and cutaneous malignancies. *Mod Pathol.* 19(1):149-159.
175. Conti, P., Castellani, M.L., Kempuraj, D., Salini, V., Vecchiet, J., Tetè, S., Mastrangelo, F., Perrella, A., De Lutiis, M.A., Tagen, M., and Theoharides, T.C. 2007. Role of mast cells in tumor growth. *Ann Clin Lab Sci.* 37(4):315-322.
176. Theoharides, T.C., and Konstantinidou, A.D. 2007. Corticotropin-releasing hormone and the blood-brain-barrier. *Front Biosci.* 12:1615-1628.
177. Masini, E., Fabbroni, V., Giannini, L., Vannacci, A., Messerini, L., Perna, F., Cortesini, C., and Cianchi, F. 2005. Histamine and histidine decarboxylase up-regulation in colorectal cancer: correlation with tumor stage. *Inflamm Res.* 54 Suppl 1:S80-81.
178. Tomita, K., and Okabe, S. 2005. Exogenous histamine stimulates colorectal cancer implant growth via immunosuppression in mice. *J Pharmacol Sci.* 97(1):116-123.
179. Brookes, Z.L., Stedman, E.N., Guerrini, R., Lawton, B.K., Calo, G., and Lambert, D.G. 2007. Proinflammatory and vasodilator effects of nociceptin/orphanin FQ in the rat mesenteric microcirculation are mediated by histamine. *Am J Physiol Heart Circ Physiol.* 293(5):H2977-2985.
180. Heinke, S., Szücs, G., Norris, A., Droogmans, G., and Nilius, B. 1995. Inhibition of volume-activated chloride currents in endothelial cells by chromones. *Br J Pharmacol.* 115(8):1393-1398.
181. della Rovere, F., Granata, A., Familiari, D., D'Arrigo, G., Mondello, B., Basile, G. 2007. Mast cells in invasive ductal breast cancer: different behavior in high and minimum hormone-receptive cancers. *Anticancer Res.* 27(4B):2465-2471.
182. Ko, C., Wu, L., Antich, P., and Tang, L. 2009. Whole body optical imaging for studying inflammation-induced cancer metastasis. The 9th Annual UT Southwestern *In vivo* Cancer Cellular and Molecular Imaging Symposium. Dallas, TX.

BIOGRAPHICAL INFORMATION

Cheng-Yu Ko was born in Taipei city, Taiwan. At the National Chung Hsing University of Veterinary Medicine, her undergraduate education provided her with experiences which gave her the opportunity to receive different levels of clinical and field training. She found it was fascinating how different disciplines in basic research could lead her to find better solutions for medication. Therefore, after completion of her Bachelor's degree in Veterinary Medicine, she received research training in Veterinary Microbiology under the supervision of Dr. Poa-Chun Chang who is the person who motivated her to take the first step in becoming a research scientist. Research in Veterinary Microbiology gave her a better understanding of animal vaccine development. With that understanding, along with her previous education in veterinary medicine, she started her Ph.D. study in Bioengineering of the University of Texas at Arlington in 2005. Under the supervision of Dr. Liping Tang, she found it was very interesting to continue the investigation of biomaterial-mediated inflammation for the application of cancer metastasis study and therapy development. Her plan is to complete her Doctor of Philosophy in Biomedical Engineering at the joint program of the University of Texas at Arlington and the University of Texas Southwestern Medical Center at Dallas in May 2010. She will look for a research scientist position in order to pursue her interests in vaccine adjuvant development.